การออกแบบและการจำลองกระบวนการรวมของการผลิตไบโอดีเซล การรีฟอร์มของกลีเซอรอล และการผลิตกรีนดีเซล

นายบำรุง สูงเนิน

จุฬาลงกรณ์มหาวิทยาลัย
Chulalongkorn University

บทคัดย่อและแฟ้มข้อมูลฉบับเต็มของวิทยานิพนธ์ตั้งแต่ปีการศึกษา 2554 ที่ให้บริการในคลังปัญญาจุฬาฯ (CUIR)
เป็นแฟ้มข้อมูลของนิสิตเจ้าของวิทยานิพนธ์ ที่ส่งผ่านทางบัณฑิตวิทยาลัย
The abstract and full text of theses from the academic year 2011 in Chulalongkorn University Intellectual Repository (CUIR)
are the thesis authors' files submitted through the University Graduate School.

วิทยานิพนธ์นี้เป็นส่วนหนึ่งของการศึกษาตามหลักสูตรปริญญาวิศวกรรมศาสตรมหาบัณฑิต
สาขาวิชาวิศวกรรมเคมี ภาควิชาวิศวกรรมเคมี
คณะวิศวกรรมศาสตร์ จุฬาลงกรณ์มหาวิทยาลัย
ปีการศึกษา 2557
ลิขสิทธิ์ของจุฬาลงกรณ์มหาวิทยาลัย

DESIGN AND SIMULATION OF COMBINED BIODIESEL PRODUCTION, GLYCEROL REFROMING AND GREEN DIESEL PRODUCTION

Mr. Bamrung Sungnoen

A Thesis Submitted in Partial Fulfillment of the Requirements
for the Degree of Master of Engineering Program in Chemical Engineering
Department of Chemical Engineering
Faculty of Engineering
Chulalongkorn University
Academic Year 2014
Copyright of Chulalongkorn University

Thesis Title	DESIGN AND SIMULATION OF COMBINED BIODIESEL PRODUCTION, GLYCEROL REFROMING AND GREEN DIESEL PRODUCTION
By	Mr. Bamrung Sungnoen
Field of Study	Chemical Engineering
Thesis Advisor	Professor Suttichai Assabumrungrat, Ph.D.
Thesis Co-Advisor	Kanokwan Ngaosuwan, D.Eng.

Accepted by the Faculty of Engineering, Chulalongkorn University in Partial Fulfillment of the Requirements for the Master's Degree

.....Dean of the Faculty of Engineering
(Professor Bundhit Eua-arporn, Ph.D.)

THESIS COMMITTEE

.....Chairman
(Akawat Sirisuk, Ph.D.)

.....Thesis Advisor
(Professor Suttichai Assabumrungrat, Ph.D.)

.....Thesis Co-Advisor
(Kanokwan Ngaosuwan, D.Eng.)

.....Examiner
(Palang Bumroongsakulsawat, Ph.D.)

.....External Examiner
(Assistant ProfessorWorapon Kiatkittipong, Ph.D.)

CHULALONGKORN UNIVERSITY

บำรุง สูงเนิน : การออกแบบและการจำลองกระบวนการรวมของการผลิตไบโอดีเซล การรีฟอร์มของกลีเซอรอลและการผลิตกรีนดีเซล (DESIGN AND SIMULATION OF COMBINED BIODIESEL PRODUCTION, GLYCEROL REFROMING AND GREEN DIESEL PRODUCTION) อ.ที่ปรึกษาวิทยานิพนธ์หลัก: ศ. ดร.สุทธิชัย อัสสะบำรุงรัตน์, อ.ที่ปรึกษาวิทยานิพนธ์ร่วม: ดร.กนกวรรณ ง้าวสุวรรณ, 173 หน้า.

ไบโอดีเซลเป็นเชื้อเพลิงทางเลือกที่ได้รับความนิยมในปัจจุบัน โดยนำมาใช้ทดแทนเชื้อเพลิงน้ำมันดีเซลจากปิโตรเลียมที่กำลังจะหมดไปในอนาคตอันใกล้ แต่อย่างไรก็ตามปัญหาที่จะเกิดขึ้นคือกลีเซอรอลที่เป็นผลพลอยเกิดขึ้นในปริมาณที่มาก ถึงแม้ว่าจะมีการนำกลีเซอรอลไปใช้ในอุตสาหกรรมเครื่องสำอางค์ อาหาร และเภสัชกรรม ซึ่งมีความต้องการความบริสุทธิ์สูง ในปริมาณที่น้อย เมื่อเร็วๆ นี้พบว่ากลีเซอรอลเป็นทางเลือกที่น่าสนใจในการผลิตไฮโดรเจนเนื่องจากให้ไฮโดรเจนได้ในปริมาณที่สูง และถูกใช้ในอุตสาหกรรมทั่วโลก น้ำมันที่มีกรดไขมันอิสระปริมาณที่สูงไม่เหมาะสำหรับเป็นวัตถุดิบที่ใช้ในการผลิตไบโอดีเซล เนื่องจากจะทำให้กระบวนการผลิตนั้นมีความซับซ้อนขึ้น แต่เมื่อนำกรดไขมันอิสระมาใช้เป็นสารตั้งต้นในกระบวนการไฮโดรทรีทติงโดยใช้ปริมาณไฮโดรเจนที่ต่ำในการผลิตกรีนดีเซลซึ่งการรวมกระบวนการเหล่านี้เข้าด้วยกันจะส่งผลดีในภาพรวมในด้านต่างๆ และยังสามารถผลิตเชื้อเพลิงทางเลือกได้หลากหลายตามความต้องการใช้งานมากขึ้น งานวิจัยนี้จึงศึกษาการจำลองกระบวนการรวมสำหรับผลิต ไบโอดีเซล ไฮโดรเจน และกรีนดีเซล โดยใช้น้ำมันถั่วเหลืองและกรดสเตียริกเป็นสารตั้งต้น โดยงานส่วนแรกเป็นการเลือกวิธีการผลิตในไบโอดีเซล การรีฟอร์มของกลีเซอรอล และกรีนดีเซลแต่ละส่วน เพื่อที่จะนำกระบวนการที่เหมาะสมเหล่านี้มารวมเป็นกระบวนการเดียวกันเป็นกรณีศึกษาพื้นฐาน งานส่วนที่สองคือการปรับปรุงกระบวนข้างต้นซึ่งแบ่งเป็นสามกระบวนการปรับปรุง โดยส่วนแรกของการปรับปรุงสามารถลดการใช้หอกลั่นในกระบวนการทำกลีเซอรอลให้บริสุทธิ์ และยังส่งผลให้ได้ทั้งปริมาณของไฮโดเจนและกรีนดีเซลเพิ่มขึ้น ในงานส่วนที่สองน้ำมันพืชที่ไม่ทำปฏิกิริยาสามารถนำกลับมาใช้เป็นสารตั้งต้นทำให้พลังงานลดลงจาก 14.02 เป็น 13.85 เมกะวัตต์ และยังสามารถนำน้ำที่เหลือใช้นำกลับมาใช้ใหม่โดยไม่ต้องผ่านกระบวนการบำบัด งานส่วนที่สามทำการปรับปรุงพลังงานของโรงงาน ซึ่งผลที่ได้คือสามารถลดการใช้พลังงานความร้อนจากกรณีศึกษาพื้นฐานลงมาได้ 47.24 เปอร์เซ็นต์ นอกจากนี้เมื่อเปรียบเทียบกับโรงงานทั้งสามของการผลิตไบโอดีเซล การรีฟอร์มของกลีเซอรอล และการผลิต กรีนดีเซลที่ภาวะการดำเนินการเดียวกัน เปรียบเทียบกับการรวมกระบวนการที่เสนอ พบว่าสามารถลดจำนวนพลังงานลงได้ 31.41 เปอร์เซ็นต์ โดยพลังงานโดยส่วนใหญ่ของโรงงานงานที่เสนอนี้มาจากหอกลั่นไบโอดีเซลและหอกลั่นเมทานอล จากผลการจำลองทั้งหมดนี้ชี้ชัดให้เห็นว่าการรวมกระบวนการที่เสนอนี้มีประสิทธิภาพสำหรับการผลิตพลังงานทางเลือกแก่มนุษยชาติเพื่อนำไปใช้ต่อไป

ภาควิชา วิศวกรรมเคมี ลายมือชื่อนิสิต .....

สาขาวิชา วิศวกรรมเคมี ลายมือชื่อ อ.ที่ปรึกษาหลัก .....

ปีการศึกษา 2557 ลายมือชื่อ อ.ที่ปรึกษาร่วม .....

5670263121 : MAJOR CHEMICAL ENGINEERING
KEYWORDS: GLYCEROL REFORMING / HYDROTREATING PROCESS / COMBINATION / GREEN DIESEL PRODUCTION / CONCEPTUAL DESIGN / BIODIESEL PRODUCTION / HEAT INTEGRATION / HOMOGENEOUS / HYDROGEN PRODUCTION / PROCESS IMPROVEMENT / BIODIESEL PRODUCTION

BAMRUNG SUNGNOEN: DESIGN AND SIMULATION OF COMBINED BIODIESEL PRODUCTION, GLYCEROL REFROMING AND GREEN DIESEL PRODUCTION. ADVISOR: PROF. SUTTICHAI ASSABUMRUNGRAT, Ph.D., CO-ADVISOR: KANOKWAN NGAOSUWAN, D.Eng., 173 pp.

Biodiesel, an alternative renewable and biodegradable fuel, has been attractive to substitute petroleum diesel, the large amounts of glycerol as a byproduct will be a problem because of the limitation of glycerol applications. Recently, hydrogen production using glycerol as a main reactant has been attractive, because it can use for several processes. For biodiesel production, oil with high free fatty acids (FFAs) content is unsuitable feedstock due to this make the biodiesel process more complicated and using more equipment than virgin oil. In contrast, if FFAs is utilized in hydrotreating process with low amount of hydrogen as one of reactant. Moreover, a novel process by combination of three alternative fuels involving three processes of biodiesel production, hydrogen production via glycerol reforming and hydrotreating of free fatty acid might show the beneficially overall process and produces a variously alternative fuel. This research studied the simulation of combination process for production of biodiesel, hydrogen and green diesel using soybean oil and stearic acid as raw materials. Firstly, the individual process including of biodiesel production, glycerol steam reforming, and green diesel production was investigated to choose the suitable process for combination as base case. After that, this base case was improved by: (1) glycerol purification column can be neglected from the process. This is leading to produce more hydrogen and green diesel than that of the base case because of methanol reforming; (2) hot unconverted oil was recycle to mix with fresh oil which it can reduce the total energy consumption from 14.02 to 13.85 MW. Moreover, high purity of condensed water can be directly used as the steam. (3) furnace combustor was installed to produce heat from fuel gas which this gas produces large amount of energy and return to the process. Pinch analysis showed that the proposed process offers energy saving of 47.24% comparing to the base case. Furthermore, the proposed process can also decrease the total energy consumption to 31.41% comparing to the conventional biodiesel production, glycerol steam reforming and hydrotreating at the same operating condition. It was found that the main energy consumption from the proposed process was obtained from the FAMEs purification and methanol recovery columns. This proposed process showed the efficiency for producing three alternative energy for humanity.

Department:	Chemical Engineering	Student's Signature	.....
Field of Study:	Chemical Engineering	Advisor's Signature	.....
Academic Year:	2014	Co-Advisor's Signature	.....

ACKNOWLEDGEMENTS

I would like to respect to my advisor, Professor Suttichai Assabumrungrat, and my co-advisor, Dr. Kanokwan Ngaosuwan, for their suggestions about my work. I have an excellent experiences from learning with them which I can using in the future.

In my thesis, I greatly respect to thesis committee commendation who Dr. Akawut Sirisuk, Dr. Palang Bamroongsakulsawat, and Assistant Professor Worapon Kiatkittipong. Furthermore, I appreciatively acknowledge the supports from the Thailand Research Fund for financial support.

For my good friends such as Mr. Agachon Phuluanglue, Mr. Pichayapan Kongpanna, Mr. Kritchart Wongwailikhit, Mr. Jutipong Poosumas and others who provided sincere friendship, supported and suggested any idea on my work with their help.

Finally, I would like to devote this thesis to my beloved parents. They always support me when I encountered with any problems. I can say that I could not achieve my degree without their encouragements. I love them much more than anything.

จุฬาลงกรณ์มหาวิทยาลัย
Chulalongkorn University

CONTENTS

Page

จุฬาลงกรณ์มหาวิทยาลัย
Chulalongkorn University

Page

จุฬาลงกรณ์มหาวิทยาลัย
Chulalongkorn University

Page

จุฬาลงกรณ์มหาวิทยาลัย
CHULALONGKORN UNIVERSITY

Page

จุฬาลงกรณ์มหาวิทยาลัย
Chulalongkorn University

LIST OF FIGURES

Page

CHULALONGKORN UNIVERSITY

Page

จุฬาลงกรณ์มหาวิทยาลัย
CHULALONGKORN UNIVERSITY

Page

จุฬาลงกรณ์มหาวิทยาลัย
CHULALONGKORN UNIVERSITY

Page

จุฬาลงกรณ์มหาวิทยาลัย
CHULALONGKORN UNIVERSITY

Page

จุฬาลงกรณ์มหาวิทยาลัย
Chulalongkorn University

LIST OF TABLES

Page

จุฬาลงกรณ์มหาวิทยาลัย
Chulalongkorn University

Page

Chulalongkorn University

Page

จุฬาลงกรณ์มหาวิทยาลัย
CHULALONGKORN UNIVERSITY

Page

NOMENCLATURE

APGR	Aqueous phase glycerol reforming
ASTM	American Society for Testing and Materials
BD-WASH	Liquid-liquid extraction
C [number]	Cooling unit
C15	Carbon number 15
C18	Carbon number 18
CSTR	Mechanically stirred tank reactor
DC-BD	Methanol recovery column
DC-FAME	FAMEs purification column
DC-GLY	Glycerol purification column
FAME	Fatty acid methyl esters
FAN [number]	Fan, compressor
FILTER	Solid filtration
FURNACE	Furnace combustor
GATR	Glycerol reforming via autothermal
GDR	Glycerol dry reforming
GSM	Glycerol steam reforming
GSW	Glycerol reforming via supercritical water
HDO	Hydrodeoxygenation
HEPD	N-heptadecane
HEXD	N-hexadecane
HWGS	High water-gas shift reactor
HX [number]	Heat exchanger, preheating unit
LWGS	Low water-gas shift reactor
MIX [number]	Mixer
NRTL	Non-Random Two Liquid model
OCTD	N-octadecane
OCTDL	L-octadecanol

จุฬาลงกรณ์มหาวิทยาลัย
Chulalongkorn University

NOMENCLATURE *(continue)*

P	Pressure, atm
P [number]	Pump
PEND	N-pentadecane
PENG-ROB	Peng-Robinson equation of state
PSA	Pressure-swing adsorption unit
QSPTL	Heat splitter
REFORMER	Reforming reactor
R-HDO1	Hydrotreating reactor (rate base)
R-HDO2	Hydrotreating reactor (equilibrium)
R-NUET	Neutralization reactor
R-TRAN	Transesterification reactor
SA	Stearic acid
SCM	Supercritical methanol
SEP [number]	Phase separator
SPTL [number]	Component splitter
SRK	Soave-Redlich-Kwong Equation of State
T	Temperature, K
UNIFAC	UNIQUAC Functional-group Activity Coefficients
V [number]	Valve
WGFR	Water to glycerol feed ratio
WGMR	Water to glycerol-methanol feed ratio
ΔT_{min}	Minimum approach temperature, K

จุฬาลงกรณ์มหาวิทยาลัย
Chulalongkorn University

CHAPTER I INTRODUCTION

1.1 Motivation

Nowadays, the increasing of energy consumption of the world has resulted in the significant depletion of fossil based fuels. The International Energy Agency (IEA) predicts an investment of new fuel sources to increase the global energy demand as approximate 8 trillion dollars by 2040 [1]. Bridjanian and Samimi [2] reported increasing demand of diesel and gasoline is because of the growth of engine and machine supplying for the worldwide automobile industries. Thus, there are many researches focusing on alternative energy which could be directly used in engines for transportation sector.

Biodiesel or free fatty acid methyl ester (FAME), known as an alternative renewable and biodegradable fuel, has been attractive because it can be directly used or blended with petroleum diesel in compression–ignition engines which may avoid diesel-engine modification. Vegetable oils and their waste, fat, algae, and lipid are used as a renewable feedstock for biodiesel production. Using biodiesel can reduce carbon dioxide emission as well as hydrocarbons and exhaust gases. Although present biodiesel production is still limited due to high cost of vegetable oils which is about 80% of total cost of biodiesel production. The cost of biodiesel cost is higher than petro-diesel as approximately 1.5 times.

In biodiesel production, every 10 tons of biodiesel produces 1 ton of glycerol as a by-product. Although biodiesel can be produced for complete substitution of a fossil diesel in the future, glycerol as a byproduct will be a problem because of limited glycerol applications. Only 500 kton per year of purified glycerol are used in industries such as cosmetics, food and pharmaceutical applications [3]. By-product glycerol containing unreacted alkali catalyst and soap must be neutralized with acid and then, water and alcohol are removed in order to obtain 50-80% of crude glycerol whereas 99% or higher purity is used for feeding in pharmaceutical and cosmetic industries [4]. Distillation unit is required for glycerol purification to obtain 99% or higher purity of glycerol resulting in a higher cost of by-product treatment. Moreover, if glycerol is

directly discarded without treatments, it may be environmental hazards [5]. Thus, many researchers have been studied the processes in order to convert a glycerol to valuable products.

Recently, hydrogen production using glycerol as a main reactant has been attractive for many reasons such as it provides high hydrogen content with an economic aspect [6]. Glycerol can be converted to hydrogen via glycerol reforming using a commercial nickel-base catalyst reforming [7]. The advantages of hydrogen in comparison with other conventional fuels are non-toxic while inhaled with ambient air, untraceable by human sensory system, highly combustible fuel without water and air pollution. Hydrogen is used for several processes such as oil refinery (approximate 75% of worldwide consumption), energy sources for automotive and transportation. Thus, hydrogen production in the future also increases to serve human civilization.

Although biodiesel has been proven for many reasons to substitute petro-diesel, there are some drawbacks. Vegetable oil for biodiesel production must remove free fatty acids (FFAs) in order to avoid water formation causing soap formation via saponification reaction during transesterification in presence of alkali catalyst [4,8]. Many researchers have attempted to develop new processes in order to defeat some of biodiesel limitations.

Hydrotreating oil is known as green diesel or renewable diesel or second generation diesel or petrodiesel-like fuels. Green diesel can be obtained from vegetable oil or free fatty acids as well as biodiesel raw materials. Using free fatty acids as a raw material can be reduced via some hydrotreating reaction pathways (see in the next chapter) to produce green diesel.

In this work, we propose a novel process by combination of three alternative fuels involving three processes of biodiesel production, hydrogen production via glycerol reforming and hydrotreating of free fatty acid. The combined process with a simple diagram is given in Figure 1.1

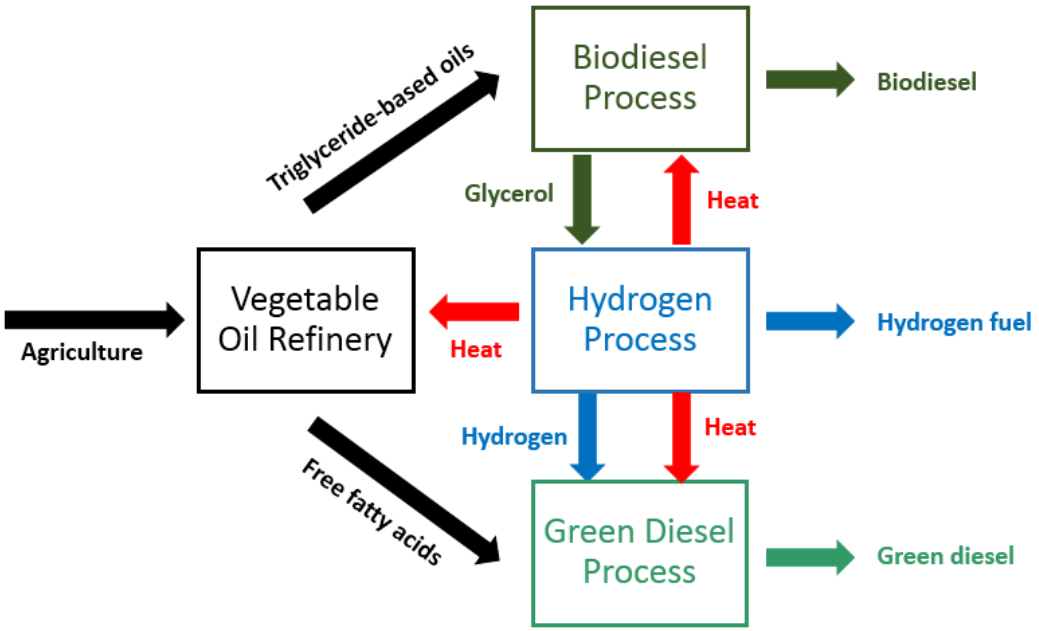

Figure 1.1 Simple diagram of the proposed combination of biofuels production processes.

The crude glycerol is fed to the reforming process in order to convert to hydrogen via glycerol reforming. Part of produced hydrogen together with free fatty acids are fed to the hydrotreating process for producing green diesel. Both the reforming and hydrotreating require operation at high temperatures and consequently high energy consumption. Process heat integration would be necessary for efficient operation of the combined processes. Based on the proposed combined process, the valuable final products are FAME, hydrogen, and petrodiesel-like fuels (green diesel).

1.2 Objective

To design and simulate a novel process which combines processes of biodiesel production, hydrogen production via glycerol reforming and green diesel production.

1.3 Scope of work

1.3.1 Simulate the proposed process consisting of biodiesel production using soybean oil, glycerol reforming and hydrotreating using stearic acid as model of a pure free fatty acid oil by Aspen Plus simulation.

1.3.2 Determine effects of major operating parameters of the combined process on its performances including FAME, hydrogen and green diesel productions, and energy consumption.

1.3.3 Apply the concept of heat integration to further improve the performances of the combined process.

1.4 Expected Output

The work should provide a conceptual design for efficient combined process for productions of biodiesel, hydrogen, and green diesel.

CHAPTER II THEORY

Fundamental concepts of biodiesel production, glycerol reforming and hydrotreating were presented in this chapter which provided basic knowledge for understanding this work.

2.1 Oil feedstocks for biodiesel production

Vegetable oils (organic oil) are mainly reactant in biodiesel production. The selection of oil as a feedstock is depended on a local availability. In Europe and United States of America use edible oils such as rape seed and soybean oil. Philippines and Malaysia also apply edible oils such as palm oil and coconut oil. India uses jatropha as non-edible oil .The global commercial biodiesel production in the percentage of oil is rapeseed oil (84%), sunflower oil (13%), palm oil (1%), soybean and others (2%). The favorable agronomic features of soybean is due to its high-quality of protein and valuable edible oil that motivating commercial process produces soybean oil for supplement in the world trading. The main fatty acid compositions of soybean are highly content of linoleic acid, moderate oleic acid and low palmitic acid, stearic acid and linolenic acid as shown in Table 2.1 [8]

จุฬาลงกรณ์มหาวิทยาลัย
Chulalongkorn University

Table 2.1 Typical fatty acid composition (wt %) of soybean oil is compared with others oils (Orthoefer 1996) [8].

Fatty acid		Soybean	Canola	Cottonseed	Sunflower	Peanut
Lauric	12:0	–	–	–	0.5	–
Myristic	14:0	0.1	–	0.9	0.2	0.1
Palmitic	16:0	11.0	3.9	24.7	6.8	11.6
Palmitoleic	16:1	0.1	0.2	0.7	0.1	0.2
Stearic	18:0	4.0	1.9	2.3	4.7	3.1
Oleic	18:1	23.4	64.1	17.6	18.6	46.5
Linoleic	18:2	53.2	18.7	53.3	68.2	31.4
Linolenic	18:3	7.8	9.2	0.3	0.5	–
Arachidic	20:0	0.3	0.6	0.1	0.4	1.5
Gadoleic	20:1	–	1.0	–	–	1.4
Eicosadienoic	20:2	–	–	–	–	0.1
Behenic	22:0	0.1	0.2	–	–	3.0
Lignoceric	24:0	–	0.2	–	–	1.0

2.2 Transesterification for biodiesel production

Transesterification for biodiesel production is a reaction between oil and methanol as alcohol that the organic alkoxy group of triglyceride is exchanged with the organic alkoxy group of methanol [10, [9]]. In general, transesterification are often catalyzed by strong acid or base catalyst [10]. The product of transesterification are fatty acid methyl ester and glycerol. The basic reaction is depicted in Figure 2.1

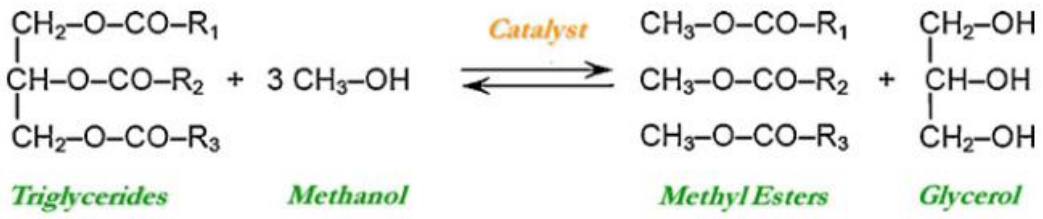

Figure 2.1 Transesterification for biodiesel production [10].

In mechanism detail, transesterification composes of three steps for complete reaction, the first step is one mole of triglyceride convert to one mole of diglyceride, which is followed by the subsequent higher glycerides to lower glycerides and glycerol in the last step. Each of steps provide the one mole of FAME [10]. (Figure 2.2)

จุฬาลงกรณ์มหาวิทยาลัย
Chulalongkorn University

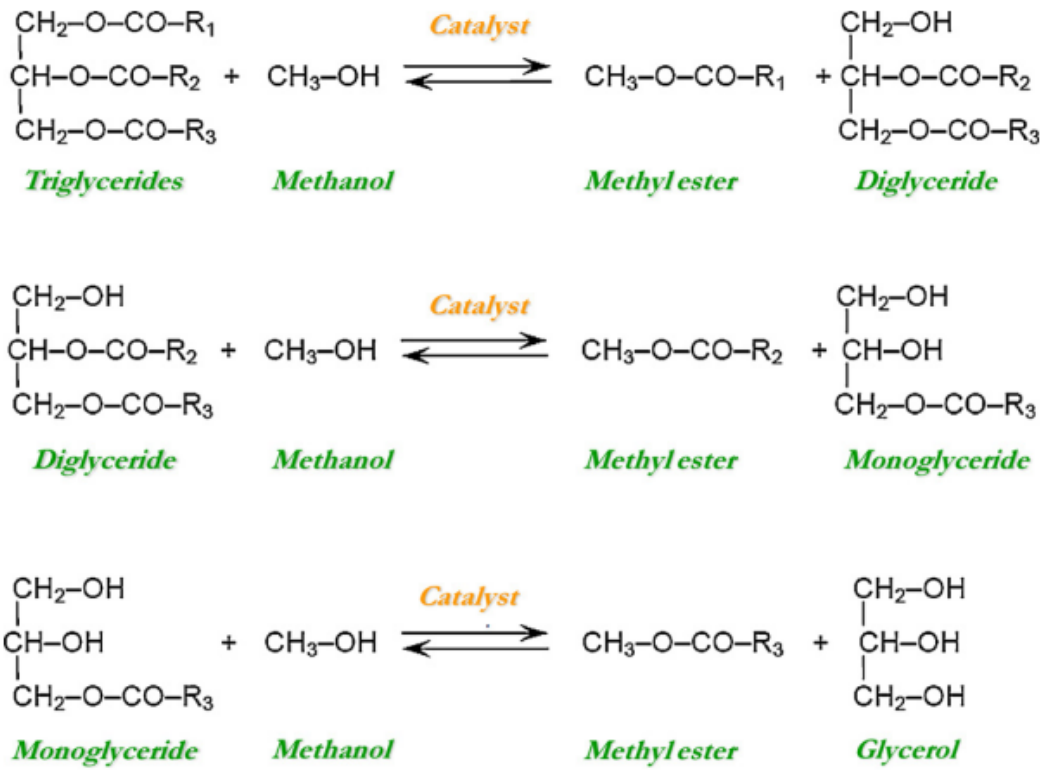

Figure 2.2 Transesterification reaction steps [10].

2.3 Esterification for biodiesel production

Esterification is the reaction which offers FAME and water via fatty acids react with methanol in presence of acid catalyst as shown in Figure 2.3

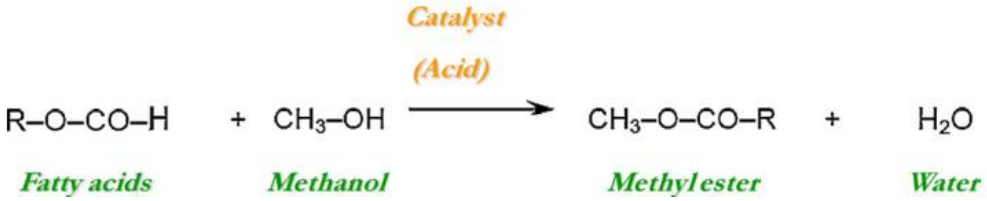

Figure 2.3 Esterification reactions in biodiesel production [10].

This reaction is usually used in biodiesel production when oil feedstocks contain an excessive free fatty acids in presence of an acid catalyst [11].

2.4 Saponification in biodiesel production

Sodium salt or potassium salt of fatty acid is known as natural soap, is prepared by a reaction called saponification where one of organic reaction. The original process was produced by either animal fat or boiling lard reacted with sodium hydroxide or

potassium hydroxide as reactants and glycerol and crude soap as products. The following reaction is shown in Figure 2.4 [12]. This reaction provides alkali soap as undesirable by-product of alkali-catalyzed biodiesel production causes the lower FAME yield, etc.

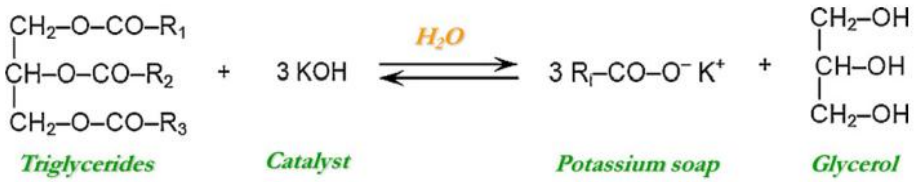

Figure 2.4 Saponification reaction [10].

2.5 Glycerol reforming process

2.5.1 Glycerol steam reforming (GSM)

The alternative hydrogen production process using glycerol and water as the reactants. Conventional glycerol steam reforming is an extremely endothermic reaction and may be operated at high temperature (>500 K). Glycerol reforming is combined from decomposition of glycerol and water-gas shift reaction as shown below [13, 14]

Glycerol decomposition

$$C_3H_8O_3 \rightleftharpoons 3CO + 4H_2 \ (\Delta H_r^{298K} = 251 kJ/mol) \quad (2.1)$$

Water-gas shift

$$CO + H_2O \rightleftharpoons CO_2 + H_2 \ (\Delta H_r^{298K} = -41 kJ/mol) \quad (2.2)$$

Overall reaction

$$C_3H_8O_3 + 3H_2O \rightleftharpoons 3CO_2 + 7H_2 \ (\Delta H_r^{298K} = 128 kJ/mol) \quad (2.3)$$

Methanation

$$CO + 3H_2 \rightleftharpoons CH_4 + H_2O \ (\Delta H_r^{298K} = -165 kJ/mol) \quad (2.4)$$

$$CO_2 + 4H_2 \rightleftharpoons CH_4 + 2H_2O \ (\Delta H_r^{298K} = -165 kJ/mol) \quad (2.5)$$

Glycerol hydrogenolysis

$$C_3H_8O_3 + 2H_2 \rightleftarrows 2CH_4 + CO + 2H_2O \quad \Delta H_r^{298K} = -160\,kJ/mol) \qquad (2.6)$$

2.5.2 Glycerol reforming via supercritical water (GSW)

This process is operated at a supercritical condition of water. Supercritical fluid is fluid state beyond its critical temperature and critical pressure. In this state, fluid cannot be clearly defined as a gas or liquid phase. Fluid can effuse like a gas and dissolve like a liquid. Supercritical water properties are shown in Table 2.2 and Figure 2.5.

Table 2.2 Water properties at various condition [19].

	Water	**Steam**	**Subcritical water**	**Supercritical water**	
Temperature, T (K)	298	673	523	673	673
Pressure, P (atm)	0.99	0.99	49.35	246.73	493.46
Density, ρ (g/cm^3)	1	0.0003	0.80	0.17	0.58
Dielectric constant, ε	78.5	~1	27.1	5.9	10.5
pK_w	14.0	-	11.2	19.4	11.9
Heat capacity, c_p (kJ/kg/K)	4.22	2.1	4.86	13.0	6.8
Dynamic viscosity, η (mPa s)	0.89	0.02	0.11	0.03	0.07
Heat conductivity, λ (mW/m/K)	608	55	620	160	438

จุฬาลงกรณ์มหาวิทยาลัย
Chulalongkorn University

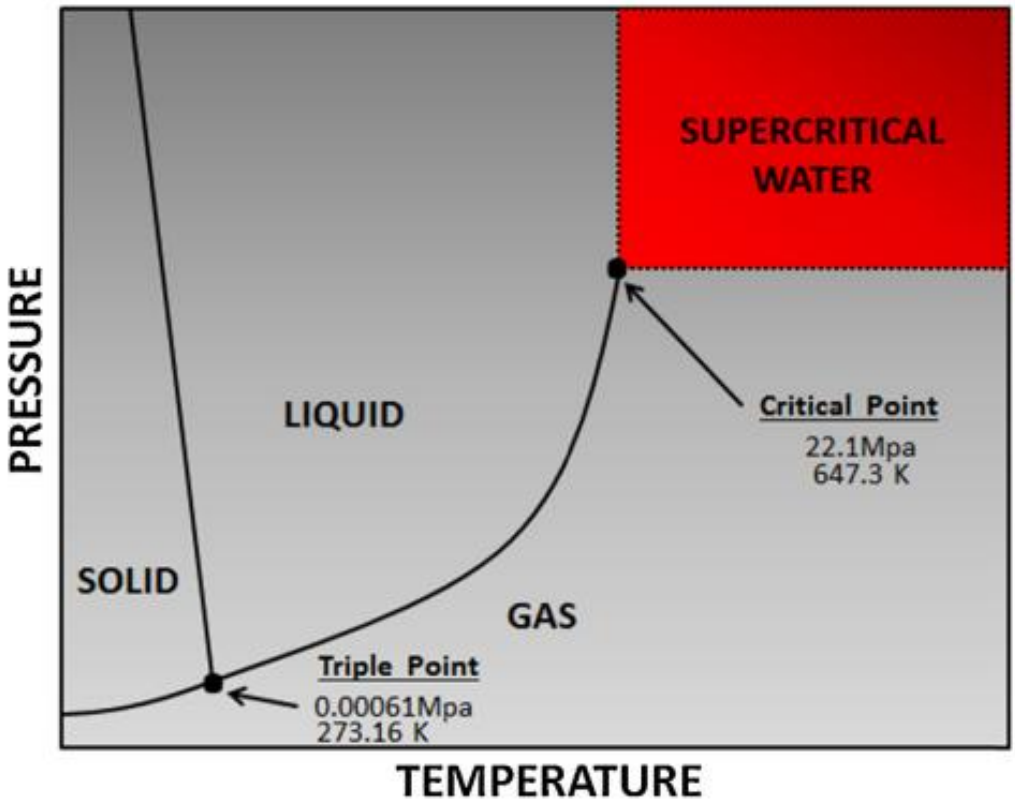

Figure 2.5 Phase diagram of water as a function of temperature and pressure [1].

The supercritical water is usually used laboratory and industry such as floral fragrance extraction. The decomposition of biomass in sub- and supercritical water state is faster than the other water state because the low value of water density and nonpolar solvent behavior (low dielectric constant) that it can dissolve with organic compound providing the homogeneous reaction. The mass transfer resistance between biomass and water is decreased at supercritical condition. Tar and coke formation are inhibited by intermediate of supercritical water [15, 16]. Moreover, the supercritical water reforming offers hydrogen selectivity, high space-time yield and beneficial endothermic reaction. In finally, hydrogen is possible to directly store without compression [2].

2.5.3 Glycerol reforming via partial oxidation (POG)

Partial oxidation of glycerol (POG) have several advantages on a start-up period because this process is naturally exothermic reaction. Furthermore, heat may be not required in a partial oxidation reactor providing an advantage than other reforming processes. The possible reactions can be described as shown below.

Glycerol decomposition

$$C_3H_8O_3 \rightleftarrows 3CO + 4H_2 \ (\Delta H_r^{298K} = 251 kJ/mol) \quad (2.1)$$

Partial oxidation can offer strongly heat of reaction that the partial combustion one mole of glycerol can provide energy itself to convert 6 mole of glycerol to carbon monoxide and hydrogen via glycerol decomposition.

Glycerol partial oxidation

$$C_3H_8O_3 + 3.5O_2 \rightleftarrows 4H_2O + 3CO_2 \ (\Delta H_r^{298K} = -1564.93 kJ/mol) \quad (2.7)$$

The stoichiometric of glycerol reforming reaction, which is three mole of water per one mole of glycerol (Equation 2.3), can be used to adjust the synthesis gas ratio with no significantly affecting against the energy consumption. However, the excessive water will extinguish the reaction. If the oxygen is insufficient supply in reaction, the partial oxidation can be occurred via

$$C_3H_8O_3 + 0.5O_2 \rightleftarrows 4H_2 + CO_2 + 2CO \ (\Delta H_r^{298K} = -31.79 kJ/mol) \quad (2.8)$$

If the oxygen is sufficient supply in reaction the partial oxidation can be occurred via

$$C_3H_8O_3 + 1.5O_2 \rightleftarrows 4H_2 + 3CO_2 \ (\Delta H_r^{298K} = -597.73 kJ/mol) \quad (2.9)$$

Other reactions can be described as shown below;

Glycerol dehydrogenation to glyceraldehyde

$$C_3H_8O_3 \rightleftarrows C_3H_6O_3 + H_2 \quad (\Delta H_r^{298K} = -38.64 kJ/mol) \tag{2.10}$$

Glycerol dehydration

Glycerol can dehydrate to hydroxyacetone.

$$C_3H_8O_3 \rightleftarrows C_3H_6O_2 + H_2O \quad (\Delta H_r^{298K} = -24.9 kJ/mol) \tag{2.11}$$

Hydroxyacetone can dehydrate to acrolein.

$$C_3H_6O_2 \rightleftarrows C_3H_4O + H_2O \tag{2.12}$$

Glyceraldehyde can dehydrate to 2-oxopropanal.

$$C_3H_6O_3 \rightleftarrows C_3H_4O_2 + H_2O \tag{2.13}$$

2-Oxopropanal decomposition to acetaldehyde

$$C_3H_4O_2 \rightleftarrows CH_3CHO + CO \tag{2.14}$$

Acetaldehyde decomposition to methane

$$CH_3CHO \rightleftarrows CH_4 + CO \tag{2.15}$$

จุฬาลงกรณ์มหาวิทยาลัย
CHULALONGKORN UNIVERSITY

Glycerol partial oxidation on Pt catalyst

$$C_3H_8O_3 \rightleftarrows C_2H_4 + 2H_2O + CO \tag{2.16}$$

Water-gas shift

$$CO + H_2O \rightleftarrows CO_2 + H_2 \quad (\Delta H_r^{298K} = -41 kJ/mol) \tag{2.2}$$

Methanation

$$CO + 3H_2 \rightleftarrows CH_4 + H_2O \quad (\Delta H_r^{298K} = -165 kJ/mol) \tag{2.4}$$

$$CO_2 + 4H_2 \rightleftarrows CH_4 + 2H_2O \quad (\Delta H_r^{298K} = -165 kJ/mol) \tag{2.5}$$

Coke formation

Ethylene decomposition

$$C_2H_4 \rightleftarrows \text{Polymers} \rightleftarrows 2C + 2H_2 \quad (2.17)$$

Methane decomposition

$$CH_4 \rightleftarrows C + 2H_2 \quad (2.18)$$

Boudouard reaction

$$CO \rightleftarrows 0.5C + 0.5CO_2 \quad (2.19)$$

Carbon monoxide and carbon dioxide reduction

$$CO + H_2 \rightleftarrows C + H_2O \quad (2.20)$$

$$CO_2 + 2H_2 \rightleftarrows C + 2H_2O \quad (2.21)$$

Hydrogen and oxygen oxidation

$$O_2 + 2H_2 \rightleftarrows 2H_2O \quad (2.22)$$

$$CO + 0.5O_2 \rightleftarrows CO_2 \quad (2.23)$$

Hydrogen production can be obtained from various reactions with the different reaction pathways. Thus, the sufficient oxygen supply in partial oxidation of glycerol is direct effect to amount of hydrogen at maximum yield and minimized glycerol decomposition and dehydration [17].

2.5.4 Glycerol reforming via autothermal reforming (ATR)

Principle of glycerol reforming via autothermal reforming is combined steam reforming and partial oxidation reaction which occurs simultaneously. The steam reforming is naturally endothermic reaction, while partial oxidation is naturally exothermic reaction. Thus, autothermal reforming reactions are provided self-energy in reaction which could not require the external energy consumption. The possible glycerol reforming via autothermal reforming including side reactions are following;

Glycerol stream reforming

$$C_3H_8O_3 + 3H_2O \rightleftarrows 3CO_2 + 7H_2 \quad (\Delta H_r^{298K} = 128\,kJ/mol) \qquad (2.3)$$

Glycerol oxidation

$$C_3H_8O_3 + 0.5O_2 \rightleftarrows 4H_2 + CO_2 + 2CO \quad (\Delta H_r^{298K} = -31.79\,kJ/mol) \qquad (2.8)$$

$$C_3H_8O_3 + O_2 \rightleftarrows 4H_2 + 2CO_2 + CO \quad (\Delta H_r^{298K} = -314.76\,kJ/mol) \qquad (2.24)$$

$$C_3H_8O_3 + 1.5O_2 \rightleftarrows 4H_2 + 3CO_2 \quad (\Delta H_r^{298K} = -597.73\,kJ/mol) \qquad (2.9)$$

$$C_3H_8O_3 + 3.5O_2 \rightleftarrows 4H_2O + 3CO_2 \quad (\Delta H_r^{298K} = -1564.93\,kJ/mol) \qquad (2.7)$$

Water-gas shift

$$CO(g) + H_2O \rightleftarrows CO_2 + H_2 \quad (\Delta H_r^{298K} = -41\,kJ/mol) \qquad (2.2)$$

Methanation

$$CO + 3H_2 \rightleftarrows CH_4 + H_2O \quad (\Delta H_r^{298K} = -206.11\,kJ/mol) \qquad (2.4)$$

$$CO_2 + 4H_2 \rightleftarrows CH_4 + 2H_2O \quad (\Delta H_r^{298K} = -164.94\,kJ/mol) \qquad (2.5)$$

Methane-carbon dioxide reforming

$$CO_2 + CH_4 \rightleftarrows 2H_2 + 2CO \quad (\Delta H_r^{298K} = 247.28\,kJ/mol) \qquad (2.25)$$

Coke formation

$$2CO \rightleftarrows C + CO_2 \quad (\Delta H_r^{298K} = -172.43\,kJ/mol) \qquad (2.26)$$

$$CH_4 \rightleftarrows C + 2H_2 \quad (\Delta H_r^{298K} = 74.85\,kJ/mol) \qquad (2.27)$$

$$CO + H_2 \rightleftarrows C + H_2O \quad (\Delta H_r^{298K} = -131.26\,kJ/mol) \qquad (2.20)$$

The glycerol reforming via auto thermal reforming is combination of glycerol steam reforming and partial oxidation of glycerol. Therefore, the overall reaction can be expressed as following.

$$C_3H_8O_3 + a\left(O_2 + 3.77N_2\right) + bH_2O \rightarrow cH_2 + dCO + eCO_2 + fCH_4 + gH_2O + 3.77aN_2 \quad (2.28)$$

where: $a - g$ are the stoichiometric coefficients depended on the temperature and pressure of reformer, oxygen-glycerol feed ratio and water-glycerol feed ratio [3].

2.5.5 Aqueous-phase glycerol reforming (APR)

Aqueous-phase glycerol reforming is one branch of glycerol reforming process which provides less energy consumption in the reaction. At the condition of APR process can drive a favorable condition of the water-gas shift reaction. The multiple reactors in the general steam reforming process can be replaced by the single-step reactor because hydrogen can be produced with low amounts of carbon monoxide. Furthermore, at APR condition is possible to avoid undesirable decomposition reactions as naturally taking place at the high reaction condition. The main reaction is shown below [18]:

จุฬาลงกรณ์มหาวิทยาลัย
Chulalongkorn University

Aqueous-phase glycerol reforming reaction

$$C_3H_8O_3(l) + 3H_2O(l) \xrightleftharpoons{r_{ref}} 3CO_2(g) + 7H_2(g) \quad (2.29)$$

2.5.6 Glycerol dry reforming (GDR)

Glycerol dry reforming process is an alternative reaction to convert carbon dioxide to hydrogen gas as a valuable product. The possible reactions of glycerol dry reforming and their side reactions are shown below [19, 20]

Dry reforming of glycerol

$$C_3H_8O_3 + CO_2 \rightleftharpoons 4CO + 3H_2 + H_2O \quad (2.30)$$

Glycerol decomposition

$$C_3H_8O_3 \rightleftarrows 3CO + 4H_2 \left(\Delta H_r^{298K} = 251 kJ/mol\right) \quad (2.1)$$

Water-gas shift

$$CO(g) + H_2O \rightleftarrows CO_2 + H_2 \left(\Delta H_r^{298K} = -41 kJ/mol\right) \quad (2.2)$$

Methanation

$$CO + 3H_2 \rightleftarrows CH_4 + H_2O \left(\Delta H_r^{298K} = -206.11 kJ/mol\right) \quad (2.4)$$

$$CO_2 + 4H_2 \rightleftarrows CH_4 + 2H_2O \left(\Delta H_r^{298K} = -164.94 kJ/mol\right) \quad (2.5)$$

$$2CO + 2H_2 \rightleftarrows CH_4 + CO_2 \quad (2.31)$$

Coke formation and carbon gasification

$$2CO \rightleftarrows C + CO_2 \left(\Delta H_r^{298K} = -172.43 kJ/mol\right) \quad (2.26)$$

$$CH_4 \rightleftarrows C + 2H_2 \left(\Delta H_r^{298K} = 74.85 kJ/mol\right) \quad (2.32)$$

$$C + H_2O \rightleftarrows CO + H_2 \left(\Delta H_r^{298K} = -131.26 kJ/mol\right) \quad (2.33)$$

$$C + 2H_2O \rightleftarrows CO_2 + 2H_2 \quad (2.34)$$

2.6 Hydrotreating of vegetable oil

Bio-hydrogenated diesel (BHD), also known as green diesel, is an alternative renewable energy which can be derived from biomass such as vegetable oils and their fatty acids. The molecular structure of BHD has similar with fossil diesel [21]. Although the reaction pathway has not been completely understood, the main hydrotreating reaction of vegetable oil is following through reaction steps by step 1: unsaturated triglycerides are converted to saturated triglycerides via hydrogenation reaction, step 2: saturated triglycerides are converted to free fatty acids via hydrogenolysis, step 3: free fatty acids are converted to green diesel via the three

pathways of hydrodeoxygenation (HDO), decarbonylation (DCO), or decarboxylation (DCO_2) and end at step 4: the isomerization or cracking take place as shown in Figure 2.6 [22].

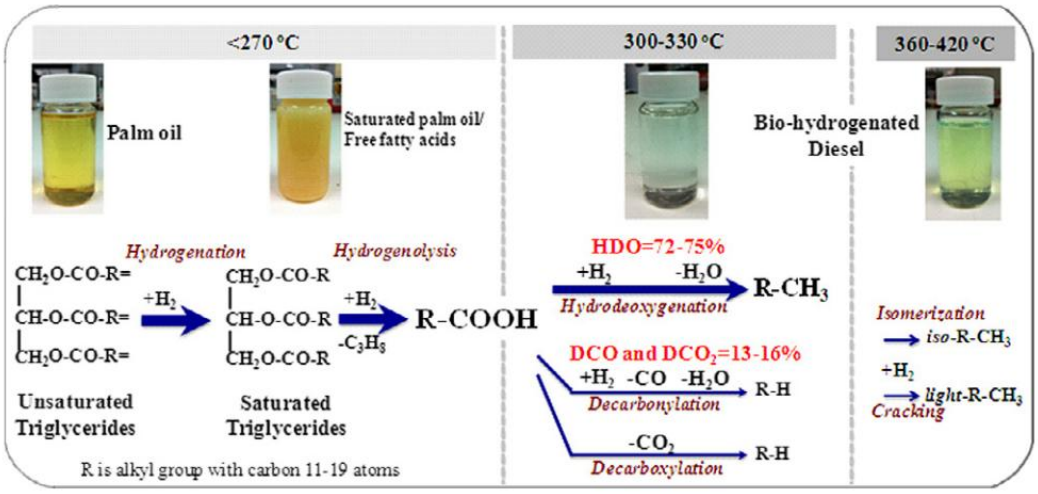

Figure 2.6 Reaction pathway for conversion of vegetable oil [22].

จุฬาลงกรณ์มหาวิทยาลัย
Chulalongkorn University

CHAPTER III LITERATURE REVIEWS

In this chapter, literature reviews are divided into three parts. Firstly, a reviews of biodiesel production processes, secondly, a reviews of glycerol reforming processes and finally, a reviews of hydrotreating of vegetable oils were presented.

3.1 Biodiesel production

In 1853, E. Duffy and Patrick studied glycerol production via transesterification of vegetable oil which biodiesel was obtained as a by-product. After that, Rudolph Diesel, who was a German inventor and mechanical engineer invented the first diesel engine. Owning to the energy crisis, biodiesel was also recommended as fuel in the diesel engine.

At the present, biodiesel plant have widely installed in many zones in the world such as North America, Latin America and Europe. For example, the biodiesel magazine has reported 145 of biodiesel plants using various feedstocks in USA with 2,601.15 MMgy (million gallons per year) of total biodiesel capacities. In additional, 16 plants of biodiesel have under constructed and 4 plants of biodiesel have under proposed [27]. The biodiesel plant using only soybean as oil feedstock in USA are given in Table 3.1.

In generally, biodiesel production can be classified into four processes, including the conventional homogeneous catalytic process, heterogeneous catalytic process, enzymatic catalytic process and supercritical methanol process as concluded in Table 3.2 – 3.5 and Figure 3.1.

Chulalongkorn University

Table 3.1 Biodiesel plant using only soybean as oil feedstock in USA [27].

Name	City	State	Capacity per year	
			MMgy	Tonnes
AC&S Inc.	Nitro	West Virginia	3	9,993.46
Ag Processing Inc. - Algona	Algona	Iowa	60	199,869.10
Ag Processing Inc. - Sergeant Bluff	Sergeant Bluff	Iowa	30	99,934.56
Ag Processing Inc. - St. Joseph	St. Joseph	Missouri	30	99,934.56
Ag Solutions Inc.	Gladstone	Michigan	5	16,655.76
Cargill Inc. - Iowa Falls	Iowa Falls	Iowa	56	186,544.50
Cincinnati Renewable Fuels LLC	Cincinnati	Ohio	60	199,869.10
Deerfield Energy LLC	Deerfield	Missouri	30	99,934.56
Delta American Fuel LLC	Helena	Arkansas	40	133,246.08
Elevance Natchez Inc.	Natchez	Mississippi	80	266,492.16
Incobrasa Industries Ltd.	Gilman	Illinois	32	106,596.86
JNS Biofuels	New Albany	Mississippi	7.5	24,983.64
Louis Dreyfus Agricultural Industries LLC	Claypool	Indiana	90	299,803.68
Mid-America Biofuels	Mexico	Missouri	50	166,557.60
Minnesota Soybean Processors	Brewster	Minnesota	30	99,934.56
Owensboro Grain Biodiesel LLC	Owensboro	Kentucky	45	149,901.84
Paseo-Cargill Energy LLC	Kansas City	Missouri	56	186,544.51
Peach State Labs Inc.	Rome	Georgia	10	33,311.52
Seminole Biodiesel	Bainbridge	Georgia	5	16,655.76
Stepan Co. - Joliet	Joliet	Illinois	21	69,954.19
W2 Fuel - Crawfordsville	Crawfordsville	Iowa	10	33,311.52
Total Number of Plants: 21		**Total Existing Capacity**	**750.5**	**2,500,029.58**

Table 3.2 Example of homogeneous catalytic biodiesel production using different oil feedstocks.

Feedstocks	Catalyst	Optimum reaction condition	Yield (wt%)	Ref.
Soybean oil	CH_3ONa	Cat conc. = 0.5, MeOH/Oil = 10:1, T = 348 K, t = 0.5 h	94	[23]
Waste tallow (chicken)	H_2SO_4	Cat conc. = 1.25, MeOH/Oil = 30:1, T = 323 K, t = 24 h	~99.01	[24]
Palm fatty acid	H_2SO_4	Cat conc. = -, MeOH/Oil = 7.2:1, T = 343 K, t = 2 h	99.6	[25]
Sunflower oil	KOH	Cat conc. = 0.55, MeOH/Oil = -, T = 343 K, t = -	96	[26]
Jojoba oil-wax	CH_3ONa	Cat conc. = 1, MeOH/Oil = 7.5:1, T = 333 K, t = 4 h	55	[27]
Brassica carinata	KOH	Cat conc. = -, MeOH/Oil = -, T = -, t = -	98.27	[28]
Canola oil	KOH	Cat conc. = 0.5, MeOH/Oil = 6:1 , T = 298 K, t = 0.33 h	86.1	[29]
Jatropha curcas	KOH	Cat conc. = -, MeOH/Oil = - , T = 303 K, t = 1 h	92	[30]
Cottonseed oils	NaOH	Cat conc. = 0.5, MeOH/Oil = - , T = 328 K, t = 1 h	77	[31]
Roselle oil	KOH	Cat conc. = 1.5, MeOH/Oil = 8:1 , T = 333 K, t = 1 h	99.4	[32]
Rubber seed oil	NaOH	Cat conc. = 1, MeOH/Oil = 6:1 , T = 333 K, t = 1 h	84.46	[33]
Mahua oil	NaOH	Cat conc. = 1, MeOH/Oil = 6:1 , T = 333 K, t = 2 h	92	[34]
Mahua oil	H_2SO_4/KOH	Cat conc. = 1/0.7, MeOH/Oil = 6:1 , T = 333 K, t = 1 h	98	[35]
Sunflower frying oil	KOH	Cat conc. = 1, MeOH/Oil = 6:1 , T = 298 K, t = 0.5 h	100	[36]
Tobacco seed oil	NaOH	Cat conc. = 1.5, MeOH/Oil = 3:1 , T = 328 K, t = 1.5 h	100	[37]
Rice bran oil	H_2SO_4	Cat conc. = 2, MeOH/Oil = - , T = 373 K, t = 8 h	98	[38]
Used frying oil	KOH	Cat conc. = 1, MeOH/Oil = 12:1 , T = 333 K, t = 2 h	72.5	[39]
Jatropha oil	H_2SO_4/ KOH	Cat conc. = 0.25-1.5/0.5, MeOH/Oil = 6:1/9:1 , T = 333 K, t = 2 h	90-95	[40]
Karanja oil	KOH	Cat conc. = 0.5, MeOH/Oil = 9:1 , T = 323±5 K, t = 2 h	80	[40]

Table 3.3 Example of heterogeneous catalytic biodiesel production using soybean oil.

Catalyst	Optimum reaction condition	Yield (wt%)	Ref.
ZnO loaded with $Sr(NO_3)_2$	Cat. = 5 wt%, MeOH/Oil = 12:1, T = 338 K, t = 4 h	94.7	[41]
Sodium silicate	Cat. = 3 wt%, MeOH/Oil = 7.5:1, T = 333 K, t = 1 h	~100	[42]
KF/ɤ-Al_2O_3	Cat. = 3.5 wt%, MeOH/Oil = 12:1, T = 338 K, t = 1 h, Frequency 53.3 W/dm^3	98.7	[43]
Li/MgO	Cat. = 9 wt%, MeOH/Oil = 12:1, T = 333 K, t = 2 h	93.9	[44]
KI/Mg-Al mixed-metal oxides	Cat. = 5 wt%, MeOH/Oil = 20:1, T = 343 K, t = 8 h	>90	[45]
Mg-Al hydrotalcite	Cat. = 5 wt%, MeOH/Oil = 13:1, T = 503 K, t = 1 h	90[a]	[46]
CaO/mesoporous silica	Cat. = 5 wt%, MeOH/Oil = 16:1, T = 333 K, t = 8 h	95.2[a]	[47]
Phosphazenium hydroxide/SiO_2	Cat. = 3.8 wt%, MeOH/Oil = 60:1, T = 348 K, t = 12 h	90[a]	[48]
$VOPO_4.2H_2O$ mixed oxide	Cat. = 2 wt%, MeOH/Oil = 1:1, T = 423 K, t = 1 h	80	[49]
$Al_2O_3/ZrO_2/WO_3$ mixed oxide	Cat. = 4 g, MeOH/Oil = 4.5:1, T = 473 K, t = 20 h	100[a]	[50]
H^+ ion exchanged ZSM-5	Cat. = 0.5 wt%, MeOH/Oil = 5:1, T = 333 K, t = 1 h	80	[51]
Mordenite zeolite	Cat. = 0.5 wt%, MeOH/Oil = 5:1, T = 333 K, t = 1 h	80	[51]
H-type faujasite zeolites	Cat. = 0.5 wt%, MeOH/Oil = 5:1, T = 333 K, t = 1 h	75	[51]
Sulfonated carbon composite	Cat. = 2 wt%, MeOH/Oil = 6:1, T = 333 K, t = 1 h	21.3[a]	[52]
CaO	Cat. = 25 wt%, MeOH/Oil = -, T = - K, t = 1 h	93	[53]
ETS-10 zeolite	Cat. = 0.03 wt%, MeOH/Oil = -, T = 398 K, t = 24 h	90	[54]
Na/NaOH/ɤ-Al_2O_3	Cat. = 1 wt%, MeOH/Oil = 9:1 -, T = 333 K, t = 2 h	96	[55]

Table 3.4 Example of biodiesel production via supercritical condition using different reactants.

Feedstock/solvent	Optimum reaction condition	Products	Yield (wt%)	Ref
Rapeseed oil/ Dimethyl carbonate	Solvent/Oil = 42:1, P=20 MPa, T= 623 K, t = 0.25 h	FAME, Glycerol carbonate, Citramalic acid	94	[56]
Rapeseed oil/ Dimethyl carbonate	Solvent/Oil = 42:1, P=20 MPa, T= 573 K, t = 2/6 h	FAME, Glycerol carbonate, Citramalic acid	97.4	[57]
Palm oil/ Dimethyl carbonate	Solvent/Oil = 29:1, P= - MPa, T= 653 K, t = 0.5 h	FAME, Glycerol carbonate	91	[58]
Rapeseed oil/ Methyl acetate	Solvent/Oil = 42:1, P= 20 MPa, T= 623 K, t = 0.75 h	FAME, Triacetin	97	[59]
Jatropha oil/ Methyl acetate	Solvent/Oil = 42:1, P= 20 MPa, T= 618 K, t = 0.5 h	FAME, Triacetin	100	[60]
Palm oil/ Methyl acetate	Solvent/Oil = 30:1, P= - MPa, T= 663 K, t = 59/60 h	FAME, Triacetin	97.6	[61]
Jatropha oil/ Methyl acetate	Solvent/Oil = 50:1, P= - MPa, T= 673 K, t = 32/60 h	FAME, Triacetin	71.9	[62]
Macauba oil/ Methyl acetate	Solvent/Oil = 50:1, P= 20 MPa, T= 598 K, t = 0.75 h	FAME, Triacetin	83	[63]
Rapeseed oil/ Methanol	Solvent/Oil = 42:1, P= 45 MPa, T= 623 K, t = 4/60 h	FAME, Glycerol	>95[b]	[64]
Soybean oil/ Methanol	Solvent/Oil = 33:1, P= - MPa, T= 593 K, t = 1/6 h	FAME, Glycerol	95[b]	[65]
Sunflower oil/ Methanol	Solvent/Oil = 40:1, P= 20 MPa, T= 673 K, t = 0.5 h	FAME, Glycerol	97[a]	[66]
Sunflower oil/ Methanol	Solvent/Oil = 42:1, P= 20 MPa, T= 623 K, t = 0.5 h	FAME, Glycerol	95[b]	[67]

Table 3.5 Example of lipase-catalyzed biodiesel production using soybean oils.

Enzyme	Solvent	Operating condition	Yield (wt%)	Ref.
Novozym 435	Not specified	Acyl acceptor = Methyl acetate, T= 313 K, t = 14 h	92	[68]
IM *P. cepacia lipase*	Water	Acyl acceptor = Methanol/Ethanol, T= 308 K, t = 1 h	67/65	[69]
Novozym 435	Not specified	Acyl acceptor = Methanol , T= 303 K, t = 3.5 h	97	[70]
IM *R. oryzae lipase*	Not specified	Acyl acceptor = Methanol , T= RT[c], t = - h	90	[71]
Lipozyme TL IM	Not specified	Acyl acceptor = Methanol , T= 313 K, t = 12 h	98	[72]
Recombinant *LipB68 P. fluorescens lipase*	Not specified	Acyl acceptor = Methanol , T= 293 K, t = 12 h	92	[73]
Lipozyme IM-77	n-Hexane	Acyl acceptor = Methanol , T= - K , t = - h	92.2	[74]
P. fluorescens lipase	Not specified	Acyl acceptor = Methanol , T= 308 K, t = 90 h	80	[75]
C. rugosa lipase	Not specified	Acyl acceptor = Methanol , T= 308 K, t = 90 h	80	[75]
P. cepacia lipase	Not specified	Acyl acceptor = Methanol , T= 308 K, t = 90 h	100	[75]
IM *M. miehei lipase*	n-Hexane	Acyl acceptor = Ethanol , T= 308 K, t = 8 h	95.6	[76]
Novozym 435	Not specified	Acyl acceptor = Ethanol , T= 323 K, t = 1.5 h	83.5	[77]

[a] Presented by authors as “conversion” in bibliography.

[b] Presented by authors as “solvent content” in bibliography.

[c] RT Presented by authors as “room temperature” in bibliography.

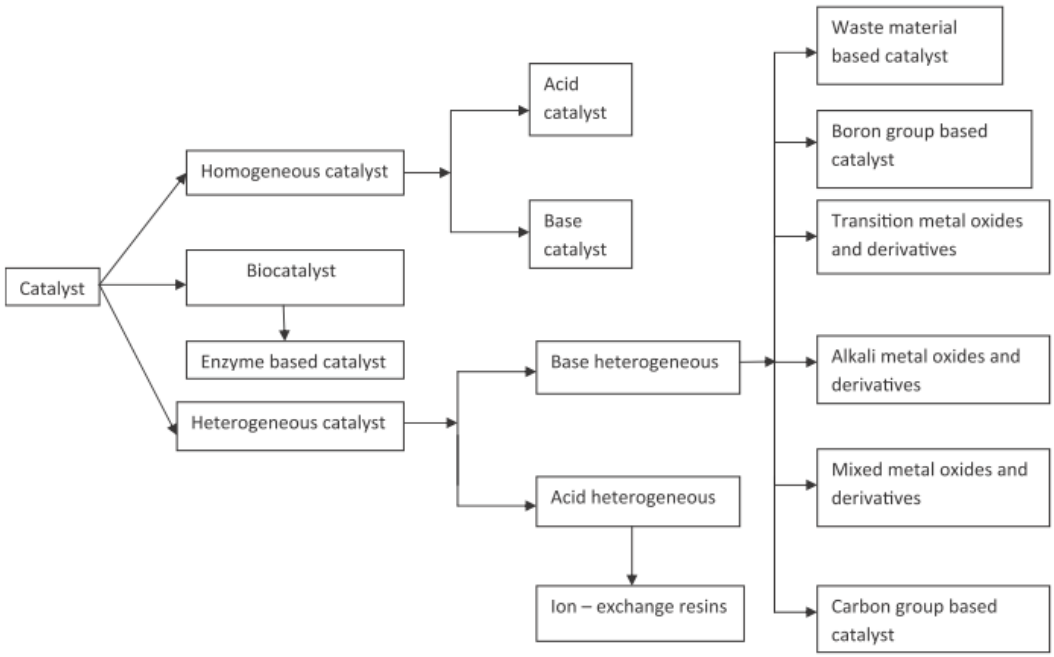

Figure 3.1 Simple chart of biodiesel catalyst classification [78].

The conventional process of biodiesel production using alkali metal as sodium hydroxide or potassium hydroxide have many advantages: (1) alkali catalyst demonstrates high biodiesel yield in a short reaction time; (2) the two phase natural of oil-methanol mixture respect to mass transfer effect, thus homogeneous catalysts have a good point because they can distribute in reaction mixture; (3) NaOH and KOH are cost effective and available in a market; (4) Both batch and continuous stirred tank reactor can be also employed [79]. Rashid et al. [80] showed an optimum condition of 1wt% NaOH, 6 molar ratio of methanol to sunflower oil, 333 K of reaction temperature, 600 rpm of agitation rate, and 2 h of reaction time producing 97.1% of biodiesel yield with acceptance on ASTM D 6751 specifications. Noureddini and Zhu [81] investigated the optimum operation of transesterification of soybean oil with 6 of molar ratio of alcohol to oil and 0.20wt% of NaOH based on soybean oil. They also reported the kinetic of transesterification of soybean oil that is shown below;

$$\text{Triglyceride + Methanol} \underset{k_{-1}}{\overset{k_1}{\rightleftharpoons}} \text{FAME + Diglyceride} \quad (3.1)$$

$$\text{Diglyceride + Methanol} \underset{k_{-2}}{\overset{k_2}{\rightleftharpoons}} \text{FAME + Monoglyceride} \quad (3.2)$$

$$\text{Monoglyceride + Methanol} \underset{k_{-3}}{\overset{k_3}{\rightleftharpoons}} \text{FAME + glyceride} \quad (3.3)$$

The mean compositions of soybean oil are 12 mol% of tripalmitin, 28 mol% of triolein and 60 mol% of trilinolein. The main biodiesel composition are methyl palmitate, methyl oleate and methyl linoleate and the rate expressions are shown as:

$$r_{TG} = -k_1[TG][MeOH]+k_{-1}[DG][FAME] \quad (3.4)$$

$$r_{DG} = k_1[TG][MeOH]-k_{-1}[DG][FAME]-k_2[DG][MeOH]+k_{-2}[FAME][MG] \quad (3.5)$$

$$r_{MG} = k_2[DG][MeOH]-k_{-2}[MG][FAME]-k_3[MG][MeOH]+k_{-3}[FAME][GL] \quad (3.6)$$

$$r_{GL} = k_3[MG][MeOH]-k_{-3}[FAME][GL] \quad (3.7)$$

$$r_{FAME} = k_1[TG][MeOH] + k_2[DG][MeOH] + k_3[MG][MeOH] - k_{-1}[FAME][DG]-k_{-2}[FAME][MG]-k_{-3}[FAME][GL] \quad (3.8)$$

where: TG, DG, MG, GL, MeOH, and FAME represent triglyceride, diglyceride, monoglyceride, glycerol, methanol, and methyl ester and rate constants are shown in Table 3.6

Table 3.6 Kinetic constant for transesterification of soybean oil and methanol using NaOH as base homogeneous catalyst.

Rate constant	**Apparent pre-exponential factor** $\left[\text{L}\cdot\text{mol}^{-1}\cdot\text{s}^{-1}\right]$	**Apparent Activation Energy** $\left[\text{cal}\cdot\text{mol}^{-1}\right]$
k_1	3.9×10^{7}	13,145
k_{-1}	5.78×10^{5}	9,932
k_2	5.906×10^{12}	19,860
k_{-2}	9.888×10^{9}	14,639
k_3	5.335×10^{3}	6,421
k_{-3}	02.1×10^{4}	9,588

In fact, sodium hydroxide is a precursor of sodium methoxide as a true catalyst of biodiesel production which showed at least 98% of oil conversion in 0.5 h even applied 0.5 mol% of sodium methoxide [82-84]. Using sodium hydroxide as a biodiesel catalyst have effective cost but it required less amount of water to prevent a serious problem in a large scale [85]. The presence of water can provide unsatisfied reaction like saponification reaction resulting in a lower activities at the similar condition [86]. Thus, sodium methoxide solution in methanol is an alternative homogeneous for biodiesel production in a large scale.

Acid-catalyzed transesterification is alternative method for biodiesel production because it simultaneously catalyze esterification and transesterification using both free fatty acids and oils [87]. The conventional biodiesel production process in presence of alkali and acid catalysts using the virgin oil and waste cooking oil are simulated by calculation tools such as HYSYS simulation by many researchers. Zhang et al. [88] investigated 8,000 tonnes/year of biodiesel process design and technological assessment of four different biodiesel production involving alkali-catalyzed process using fresh soybean oil, alkali-catalyzed process using waste cooking oil (oleic acid) in oil), acid-catalyzed process using waste cooking oil, and acid-catalyzed process using waste cooking oil with hexane extraction. The results showed the alkali-catalyzed process using fresh oil was the simplest process, because of low unit operations and it was also recommended on a commercial scale. West et al. [89] proposed heterogeneous-catalyzed biodiesel production process using waste cooking oil over SnO with 8000 tonnes/year of biodiesel capacities. They reported biodiesel production using heterogeneous acid catalyzed process had the lowest total capital investment and highest rate of return compared to alkali-catalyzed process, homogeneous acid-catalyzed process, and supercritical methanol process. However, using solid catalyst for both laboratory scale and industrial scale might be deactivated by leaching of methanol, which it offers homogeneous reaction, and agglomeration. Lee and co-workers [90] studied economic analysis of biodiesel production processes using fresh canola oil (triolein) and waste canola oil (oleic acid) and supercritical methanol which the process flow diagram and operating conditions for alkali-catalyzed process and acid-catalyst processes were derived from Zhang et al. [88] and West et al. [89]. Alkali and acid catalytic biodiesel productions proposed by Lee et al. [90] were demonstrated

in the Figure 3.2 – 3.5. In this work, the properties of triolein as triglyceride model in the Hysys simulation is not accuracy. Thus, the data of means boiling point of triolein was obtained from experiment using thermogravimetric analysis (TGA). Non-random two liquid as thermodynamic model was chosen to predict any necessary missing parameters such as binary interaction between components for calculation. Furthermore, Peng-Robinson equation of state was applied when the operating pressure is more than 10 bars. The economic result showed alkali-catalyzed process using vegetable oil had the lowest total capital investment (by 11.1 million dollars for a 40,000 tons/year) and total energy consumption (2349 kW) comparing with waste cooking oil process and supercritical methanol process in the same of biodiesel capacity. In additional, biodiesel production using waste cooking oil had the highest energy consumption because of spending for two methanol distillations column as methanol recovery particularly a methanol distillation column in Figure 3.3.

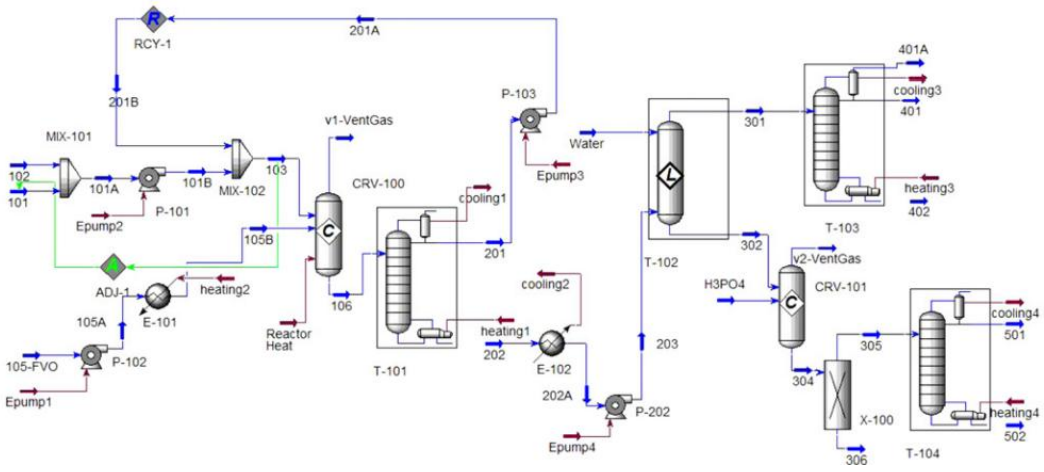

Figure 3.2 Alkali-catalyzed biodiesel process from fresh oils, Lee et al [90].

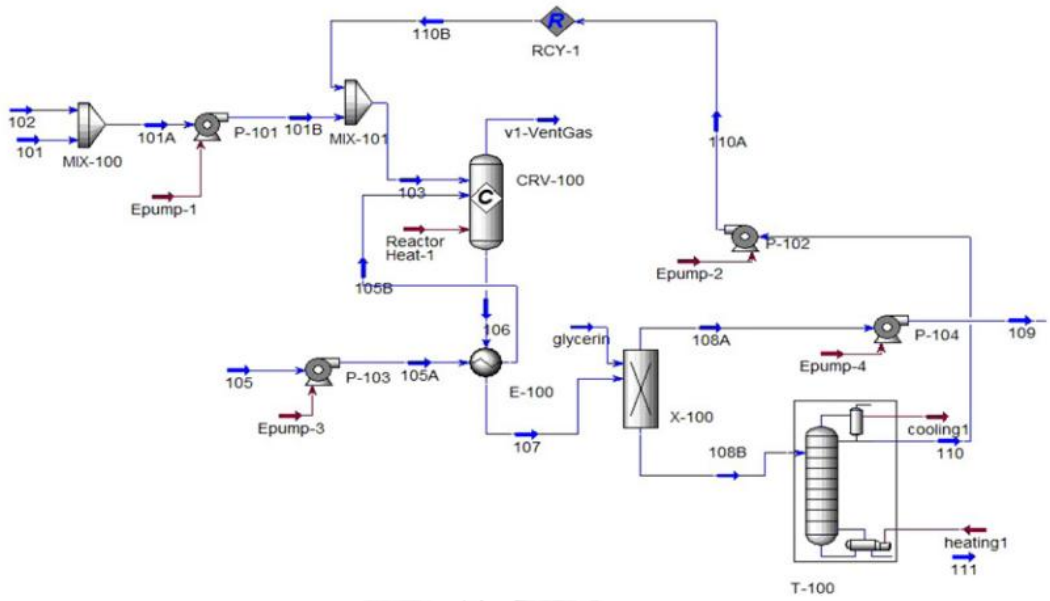

Figure 3.3 Pretreatment acid-catalyzed biodiesel process from waste cooking oils, Lee et al [90].

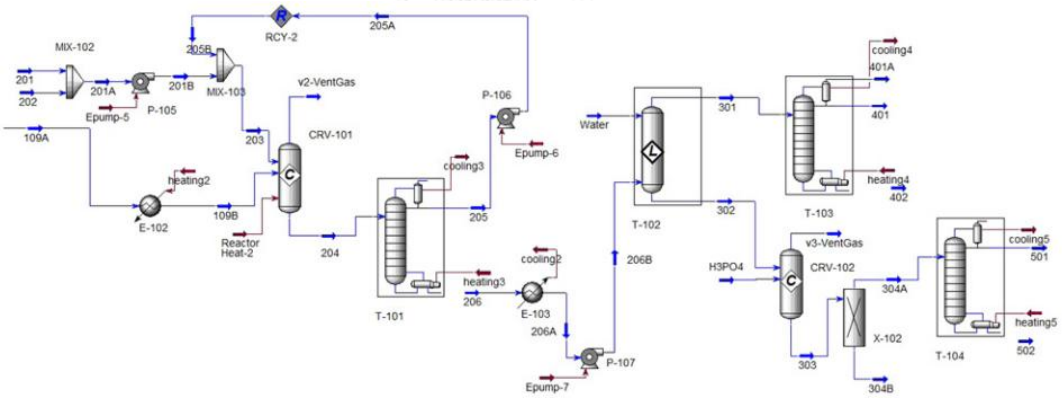

Figure 3.4 After pretreatment of alkali biodiesel process from waste cooking oils proposed by Lee et al [90].

In summary, the simple diagram for conventional biodiesel production with high free fatty acid contents in feedstocks is shown in Figure 3.5.

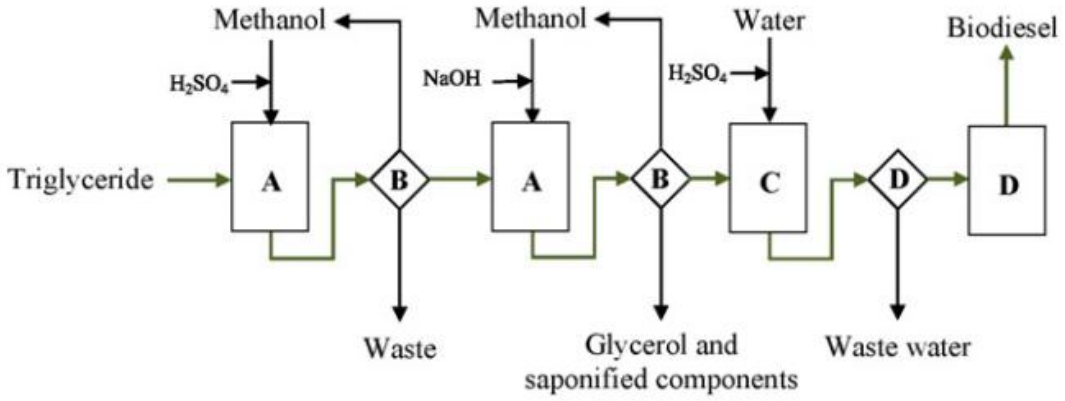

Figure 3.5 Two step of conventional biodiesel production with high free fatty acid contents in feedstock: (A) reactor, (B) product separation and methanol recovery unit, (C) water washing unit, (D) separation unit and (E) biodiesel drying unit [91].

3.2 Hydrogen production process using glycerol

Glycerol is an alternative biomass for hydrogen production. Glycerol is a key by-product of biodiesel production via transesterification of fats and oils which obtained from a various plants, animals and waste cooking oils. Glycerol can be converted to hydrogen via a difference processes as Glycerol stream reforming (GSM), Glycerol reforming via supercritical water (GSW), Partial oxidation of glycerol (POG), Autothermal glycerol reforming (GATR), Aqueous-phase glycerol reforming (AGPR) and Glycerol dry reforming (GDR) [14, 16, 19, 20, 92, 93]. Glycerol reforming processes have been intensively studied by many researcher by many fields such as the performance of catalysts [94-104], kinetic and thermodynamic analyses [5, 94, 104, 105], multifunctional reactor [106], and process simulations which the example of proposed processes are given in Figure 3.6 [107] and 3.7 [108]. Various hydrogen production via glycerol reforming as reported in the literature are summarized in Table 3.7.

Glycerol steam reforming process have been more attractive by many researchers because this process is similar to the conventional steam reforming process

comparing with others glycerol reforming process. The amounts of hydrogen are depended on the temperature of reformer because both glycerol decomposition and reverse water-gas shift reaction are naturally endothermic reaction providing a high temperature. The main products are commonly hydrogen, carbon monoxide and carbon dioxide. Although, hydrogen can obtain at low temperature via water-gas shift reaction, the undesirable products such as methane was occurred from methanation due to this reaction favors at low temperature. The catalysts are also necessary for GRM process because the high temperature does not suitable condition in term of economy and hydrogen selectivity [14].

จุฬาลงกรณ์มหาวิทยาลัย
Chulalongkorn University

Table 3.7 Main advantages and disadvantages of different glycerol reforming types.

Glycerol reforming types	Advantages	Disadvantages
Glycerol steam reforming (GSR)	• Higher efficiency and product quality such as higher hydrogen yield. • Lower side reactions.	• Energy is extremely required in glycerol steam reforming because of its naturally endothermic reaction. The total cost may be increased at high operating conditions. • High water to glycerol feed ratio (WGFR)
Glycerol reforming via supercritical water (GSW)	• The decomposition of biomass in sub- and supercritical water is faster than other water state. • Tar and coke formation are inhibited by intermediate of supercritical water. • Hydrogen is possible to directly store without compression.	• High reaction conditions including of high pressure system (>20 MPa) comparing with the conventional steam reforming (0.2-0.3 MPa) • The high cost of suitable materials is a weak points because equipment such as reactor structure, pipeline are also required mechanical strength to ensure safety in aggressive pressure.
Glycerol reforming via autothermal reforming (GATR)	• The autothermal reforming process decrease energy consumption, because the thermal energy required is generated by the partial oxidation of glycerol that this process consumes the thermal energy its producing.	• The H_2 and O_2 gases may offer the explosive mixture which the upper explosive limit of H_2-O_2 mixture at 1 bar is 0.952 of H_2 mol fraction in O_2.

Table 3.7 Main advantages and disadvantages of different glycerol reforming types *(continued).*

Glycerol reforming types	Advantages	Disadvantages
Aqueous-phase glycerol reforming (APGR)	• APGR can be operated in single reactor at mild temperature around 500 K. • Water is unnecessary to vaporize as a steam resulting to the energy saving occurs in this process. • APGR process promote the hydrogen production because as water-gas shift reaction thermodynamically favors toward low temperature and very low CO concentration in product stream.	• APGR is necessary operated at high operating pressure comparing with the conventional hydrogen production. • Glycerol conversion is very low comparing with other hydrogen production of glycerol processes. • APGR requires long contact time (>4 h), while others hydrogen production processes require a short contact time (ms).
Glycerol dry reforming (GDR)	• This process can provide CO_2 close loop by converted CO_2, which derived from cement industry as well as the large amounts of glycerol from biodiesel production, to H_2 and CO (syngas)	• This process provides the highest coke comparing to the other hydrogen production of glycerol processes which the large of coke deposition can be explained by the converting of CO_2 reactant to undesirable reaction as coke formation. • Catalyst contributes to a short cycle life and subsequent deactivation.

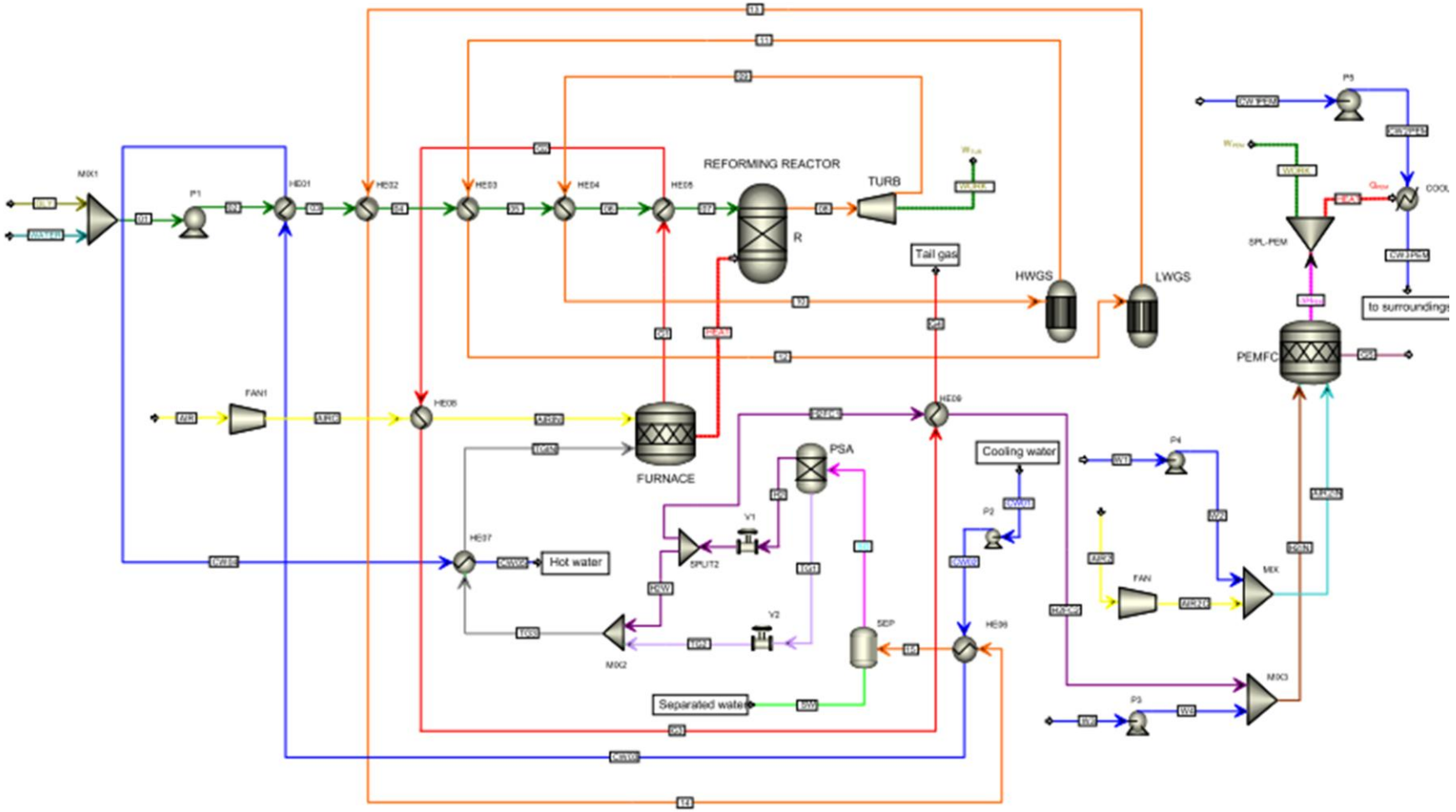

Figure 3.6 Heat-integrated flow-sheet for production of hydrogen and electrical power via supercritical water reforming of glycerol [55].

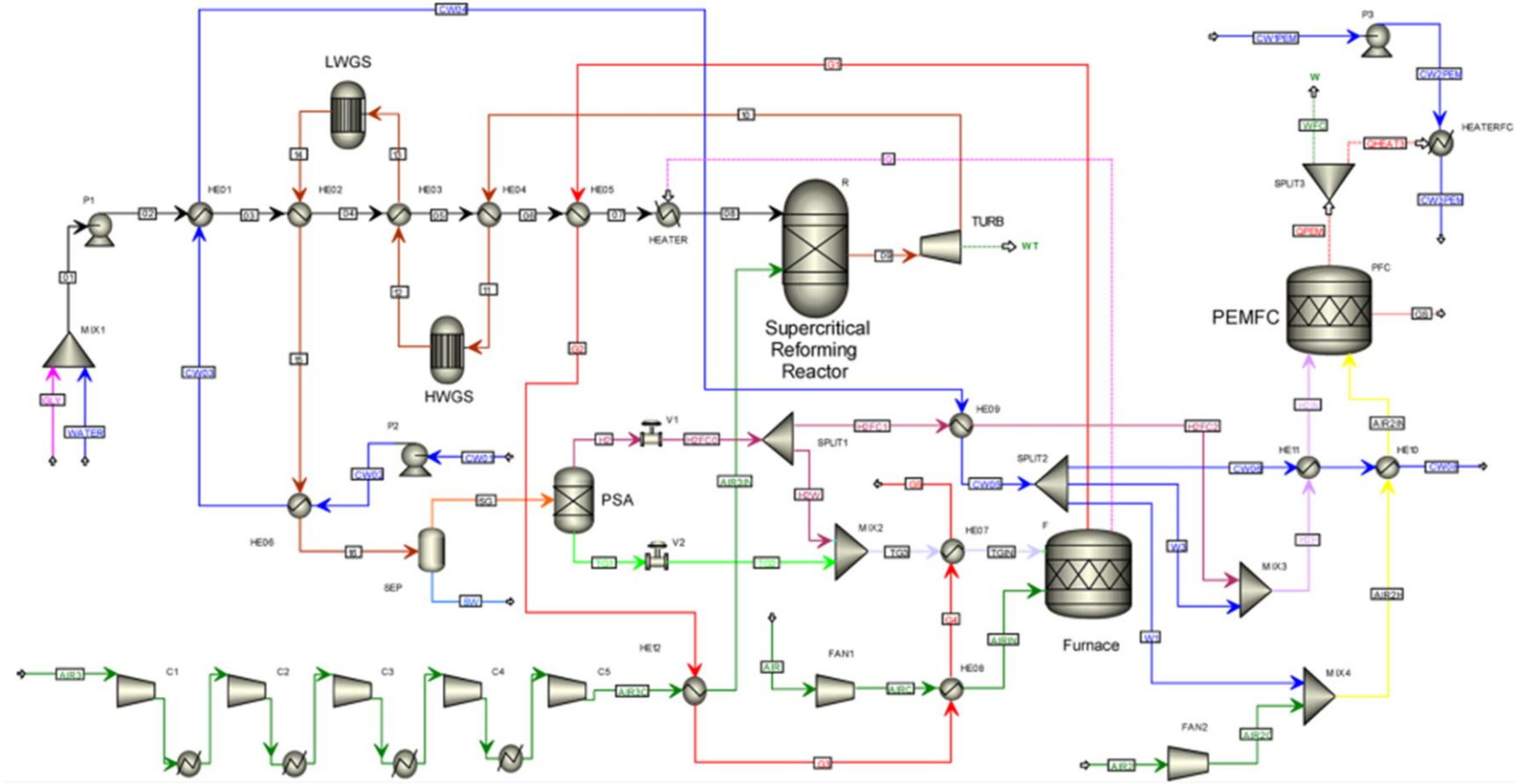

Figure 3.7 Heat-integrated flow-sheet for producing hydrogen and electrical power ATR via supercritical water reforming of glycerol [56].

Wang et al. [104] investigated thermodynamic of glycerol steam reforming and kinetics analysis of Ni-Mg-Al catalysts at different ratios of Ni, Mg and Al compositions in a fixed bed reactor under atmospheric pressure and temperature range of 723-923 K. They reported the influence temperature against glycerol conversion and products as given in Figure 3.8. In additional, the optimal steam to carbon ratio (S/C) is 3 to 4.5 and the hydrogen yield as shown in Figure 3.9.

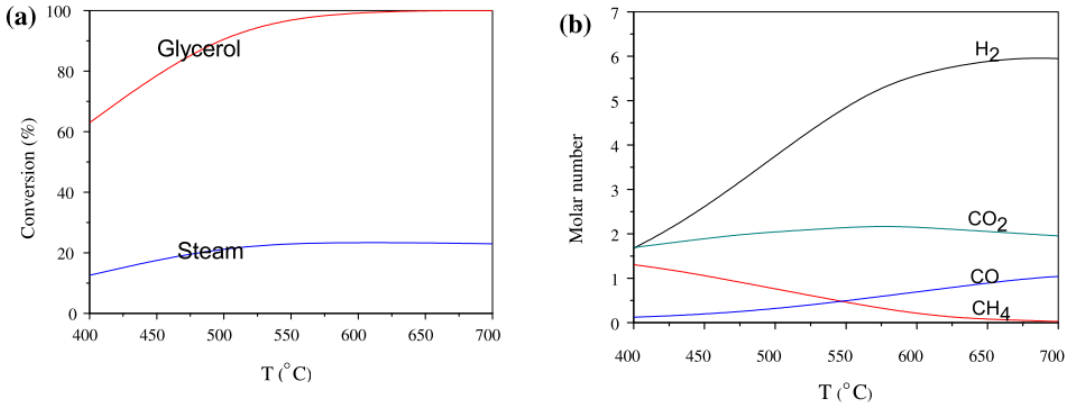

Figure 3.8 Influence of temperature against glycerol conversion (a) and products (b) [104].

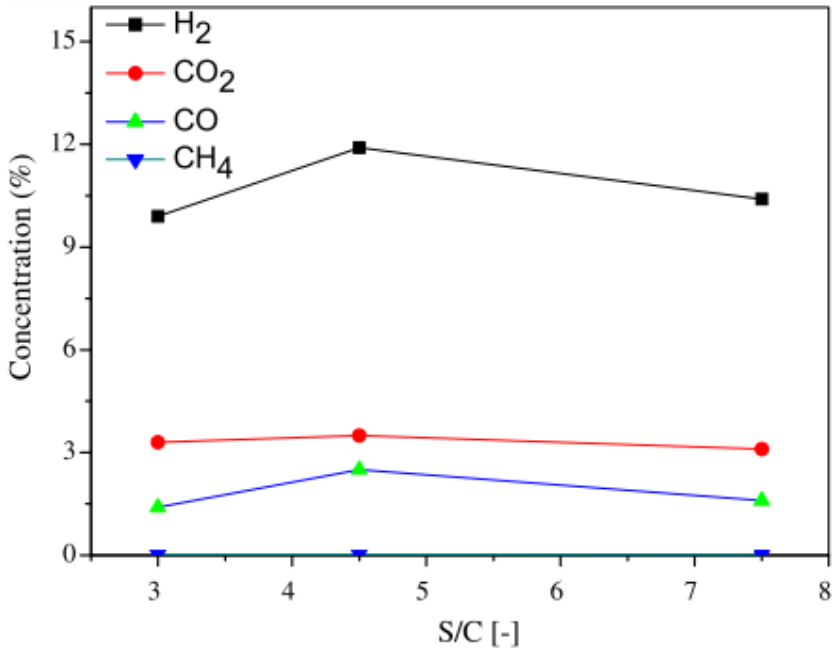

Figure 3.9 Influence of S/C against products distribution in GRM [104].

Effect of water concentration against reaction may be neglected since the value of steam to carbon ratio is 3 while the stoichiometric ratio of GRM is only 1. Thus, the

pseudo-first order with respect to glycerol can be applied to express as the rate equation. Furthermore the pseudo-first order kinetic model for rate expression was applied because it is widely permitted to compare data from different sources on the catalyst activities in complex steam reforming reaction such as methanol or ethanol steam reforming.

Pseudo-first order kinetic model

$$C_3H_8O_3 + 3H_2O \rightleftarrows 3CO_2 + 7H_2 \quad (3.9)$$

$$r_{H_2} = k' \left[C_3H_8O_3\right] \quad (3.10)$$

The values of the apparent reaction rate for pseudo first order kinetic model of three Ni-Mg-Al catalysts are given in Table 3.8

Table 3.8 Kinetic parameters for GRM using three Ni-Mg-Al catalysts at 673-873 K.

Catalyst x^aNi-y^bMg-z^cAl	**Apparent pre-exponential factor** $\left[\text{mol min}^{-1}\text{ g}^{-1}\text{cat.}\right]$	**Apparent Activation Energy** $\left[\text{kJ/mol}\right]$
0.451Ni-0.241Mg-0.308Al	5.7×10^5	131.6
0.344Ni-0.185Mg-0.471Al	2.18×10^2	74.6
0.241Ni-0.261Mg-0.498Al	4.12	37.8

x^a, y^b, z^c = mass fraction of NiO, MgO, and Al_2O_3, respectively

Hajjaji et al. [5] investigated the optimal conditions of GRM that maximizing the hydrogen production with the minimizing the methane and carbon monoxide contents and coke formation. The best operating condition for GRM process can be achieved using the water to glycerol feed ratio (WGFR) equal to 9 or the ratio of steam to carbon feed equal to 3, at reformer temperature of 950 K and atmospheric pressure.

Hydrogen production as a function of WGFR and reformer temperature is given in Figure 3.10.

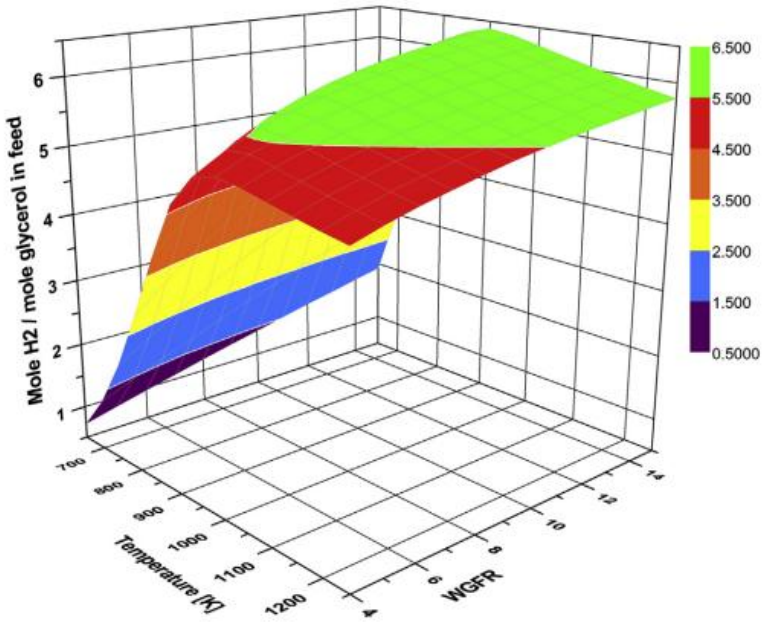

Figure 3.10 Hydrogen production as a function of the WGFR and reformer temperature at 1 atm [5].

Hajjaji et al. [5] demonstrated the conventional hydrogen production system for fuel cell applications and detailed flowchart of the SGR process are shown in Figure 3.11 and 3.12, respectively.

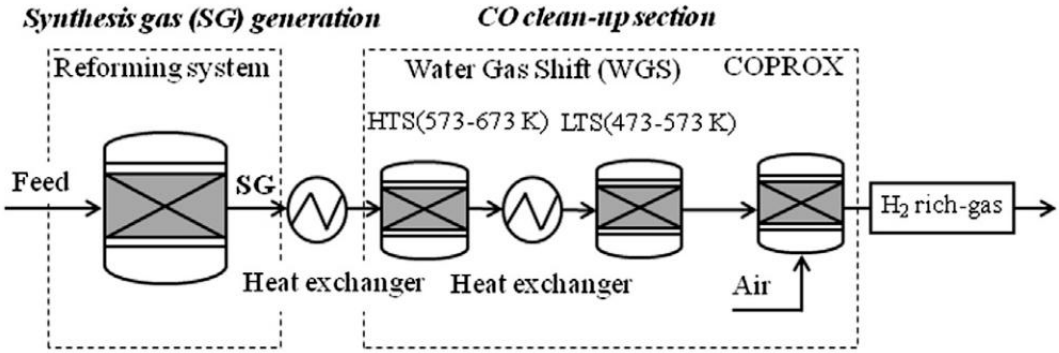

Figure 3.11 Conventional hydrogen production system for fuel cell applications [5].

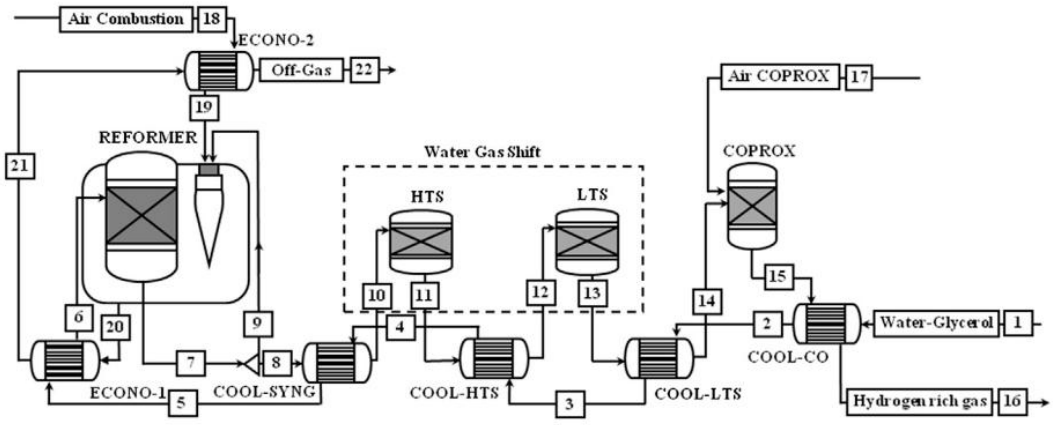

Figure 3.12 Detailed flowchart of the SGR process Label numbers 1-6: Water-Glycerol 7-16: Synthesis gas 17: Air COPROX 18-19: Air Combustion 22: Off-Gas [5].

Adhikari et al. [6] studied the kinetics and reactor modeling using COMSOL software of hydrogen production from GSR over Ni/CeO_2 catalysts at 879-1373 K of temperature range. They reported the kinetic parameters for GSM over Ni/CeO_2 catalyst were 103.4 kJ/mol of apparent activation energy, 8135.5 of rate constant, and 0.233 of reaction order that the kinetic model based on a pseudo-nth order model as:

Pseudo-*n*th order kinetic model

$$C_3H_8O_3 + 3H_2O \rightleftarrows 3CO_2 + 7H_2 \tag{3.11}$$

$$r_{H_2} = k\left[C_3H_8O_3\right]^n \tag{3.12}$$

จุฬาลงกรณ์มหาวิทยาลัย
Chulalongkorn University

In several publications for hydrogen production, sorption enhanced in steam reforming process have been investigated by many researchers. CaO-based sorbent has been shown the efficiency for hydrogen production because this sorbent can shift the equilibrium forward by entraps carbon dioxide generating during water-gas shift reaction and decrease methane production as undesirable by-product via methanation. Fermoso et al. [109] studied the hydrogen purity in GSM in a fixed bed reactor using a mixture of Ni/Co catalyst derived from hydrotalcite-like material (HT) and dolomite ($CaMg(CO_3)_2$) as Ca precursor of CO_2 sorbent. High purity (99.7 vol.%) and high yield (88%) of H_2 can be achieved in one-stage sorption enhanced steam reforming (SESR)

process at atmospheric pressure and at 823-873 K using steam to carbon ratio of 3. In additional, the lowest amounts of methane is 848 K.

Glycerol reforming process as well as other reforming process which has a challenges in order to achieve for the commercial scale. The steam reforming process offers the higher efficiency and product quality such as higher hydrogen yield, lower side reaction rate [17]. However, the main challenges of GSR this process can be written as: (1) many researchers have reported hydrogen limitation which cannot provide hydrogen yield at its upper stoichiometric coefficient; (2) the glycerol reforming is thermodynamically-limited reaction, thus operating conditions affect to glycerol conversion. The catalyst may be required to operate at the lower temperature; (3) the main side reactions of glycerol reforming affect to hydrogen purity and production leading to formation of methane from reaction of carbon monoxide, carbon dioxide and glycerol hydrogenolysis; (4) the catalyst is deactivated by coke during reaction resulting to both product and hydrogen purity in long operation. Thus, the coke formation might be concerned for glycerol steam reforming as well as the other steam reforming reaction; (5) releasing of by-products such as carbon dioxide is concerned in the environmental issue; (6) energy is extremely required in glycerol steam reforming because of its naturally endothermic reaction. Thus, the total cost may be increased at high operating conditions [14]. The proposed combination process can provide extra energy for GSM process using the combustion of syngas from hydrotreating process.

จุฬาลงกรณ์มหาวิทยาลัย
Chulalongkorn University

3.3 Hydrotreating of vegetable oil

Renewable fuels via catalytic hydrodeoxygenation are usually classified in to three generation by Choudhary and Phillips [21]: (1) the conventional processes (e.g. alkali catalyzed-transesterification production) using edible feedstocks (e.g. vegetable oil): (2) the advance processes (e.g. gasification, hydroprocessing, and pyrolysis) using non-edible feedstocks (e.g. waste greases, lignocelluloses, refuse) and (3) the harvesting and advanced processes of ultra-high yield biomass (e.g., algae). The simple flowchart of renewable fuels production from biomass is given Figure 3.13. Both green diesel and green gasoline can be derived from hydrodeoxygenation (HDO) process. The large amounts of triglyceride-based feedstock such as unsaturated vegetable oils (C=C) and their free fatty acids feedstock such as waste cooking oils are available from

agriculture and food industry. Moreover, a few researchers patented hydroprocessing of vegetable oils that mainly produce alkane with complete conversion [[22],114]. There was no simulation result of hydrotreating process due to the complication of reaction pathway.

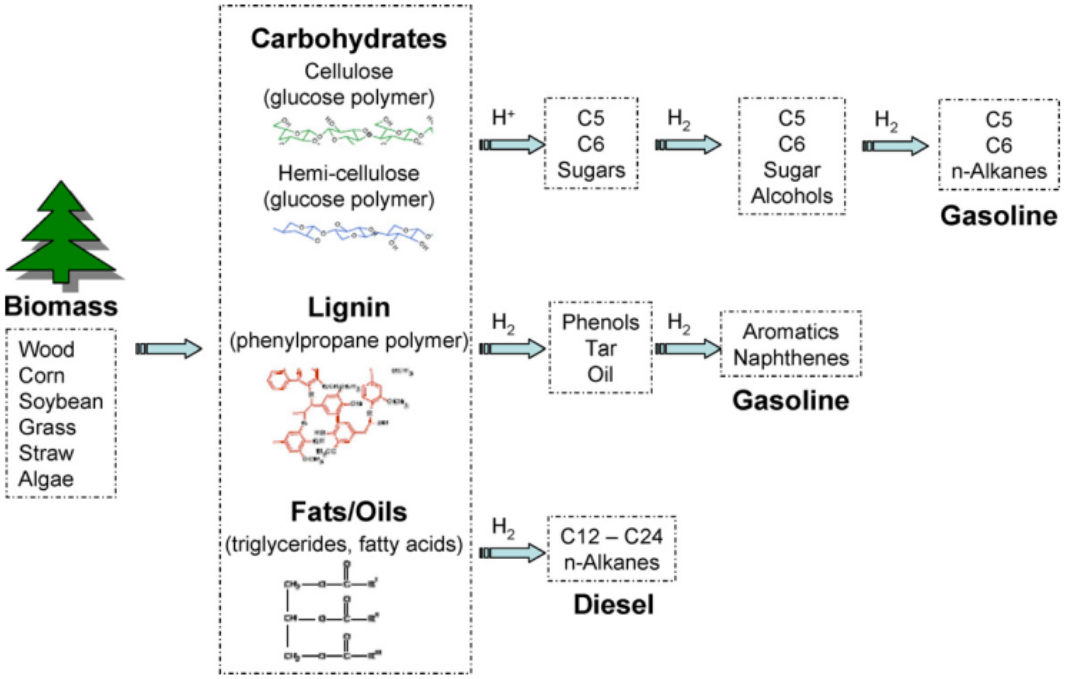

Figure 3.13 Hydrodeoxygenation of the basic building blocks of biomass to renewable hydrocarbon fuels [21].

จุฬาลงกรณ์มหาวิทยาลัย
Chulalongkorn University

The conventional hydrotreating catalyst as $NiMo/Al_2O_3$ have been studied in hydrotreating of vegetable oil and their free fatty acids. Srifa and co-workers [22] used $NiMoS_2$ /ɤ-Al_2O_3 catalyst for catalytic hydrotreating of palm oil. It was found that 90.0% of product yield with n-alkane selectivity more than 95.5% were achieved. Moreover, the result showed the five reaction pathways as hydrodeoxygenation, decarbonylation, decarboxylation, cracking, and isomerization were extensively influenced by reaction temperature. Huber et al. [110] investigated the production of liquid alkanes via hydrotreating process using vegetable oils and vegetable oil–heavy vacuum oil (HVO) mixtures over sulfided $NiMo/Al_2O_3$ as conventional hydrotreating catalysts. It was found that the reaction pathway favors to decarbonylation and decarboxylation with increasing of reaction temperature. Furthermore, the vegetable oil

blending with heavy vacuum oil exhibited increases straight chain alkanes yield which the 0.05 of sunflower oil to HVO feed weight ratio offered the maximum theoretical straight chain yield of C_{15} –C_{18} (87%) than that of pure sunflower oil (75%). Kubicka and Kaluza [111] carried out the hydrodeoxygenation of rapeseed oil over a different catalysts including of Ni, Mo, and NiMo sulfided catalysts in a fixed-bed reactor. They proposed the mechanism of triglyceride in hydrodeoxygenation that the reaction pathways is given in Figure 3.14; (1) the vegetable oil as unsaturated hydrocarbon chains are hydrogenated to saturated oil via hydrogenation reaction; (2) saturated oil can be converted to even carbon atom number of n-alkanes via hydrodeoxygenation;(3) fatty alcohol from hydrogenation is convert to even carbon atom number of n-alkanes; (4) odd carbon atom number of n-alkanes is obtained from hydrodecarboxylation.

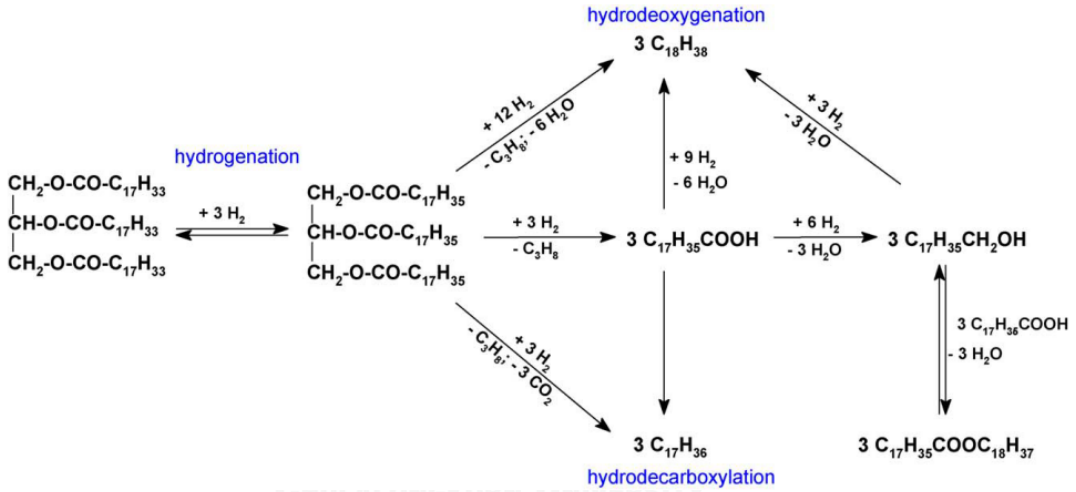

Figure 3.14 Reaction pathways involved in the conversion of triglycerides into hydrocarbons as proposed by Kubicka and Kaluza [111].

The activity of catalyst in this experiment is in the sequent as $NiMo/Al_2O_3$ > Mo/Al_2O_3 > Ni/Al_2O_3. Moreover, Ni/Al_2O_3 is unfavorable to deoxygenation pathway as compared with Mo and NiMo catalysts. In contrast, Mo/Al_2O_3 showed the high selectivity in hydrogenation (hydrodeoxygenation) pathway. Furthermore, the synergetic $NiMo/Al_2O_3$ catalysts is favorable to both hydrogenation and decarboxylation products. Simacek and co-workers [112] synthesized a three different Ni and Mo wt.% supported on alumina catalyst in rapeseed oil hydroprocessing. The result showed C_{17} –C_{18} of n-alkanes and i-alkanes are main components of organic

liquid products (OLP). They reported that free fatty acids and triglycerides were contaminated in OLP. At the high temperature around 583 K, hydrocarbons was content in OLP as well as hydrocarbons in diesel fuel. In summary, $NiMo/Al_2O_3$ sulfided catalyst showed synergetic effect that high hydrocarbons selectivity (at iso-conversion levels). Hydrogenation (Hydrodeoxygenation) and decarboxylation products occur simultaneously over $NiMo/Al_2O_3$. Ni/Al_2O_3 sulfided catalyst was favored for products from the decarboxylation pathway while Mo/Al_2O_3 is selective in hydrogenation (hydrodeoxygenation) pathway. The minor concentration of decarboxylation product was also found [25,116].

Although Ni exhibited poor selectivity in deoxygenation, a few researchers attempted to improve Ni-based catalyst for several methods. The conventional hydrodesulfurization (HDS) catalysts, including sulfided Co–Mo [113], and Ni–Mo supported on alumina for the HDO reaction, are not suitable for low sulfur content feedstock such as bio-crude-oil or biodiesel because the sulfide catalyst is reduced to metal state and then the coke formation is taking place causing the deactivation of catalyst. For this reason, it is necessary to add sulfur donor compounds into feedstocks in order to prevent desulfurization of the catalyst. Thus, the used of non-sulfide catalysts can neglected the addition of sulfur in feedstock. Yakovlev and co-workers [114] demonstrated that Ni-Cu catalyst was interested for HDO process at mild condition. Cu was found to be easy reduction at lower temperatures (<573 K) and also prevent methanation of oxy-organics around 553–623 K. In additional, the activation of oxy-compounds on the support surface CeO_2 and ZrO_2 are possible to increase the catalytic activity. Furthermore, FAMEs are deoxygenated at C–O bonds via hydrogenolysis over Ni/CeO_2 while decarboxylation occurs in presence of $Ni–Cu/ZrO_2$.catalyst

The reaction mechanism of HDO do not clearly understand due to the various products are obtained from various reactions depended on the favorable pathways of catalysts. The kinetic studies have been reported by a few researcher. Boda et al. [115] proposed the mechanism of HDO using carboxylic acid over supported oxide as $Ni-Mo/\gamma-Al_2O_3$ as demonstrated below:

Step 1: Octanal production

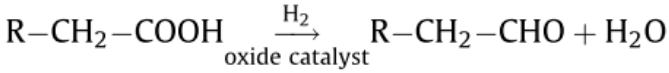

(3.13)

Step 2: Octanal consumption

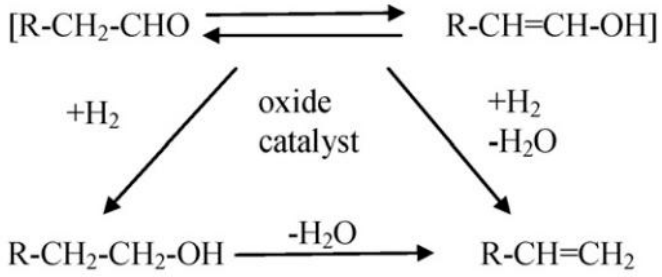

(3.14)

Step 3: Alkane formation:

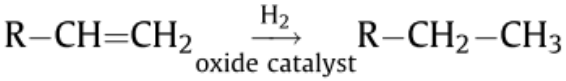

(3.15)

Langmuir–Hinshelwood–Hougen–Watson (LHHW) kinetic model is applied to rate of Ni-Mo/ɤ-Al_2O_3 oxide that alkane formation (step 3) is assumed to be a rate limiting step. Thus, the overall rate of reaction can be expressed as follow:

$$r_{Alkane} = \frac{kK_{H_2}p_{H_2}K_{CA}p_{CA}}{\left(1+K_{H_2}p_{H_2}+K_{CA}p_{CA}\right)^2} \quad (3.16)$$

where: k = Rate constant

K_{H_2} = Equilibrium adsorption coefficients of H_2

K_{CA} = Equilibrium adsorption coefficients of carboxylic acid

p_{H_2} = Hydrogen pressures

p_{H_2} = Carboxylic acid pressures

Kumar and co-workers [116] studied the kinetics of hydrodeoxygenation of stearic acid over nickel metal on different support, at initial hydrogen pressure of 7.9 atm with various reaction temperatures of 533, 543, 553, and 563 K, respectively. The products of HDO of stearic acid include n-pentadecane (PEND), n-hexadecane (HEXD), n-heptadecane (HEPD), n-octadecane (OCTD), and l-octadecanol (OCTDL). Furthermore, the used of nickel supported ɤ-Al_2O_3 catalyst (NiAl) was studied in HDO of stearic acid because it provided the higher n-heptadecane (HEPD) selectivity than other supports and 15NiAl (15wt.% of nickel loading) and 0.5 (wt./vol.)% catalyst loading were the optimal condition for HDO of SA. The possible mechanism is proposed in Figure 3.15.

จุฬาลงกรณ์มหาวิทยาลัย
Chulalongkorn University

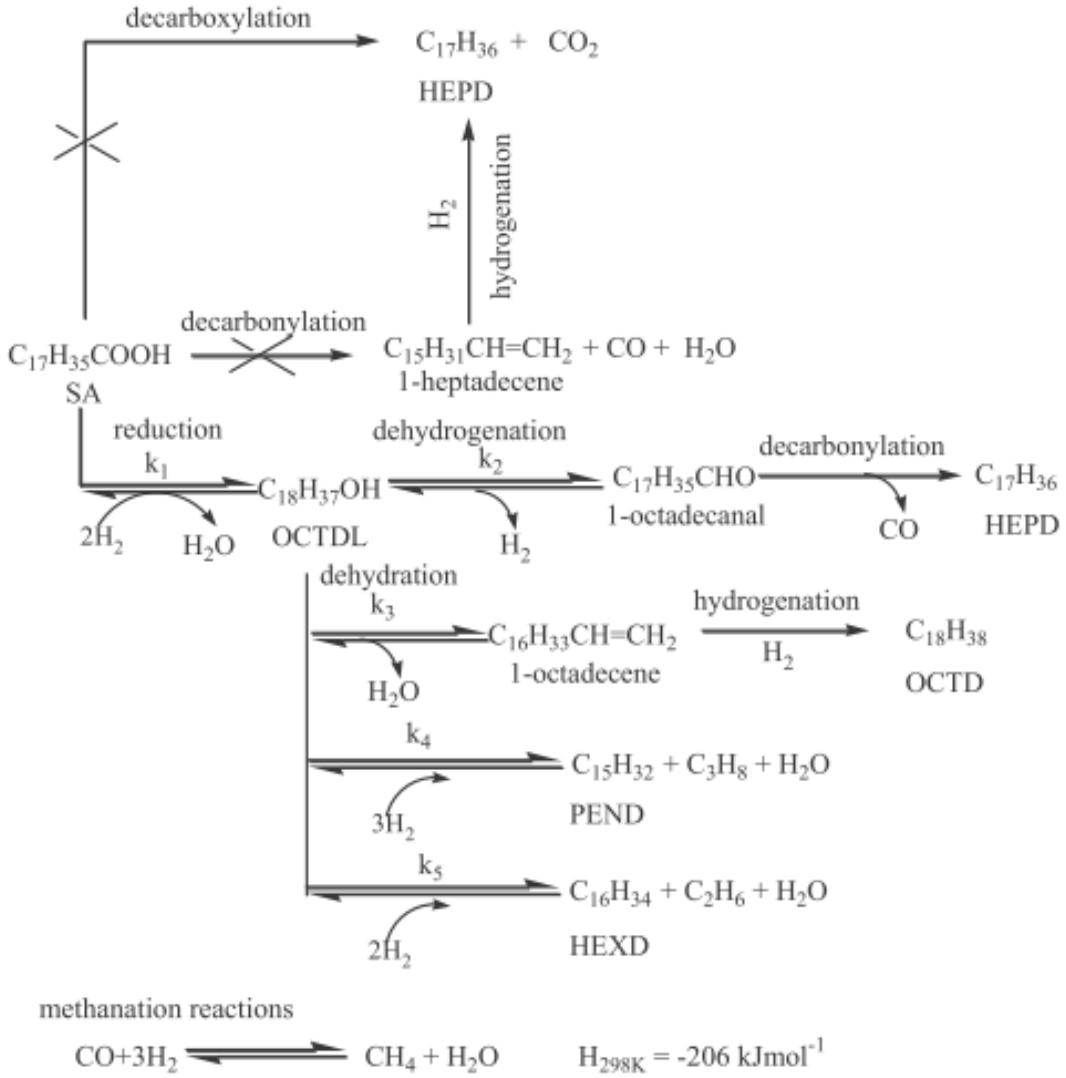

Figure 3.15 Possible pathways for hydrodeoxygenation of stearic acid in presence of supported nickel catalyst proposed by Kumar and co-workers [116].

Kinetic parameters were included internal diffusion of catalyst. Moreover, the kinetic model in Figure 3.15 which can formulate to the pseudo first order kinetic model using the excess hydrogen in the experiment. Hence, the differential equations were expressed as;

Rate of stearic acid consumption: $$\frac{dC_{SA}}{dt} = -k_1 C_{SA} \quad (3.17)$$

HEPD production rate: $$\frac{dC_{HEPD}}{dt} = k_2 C_{OCTDL} \quad (3.18)$$

OCTD production rate: $\frac{dC_{OCTD}}{dt} = k_3 C_{OCTDL}$ (3.19)

PEND production rate: $\frac{dC_{PEND}}{dt} = k_4 C_{OCTDL}$ (3.20)

HEXD production rate: $\frac{dC_{HEXD}}{dt} = k_5 C_{OCTDL}$ (3.21)

OCTDL production rate: $\frac{dC_{OCTDL}}{dt} = k_1 C_{SA} - \left(k_2 + k_3 + k_4 + k_5 \right) C_{OCTDL}$ (3.22)

Values of the apparent reaction rate for hydrodeoxygenation of stearic acid over 15NiAl catalyst are given in Table 3.7

Table 3.9 Kinetic parameters for hydrodeoxygenation of stearic acid over 15NiAl catalyst

Rate constant	**Apparent Pre-exponential Factor** $\left[s^{-1}\right]$	**Apparent Activation Energy** $\left[kJ/mol\right]$
k_1	5.57×10^{12}	175.4
k_2	1.34×10^{21}	250.0
k_3	4.77×10^{13}	190.9
k_4	5.08×10^{32}	387.7
k_5	1.08×10^{32}	377.2

จุฬาลงกรณ์มหาวิทยาลัย
Chulalongkorn University

CHAPTER IV PROCESSS SIMULATION

All processes in this work were simulated using Aspen Plus simulation. The suitable thermodynamic models have been applied for biodiesel, glycerol reforming, and green diesel production as follows: Non-Random Two Liquid model (NRTL), Soave–Redlich–Kwong (SRK), and Peng-Robinson equation of state (PENG-ROB). Furthermore, UNIFAC was used for predicting some binary interaction parameters which were not available in the simulation databank and the pressure drop in process for all equipment are neglected.

4.1 Biodiesel production process

4.1.1 Process and operating condition selection for biodiesel production process

Biodiesel production using fresh oil mainly have four processes including the conventional homogeneous catalytic process, heterogeneous catalytic process, enzymatic catalytic process and supercritical methanol process which reported by many researchers. For heterogeneous catalytic process, this process have some issues which not practical for industrial scale application. First, the natural of immiscible solution between vegetable oils and alcohols results in mass transfer limitation especially using solid catalyst, the mass transfer will extremely increasing due to the three phase of oil-alcohol-catalyst mixture. Second, although solid catalyst can be reusable, the activity of repeated catalyst will decrease along the reaction cycle. Third, the cost of heterogeneous catalyst is higher than homogeneous catalyst because mostly, they are synthesized from inorganic metals and their oxide. Fourth, heterogeneous catalyst is slower activity than that of homogeneous catalyst that may be required severe operating condition and high methanol to oil ratio and amounts of catalyst loading.

For enzymatic process, the enzymatic transesterification are several disadvantages in industrial scale such as high enzyme cost and low activity compared with conventional catalyst, easy enzyme deactivation. Furthermore, lipase activity is

decreased in long term because methanol toxicity, water deactivation and glycerol as inhibitor [91].

Although, biodiesel production via supercritical methanol process (SCM) can overcome disadvantage of previous biodiesel production processes, the high operating conditions is the main consideration [90]. The high temperature and pressure require suitable materials for reactor construction in order to offer safety in SCM plant.

In contrast, the conventional alkali catalytic biodiesel production process offers high yield in short resident time, low operating condition, effective catalyst cost, no mass transfer limitation between catalyst and reactant, using simple equipment and process. Thus, the conventional process was selected as process modelling in biodiesel section

4.1.2 Modelling validation of biodiesel production process

Kinetic parameters for transesterification of soybean oil and methanol using NaOH as a homogeneous catalyst are obtained from experimental data of Noureddini and Zhu work [81]. Figure 4.1 clearly indicates that oil conversion almost not changes after the methanol to oil molar ratio is 6 and the best conversion may obtain at 333 K (see Figure 4.2). Thus, the optimal condition of transesterification reaction is 6 of the methanol to oil molar ratio, 333 K of reaction temperature and 1 hr. of resident time. Methyl ester yield from simulation and experiment at the optimal operating condition are 92.5 and 88.0, respectively which is about 5.1% error.

จุฬาลงกรณ์มหาวิทยาลัย
CHULALONGKORN UNIVERSITY

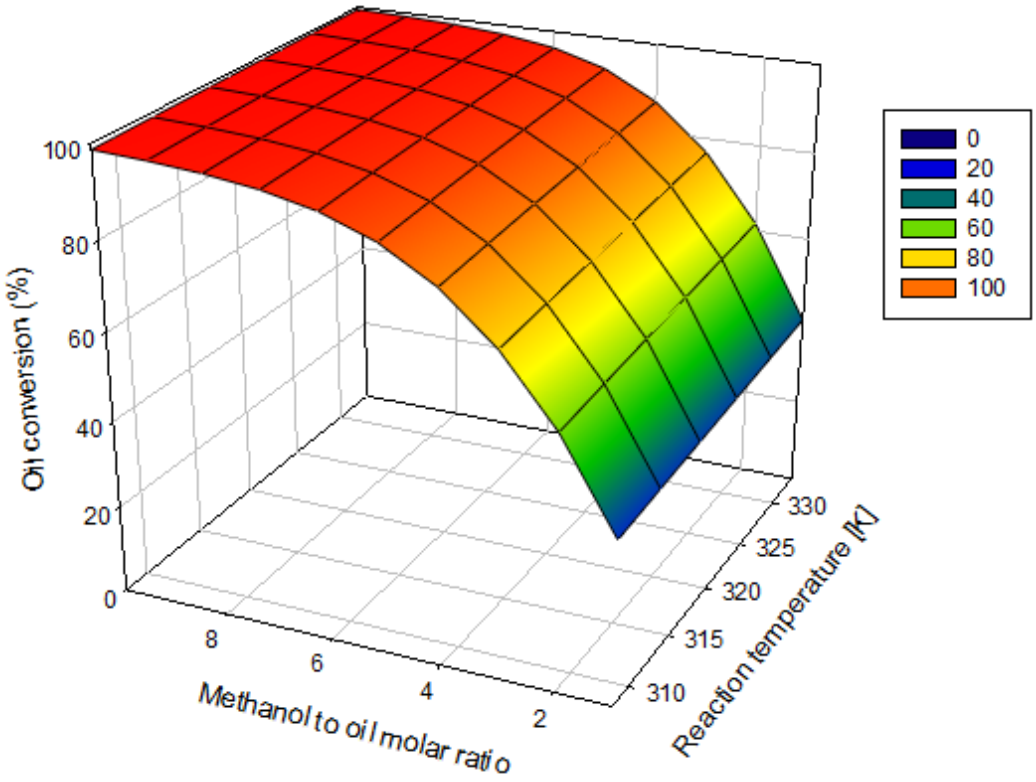

Figure 4.1 Influence of methanol to oil molar ratio (1-10) and reaction temperature (308-333 K) against oil conversion at 1 hr. of residence time.

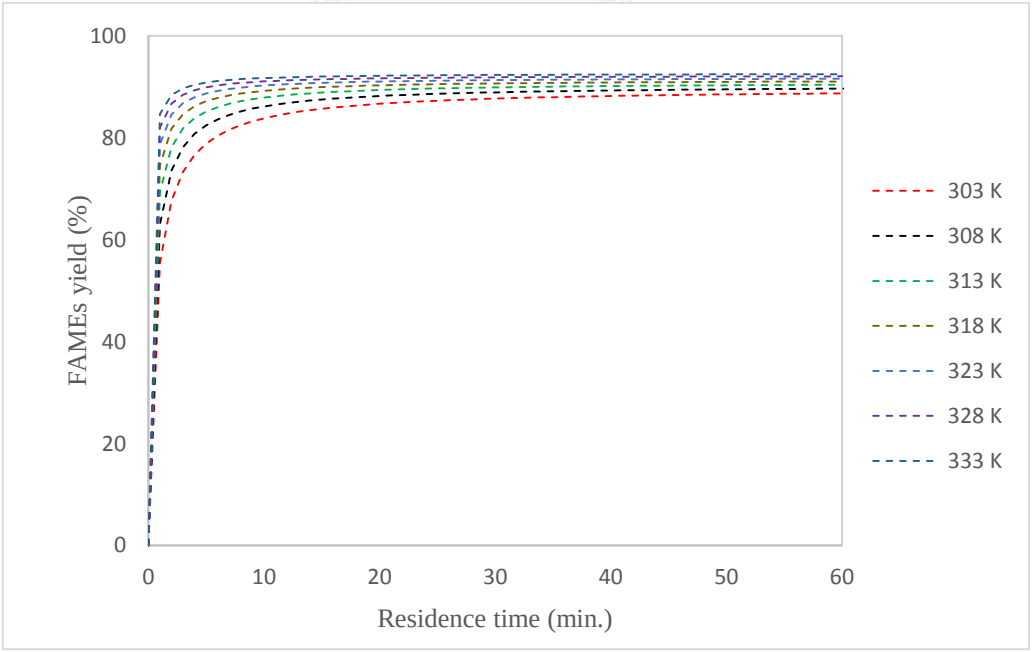

Figure 4.2 Influence of reaction temperature against methyl ester yield at 6 of methanol to oil molar ratio.

4.1.3 Process description of biodiesel production process

Figure. 4.3 shows the process flow diagram for conventional process of biodiesel production using soybean oil. This flow sheet and some of operating conditions of the conventional biodiesel production process are following Zhang et al. [88] and West et al. [89] work. Soybean oil is preheated before feeding to transesterification reactor (R-TRAN). Sodium methoxide-methanol solution is mixed with make-up methanol and methanol from recycle stream before preheating. All reactants is fed to adiabatically transesterification reactor which the reaction mixture occurred at atmospheric pressure. Transesterified product consisting of FAME, unreacted methanol, alkali catalyst and some intermediate such as diglyceride are sent to the first distillation column (DC-BD) in order to recycle methanol from overhead stream to the first mixer (MIX1). The bottom product of the first distillation column (DC-BD) after cooling is sent to extraction unit (BD-WASH) in order to separates FAME from other transesterified products using water as solvent. The isothermally neutralization reactor (R-NUET), where an alkali catalyst containing in glycerol-rich stream from extraction is neutralized by adding phosphoric acid (H_3PO_4) to produce sodium phosphate salt (Na_3PO_4. After sodium phosphate salt is sieved at filter (FILTER) from glycerol-rich stream, the second distillation column (DC-GLY) as glycerol purification unit separated other products in glycerol-rich stream in order to achieve the high purity of glycerol. FAME from water washing unit are purified under the third distillation column (DC-FAME)

จุฬาลงกรณ์มหาวิทยาลัย
Chulalongkorn University

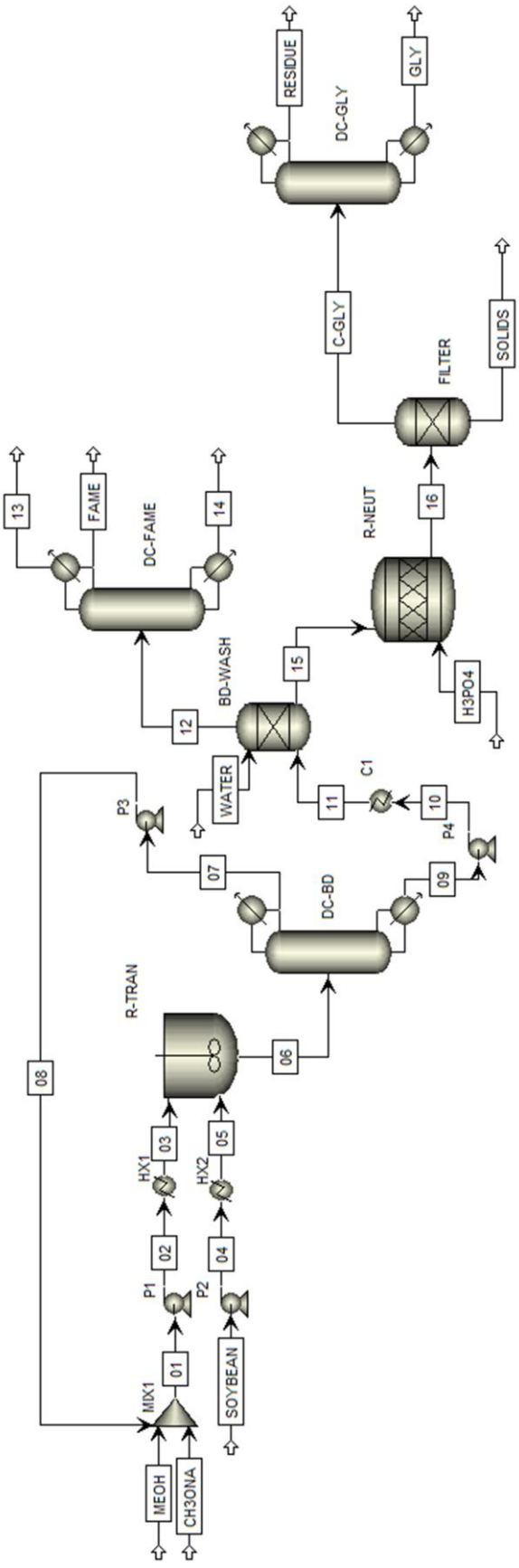

Figure 4.3 Process flow diagram for the conventional biodiesel production using alkali catalyst.

Table 4.1 Stream description of the conventional biodiesel production using alkali catalyst demonstrated in Figure 4.3.

Stream name	From	To	Stream description
MEOH		MIX1	Anhydrous methanol as raw material for biodiesel production process
CH3ONA		MIX1	Sodium methoxide-methanol solution as catalyst-alcohol feed
01	MIX1	P1	Sodium methoxide-methanol solution after adjust molar feed ratio
02	P1	HX1	Sodium methoxide-methanol solution is fed to heater to adjust temperature
03	HX1	R-TRAN	Sodium methoxide-methanol after pretreatment is fed to transesterification reactor
SOYBEAN		P2	Soybean oil as raw material for biodiesel production process
04	P2	HX2	Soybean oil is fed to heater to adjust temperature
05	HX2	R-TRAN	Soybean oil after pretreatment is fed to transesterification reactor
06	R-TRAN	DC-BD	Methanol is separated from transesterified product by distillation column (DC-BD)
07	DC-BD	P3	Anhydrous methanol at the top of the distillation column (DC-BD)
08	P3	MIX1	Anhydrous methanol recycle stream is mixed with methoxide-methanol solution
09	DC-BD	P4	Transesterified product at the bottom of the distillation column (DC-BD)
10	P4	C1	Transesterified product is cooled by cooler
11	C1	BD-WASH	Transesterified product after cooling is sent to extraction for biodiesel washing step
WATER		BD-WASH	The water as solvent in extraction for biodiesel purification
12	BD-WASH	DC-FAME	FAME-rich stream is sent to distillation column for biodiesel purification
13	DC-FAME		Off-gas mainly consists of water and methanol is spited out of process

Table 4.1 Stream description of the conventional biodiesel production using alkali catalyst demonstrated in Figure 4.3 *(continued)*.

Stream name	From	To	Stream description
14	DC-FAME		Oil residue
FAME	DC-FAME		The high purity of FAME (~99 %wt.)
H3PO4		R-NUET	Phosphoric acid
15	BD-WASH	R-NUET	Alkali catalyst in glycerol-rich stream is neutralized by phosphoric acid
16	R-NUET	FILTER	The filter sieves a solid of sodium phosphate out of process after neutralization
SOLID	FILTER		Sodium phosphate is spited out of process
C-GLY	FILTER	DC-GLY	The stream containing 85 %wt. of glycerol is sent to distillation
RESIDUE	DC-GLY		The residue mainly consists of water, methanol, FAME
GLY	DC-GLY		The high purity of glycerol (~99 %wt.)

Table 4.2 Equipment description of the conventional biodiesel production using alkali catalyst demonstrated in Figure 4.3

Model	**Name**	**Stream description**
MIXER	MIX1	Mixes crude glycerol and water for storage
PUMP	P1	Pumps sodium methoxide-methanol solution to adjust temperature
	P2	Pumps soybean oil to adjust temperature
	P3	Pumps anhydrous methanol to mixer (MIX1)
	P4	Pumps transesterified product to adjust temperature
HEATER	HX1	Preheats sodium methoxide-methanol solution to reaction temperature
	HX2	Preheats soybean oil to reaction temperature
	C1	Cools transesterified product from transesterification reactor before feeding to extraction
RCSTR	R-TRAN	Transesterification reactor
RSTOIC	R-NEUT	Neutralization reactor
RADFRAC	DC-BD	Separates methanol from the product via distillation column
	DC-FAME	Purifies FAME to ASTM specification (>99.6 %wt.)
	DC-GLY	Purifies glycerol to high grade (~99 %wt. in this work)
EXTRACT	BD-WASH	Separates FAME from other transesterified products using water as solvent
SEP	FILTER	Sieves a solid of sodium phosphate (Na_3PO_4) out of process after neutralization

4.2 Glycerol steam reforming process

4.2.1 Process and operating condition selection for glycerol steam reforming

From Chapter 3 and Table 3.7, glycerol reforming have many method to convert glycerol to hydrogen. GSW is not practical for industrial scale, because high pressure system (>20 atm) comparing with pressure the conventional steam reforming (3-25 atm). High cost of suitable materials is a weak points because equipment such as reactor construction, pipeline are also required mechanical strength to ensure safety in aggressive pressure. Although GATR can provide energy-itself. This process may require startup heat and control systems because it need to switch between lean burning and its regimes. H_2 and O_2 as product-residue stream may provide explosive mixture. Moreover, GATR is lower hydrogen yield than that of GSM. APGR can enhance hydrogen production using liquid water at mild temperature which favors water-gas shift reaction with very low CO concentration in product stream, but it need a high pressure for pressing water to liquid phase. Furthermore, it also gives the very low glycerol conversion and very high residence time comparing with other glycerol reforming process. GDR is the only one of glycerol reforming process which can utilize CO_2 as greenhouse gas to synthesis gas. Nevertheless, the main disadvantage of GDR is the coke formation resulting in carbon deposited on catalyst surface. This coke blocks active site of catalyst which catalyst contributes to short life and subsequent deactivation. The large of coke deposition can be explained by CO_2 reactant is converted to undesirable reaction as coke formation. In the other hand, GSM can handle the previously other problems: (1) coke formation can be solved by using high stream ratio; (2) glycerol can completely convert to synthesis gas with low pressure; (3) Although GSM can't produce energy like GATR, heat integration technology also help to recover heat from product to preheat feed. Moreover, GSM is not provide the explosive mixture and higher hydrogen yield. In additional, it also is stable during transition operation which it is not required switch the system. (4) GSM does not suffer with special equipment to endure a high pressure as same as GSW. Thus, GSM was selected as suitable process for hydrogen production via glycerol reforming

Hajjaji et al. [5] reported the result of thermodynamic of glycerol steam reforming. The optimal condition of this work can be achieved at 9 of WGFR, 950 K of reformer temperature, and 1 atm which the amounts of methane and coke formation are very low. Nevertheless, the operating condition of conventional steam reforming of natural gas (methane steam reforming) in industry is operated with excessive steam at high temperature (>1100 K) and high pressure (>20 atm) using nickel catalyst. Thus, the possible products of glycerol steam reforming was analyzed in function of pressure and temperature. Products of glycerol steam reforming process, which comprise of H_2, CO, CO_2, CH_4, H_2O, and C, at equilibrium were analyzed via RGibbs reactor model of Aspen Plus simulation by minimization of Gibbs free energy which the Soave-Redlich-Kwong (SRK) was selected as suitable cubic equation of state to predict vapor-liquid equilibrium behavior of all compounds, because this reaction is thermodynamically favored. Furthermore, the result can help to achieve the suitable condition ranges.

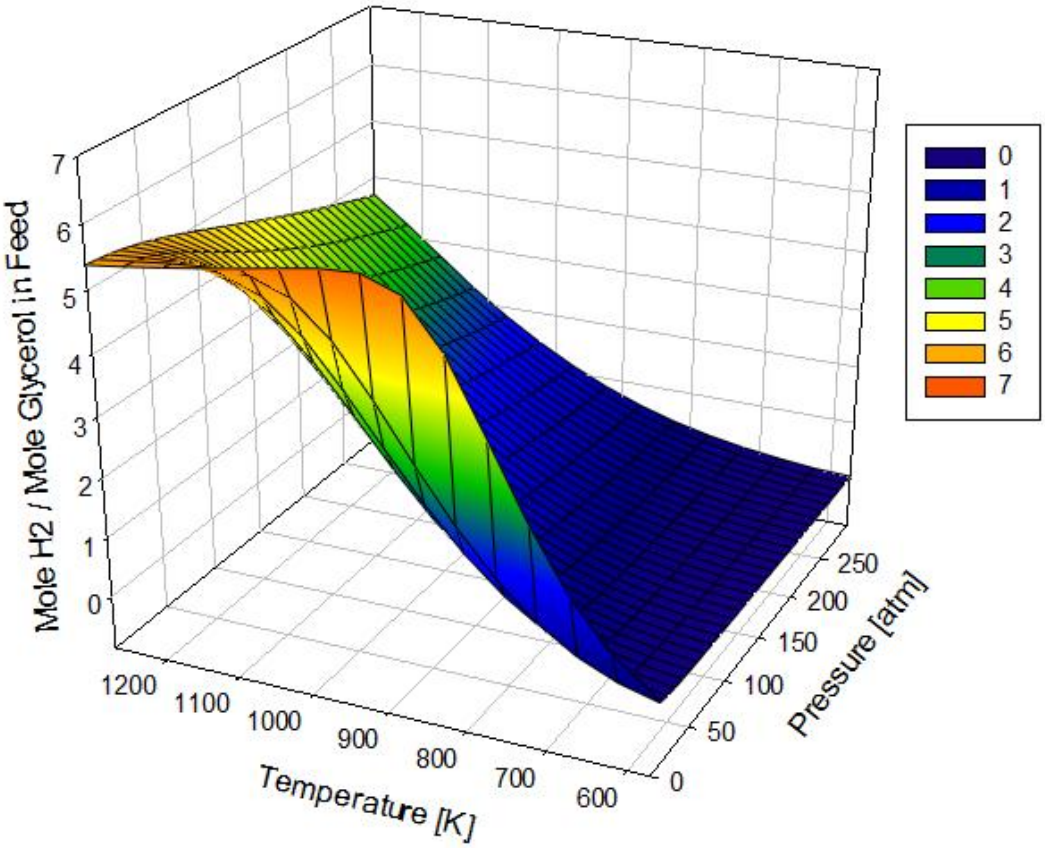

Figure 4.4 Mole of hydrogen produces per mole of glycerol in function temperature and pressure of reformer at WGFR = 9.

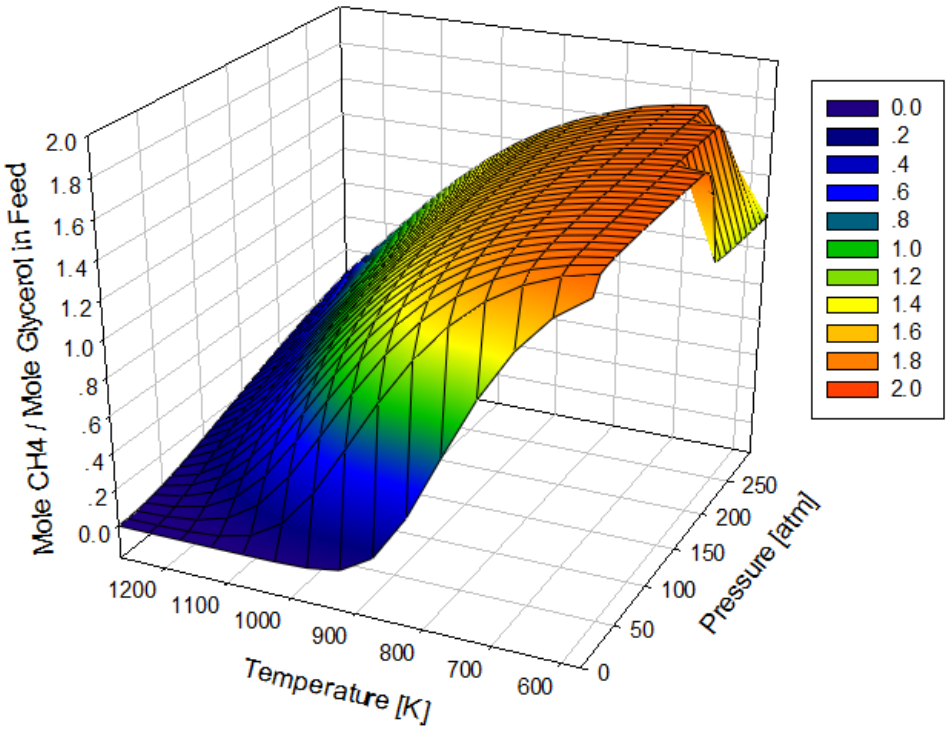

Figure 4.5 Mole of methane produces per mole of glycerol in function temperature and pressure of reformer at WGFR = 9.

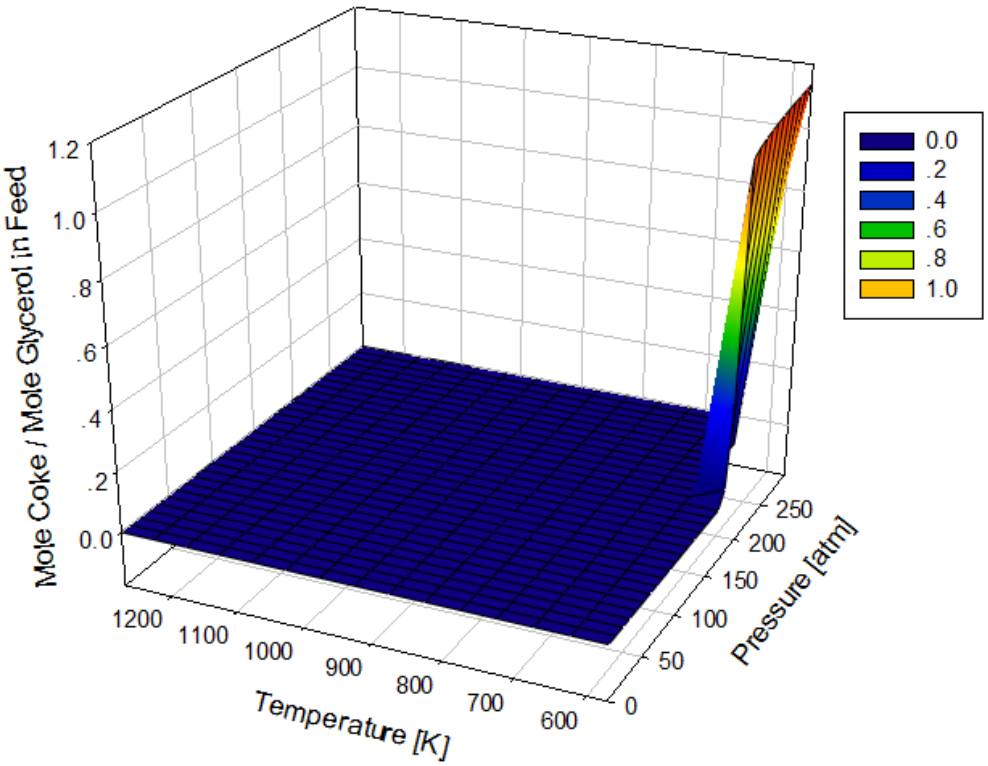

Figure 4.6 Mole of coke produces per mole of glycerol in function temperature and pressure of reformer at WGFR = 9.

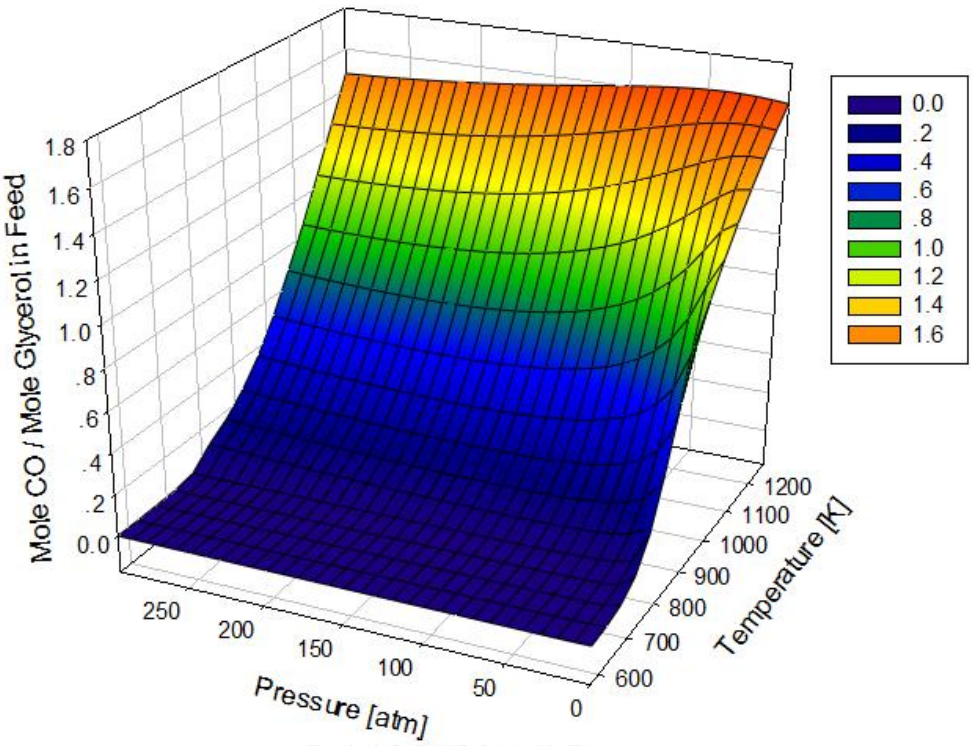

Figure 4.7 Mole of carbon monoxide produces per mole of glycerol in function temperature and pressure of reformer at WGFR = 9.

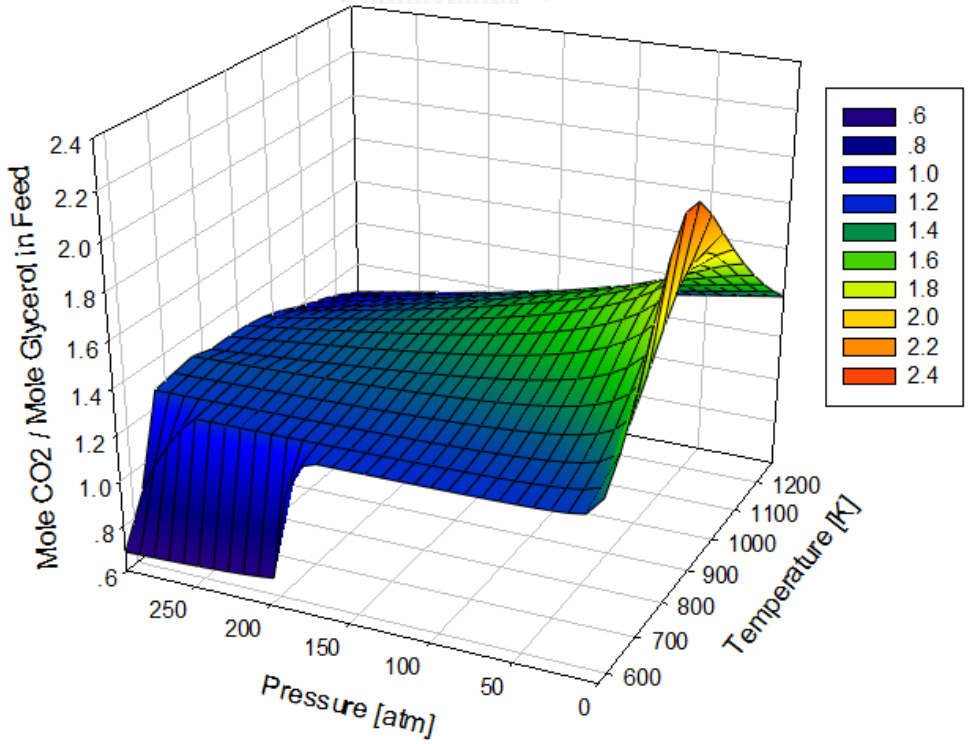

Figure 4.8 Mole of carbon dioxide produces per mole of glycerol in function temperature and pressure of reformer at WGFR = 9.

Figure 4.4 shows hydrogen yield increased when the reformer temperature increases, whereas hydrogen yield was decreased when the reformer pressure increases. This behavior can be concluded as the Le Chatelier's principle, because sum of mole product is more than the sum of mole reactant of glycerol steam reforming reaction. Figure 4.5 obviously describes hydrogen is consumed via methanation reaction at low temperature which three moles of hydrogen convert to methane. Nevertheless, methane is converted to hydrogen via methane steam reforming when the reformer temperature is high (>1150 K), Coke deposition (Figure 4.6) is not found at high temperature. Figure 4.7 shows amounts of carbon monoxide increases with temperature. This result supports the hypothesis that glycerol is rapidly decomposed to carbon monoxide as one of synthesis gas due to decomposition reaction favors high temperature. However, when the temperature of reformer increases at constant pressure cause the amounts of carbon dioxide significantly increases and subsequently decreases (Figure 4.8). This can explain by two steps: (1) carbon dioxide is produced via water-gas shift reaction at low temperature zone and (2) After that, the reverse water-gas shift reaction occurs at high temperature zone which it disturbs the amounts of hydrogen in reformer. This result is in agreement with the rate of increasing of hydrogen yield in Figure 4.4 then it decreases when the carbon dioxide content is reduced, whereas carbon monoxide greatly is increased.

Furthermore, the hydrogen yield slightly decreased between 1 to 30 atm when the temperature is greater than 1150 K. This result can completely prove that the glycerol steam reforming can use nickel catalyst and operate under the similar operating condition as same as the conventional steam reforming. Thus, the operating condition for this work was selected at 1150 K and 14.31 atm for section of glycerol steam reforming process.

4.2.2 Modelling validation of hydrogen production via glycerol reforming

Glycerol steam reforming model is referred to validate with Hajjaji et al. work [5]. Figure 4.9 demonstrates the synthesis gas composition with dry basis for equilibrium reactor which the reformer operating condition are WGFR = 6, the reformer 973 K, and the reformer pressure = 1 atm. This result shows that the product gas composition from reformer are good acceptation.

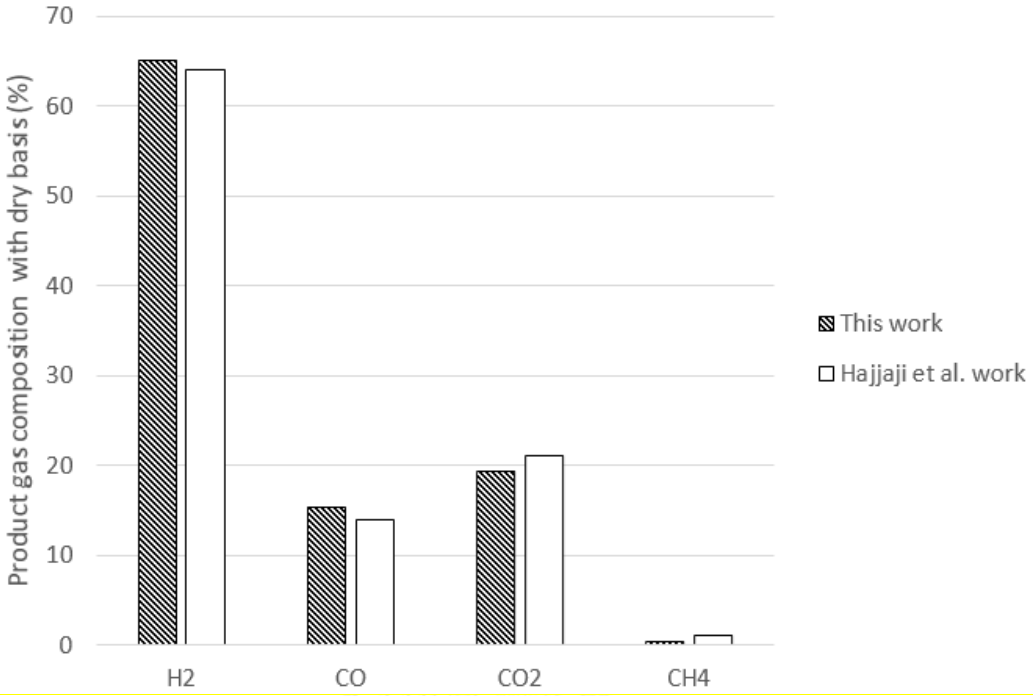

Figure 4.9 Synthesis gas composition with dry basis for equilibrium reactor (WGFR = 6, T = 973 K, P = 1 atm)

4.2.3 Process description of glycerol team reforming

In Figure 4.10, glycerol steam reforming section, the mixture of glycerol-water is preheated to the operating condition of reformer (REFORMER). Product gases are also cooled to the operating condition of high and low water-gas shift reactor (HWGS and LWGS). Off-gas, mainly consists of H_2, CO_2 and CO from the first phase separation unit (SEP1), flows to PSA, where the mean concentration of carbon dioxide can be less than 10 ppm. PSA is the most mature application for CO removal from the product gas mixture. Moreover, PSA is able to remove other product gases to achieve high purity of H_2 in the stream outlet from PSA.

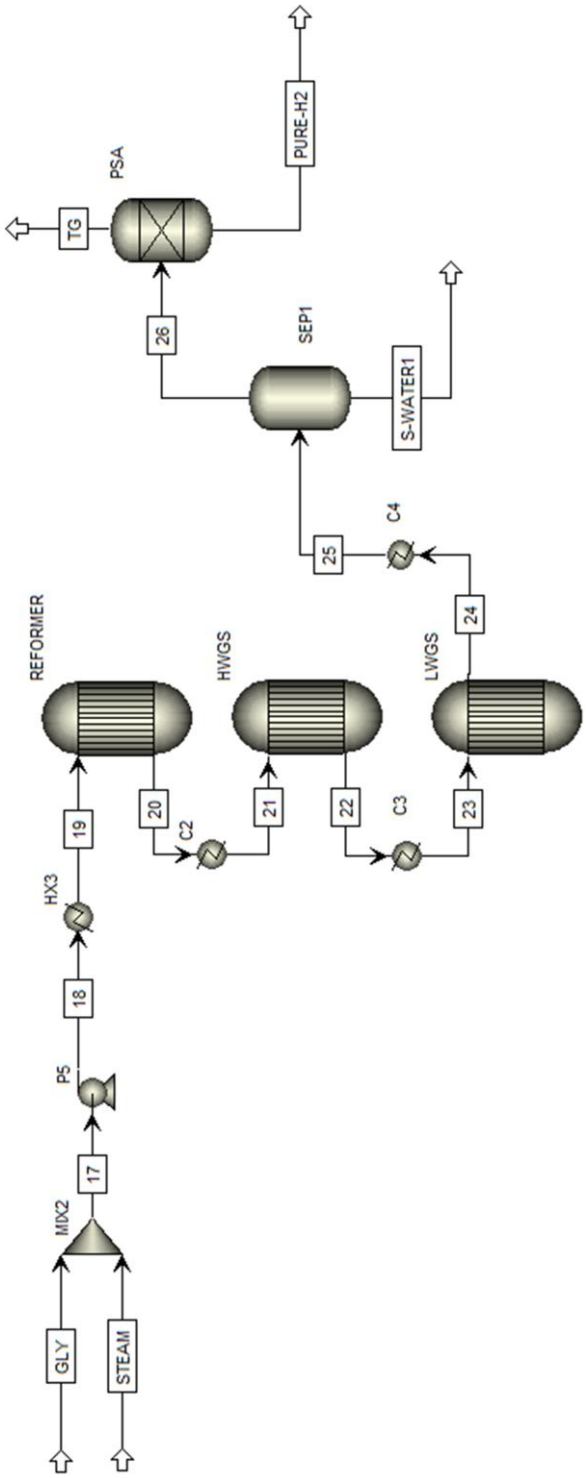

Figure 4.10 Process flow diagram for hydrogen production via glycerol steam reforming.

Table 4.3 Stream description of glycerol steam reforming demonstrated in Figure 4.10.

Stream name	From	To	Stream description
GLY		MIX2	Crude glycerol as raw material for glycerol steam reforming process
STEAM		MIX2	Water as raw material for glycerol steam reforming process
17	MIX2	P5	Glycerol-water mixture was prepared for feeding to reformer by pump
18	P5	HX3	Glycerol-water mixture was pumped to heater in order to adjust temperature
19	HX3	REFORMER	Glycerol-water mixture after pretreatment was sent to reformer
20	REFORMER	C2	Product gas form reformer were fed to cooler in order to adjust temperature
21	C2	HWGS	Product gas after adjust temperature were sent to HWGS
22	HWGS	C3	Product gas form HWGS were fed to cooler in order to adjust temperature
23	C3	LWGS	Product gas mixture after adjust temperature were sent to LWGS
24	LWGS	C4	Product gas form LWGS were fed to cooler in order to adjust temperature
25	C4	SEP1	Product gas after adjust temperature were sent to phase separation unit
S-WATER1	SEP1		Residue water from product gases mixture was withdrawn out of process
26	SEP1	PSA	Low moisture product gases were sent to H_2 purification unit (PSA)
TG	PSA		Rich-CO_2 gases consisting of CO_2, CO, H_2 and moisture were withdrawn out of process
PURE-H_2	PSA		99.99% high purity of H_2 after purification via Pressure swing adsorption

Table 4.4 Equipment description of glycerol steam reforming demonstrated in Figure 4.10**.**

Model	**Name**	**Stream description**
MIXER	MIX2	Mixes crude glycerol and water for storage
PUMP	P5	Pumps reactant to destination pressure
HEATER	HX3	Preheats reactant o reaction temperature
	C2	Cools the product gas mixture from reformer before feeding to HWGS
	C3	Cools the product gas mixture from HWGS before feeding to LWGS
	C4	Cools the product gas mixture from LWGS before feeding to phase separation unit (SEP1)
REQUIL	REFORMER	Simulates hydrogen production via glycerol steam reforming
	HWGS	Simulates water-gas shift reaction at high temperature (623 K)
	LWGS	Simulates water-gas shift reaction at low temperature (473 K)
FLASH2	SEP1	Separates moisture form the product gas mixture
SEP	PSA	Separates H_2 form others gas by Pressure swing adsorption

4.3 Hydrotreating of vegetable oil process

4.3.1 Process and operating condition selection for hydrotreating of free fatty acid

Kumar and co-workers [116] proposed the mechanism for hydrotreating of stearic acid using nickel metal with support and the value of kinetic parameters are given in Table 3.7 in the previous chapter. This kinetic model can be manipulated to pseudo first order with SA. Thus, hydrogen to SA feed molar ratio in this simulation must be operated over 1.00. SA conversion (%) from simulation (Figure 4.11) provides a good agreement of conversion as report from experimental data (Figure 4.12). at 533 to 563 K. Moreover, SA is almost achieved to 100% conversion at 563 K with low feed ratio. In additional, Figure 4.13 shows that low hydrogen to SA molar ratio offers high liquid hydrocarbon in range of C15 to C18. This result can be explained that hydrogen is consumed to produce methane via methanation as unfavorable reaction at high amounts of hydrogen feed to reactor.

The hydrogen requirement following the stoichiometric coefficients of the intermediate reaction is two moles of hydrogen and one mole of SA converting to OCTDL and followed by OCTDL converting to the various products via multiple reactions which hydrogen is used. However, the simulation result shows that almost 100%of both SA and OCTDL were also converted to green diesel products even though hydrogen consumption is nearly two moles. This result can be obliviously described that the HEPD as primary product occurring in secondary reaction offers hydrogen via dehydrogenation. Therefore, the optimal operating condition can concluded as 563 K of reaction temperature, 14.31 atm of pressure and 1.5 of hydrogen to SA feed molar ratio.

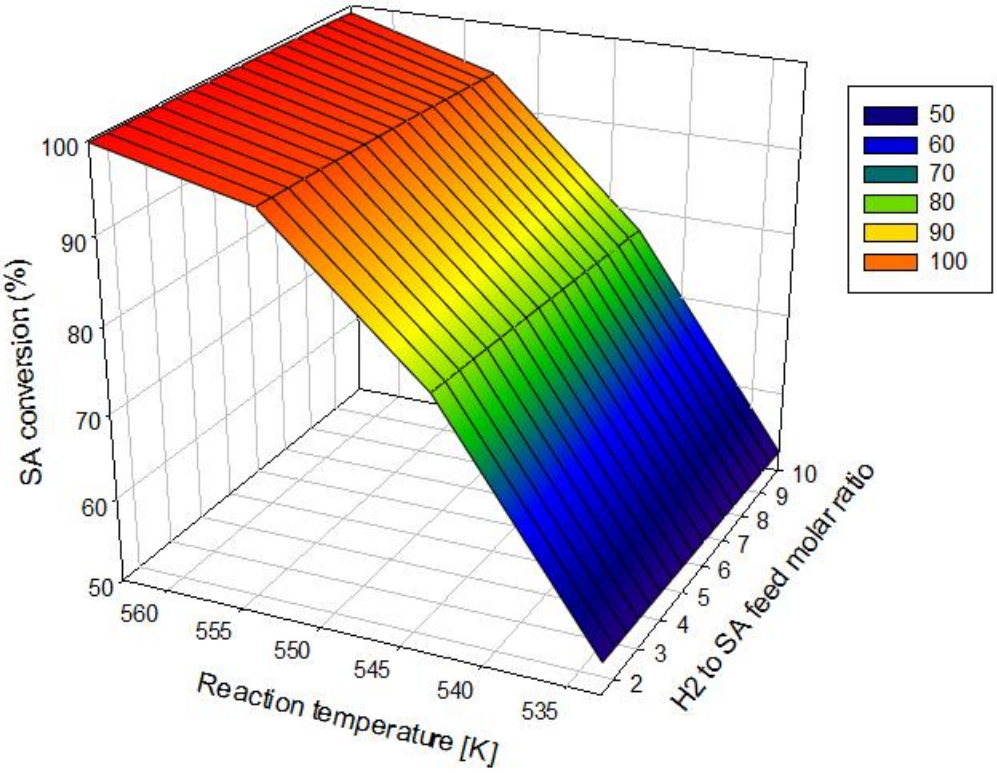

Figure 4.11 Effect of reaction temperature (533-563 K) and feed ratio (1.5-10) to SA conversion (%) at 14.31 atm of reactor pressure and 6 hr of residence time.

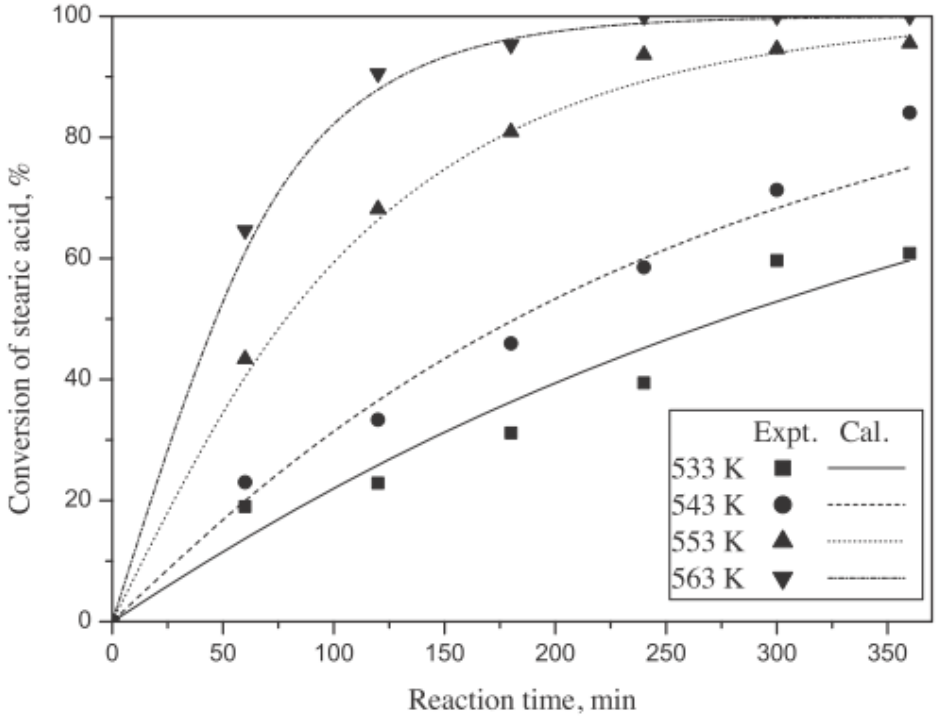

Figure 4.12 Effects of temperature on conversion of stearic acid using feed ratio = 1 is reprinted from Kumar et al. works [116].

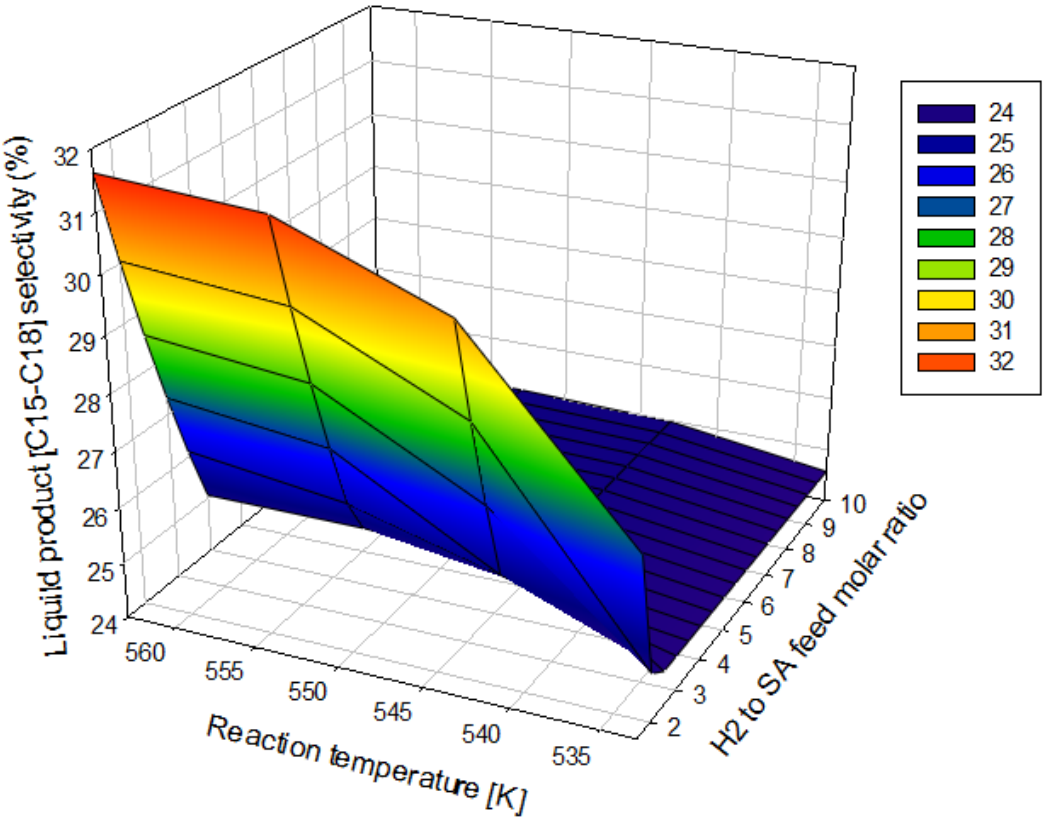

Figure 4.13 Effect of reaction temperature (533-563 K) and feed ratio (1.5-10) to liquid product selectivity (%) [C15-C18] at 14.31 atm.

จุฬาลงกรณ์มหาวิทยาลัย
Chulalongkorn University

4.3.2 Modelling validation of hydrotreating of free fatty acid

The comparison on product selectivity between simulation and experiment is shown in Figure 4.14 which the condition are validated at 95% conversion of stearic acid, 563 K of reaction temperature, and 14.31 atm.

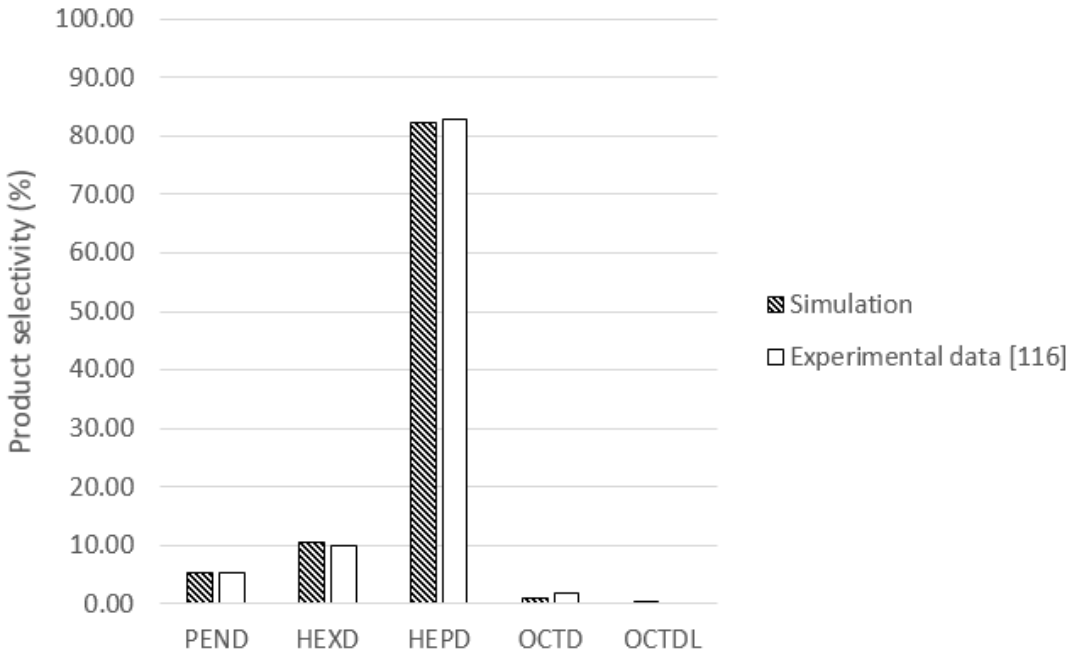

Figure 4.14 Product selectivity of hydrotreating of stearic acid using nickel supported catalyst at 95% conversion of stearic acid, 563 K of reaction temperature, and 14.31 atm.

จุฬาลงกรณ์มหาวิทยาลัย
Chulalongkorn University

4.3.3 Process description of hydrotreating of vegetable oil

Figure 4.15 illustrates the hydrotreating of stearic acid process. Stearic acid and a high purity of H_2 acid were adjusted pressure and temperature to 14.31 atm and 563 K. The multiple reactions such as hydrodeoxygenation and decarbonylation reaction can be occurred simultaneously over catalyst bed in hydrotreating reactor (R-HDO1-R-HD2). In additional, R-HDO1 is represented the reaction zone of steric acid converting to various products with different reaction pathways and R-HDO2 is represented the reaction zone of methanation. The main hydrocarbon products of HDO of steric acid consists of n-pentadecane, n-hexadecane, n-heptadecane, n-octadecane, and l-octadecanol. Gaseous portion of the stream (FLUE-GAS) comprises a residue of hydrogen, carbon monoxide, methane, ethane and propane are removed from a stream

by the second phase separator (SEP2). Crude green diesel mainly consisting of liquid hydrocarbon can be obtained in the second phase separator. These liquid mixtures are prepared for the other processes such as isomerization which it is not a main consideration in this work.

จุฬาลงกรณ์มหาวิทยาลัย
Chulalongkorn University

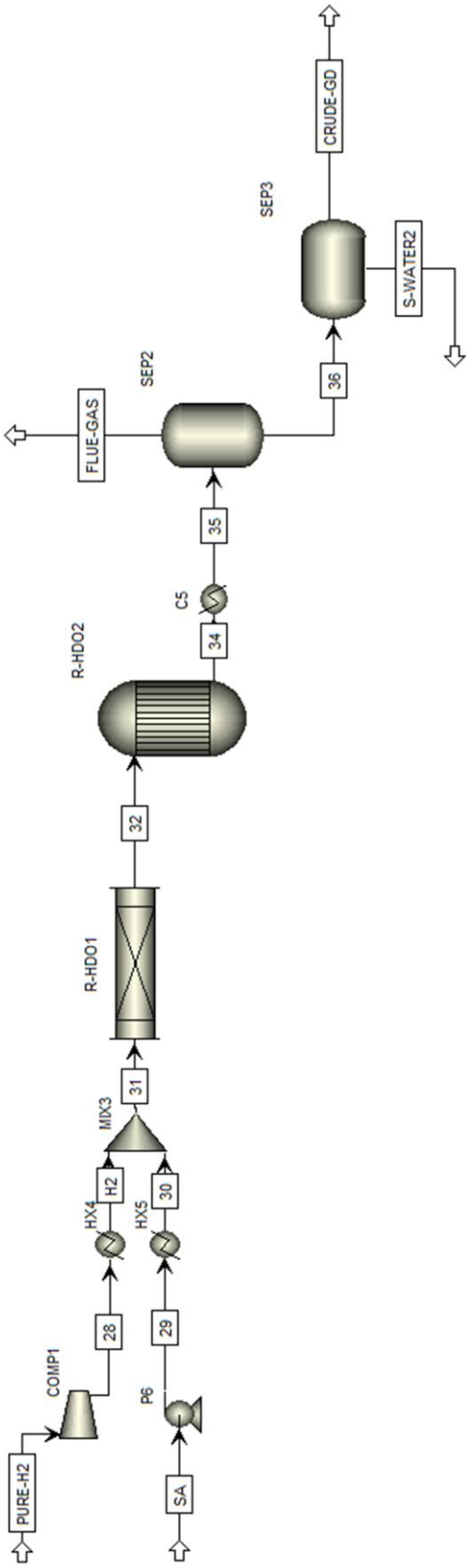

Figure 4.15 Process flow diagram for hydrotreating of stearic acid.

Table 4.5 Stream description of hydrotreating of stearic acid demonstrated in Figure 4.15.

Stream name	From	To	Stream description
PURE-H2		COMP1	The high purity of H_2 as raw material for hydrotreating of stearic acid
SA		P6	Stearic acid as raw material for hydrotreating of stearic acid
28	COMP1	HX4	High purity of H_2 was sent to preheated by compressor
29	P6	HX5	Stearic acid was sent to preheated by pump
30	HX5	MIX3	Stearic acid after pretreatment was sent to multiple-bed hydrotreating reactor
H2	HX4	MIX3	High purity of H_2 after pretreatment was sent to multiple-bed hydrotreating reactor
31	MIX3	R-HDO1	All reactants was prepared for multiple-bed hydrotreating reactor
32	R-HDO1	R-HDO2	Product mixture in hydrotreating reactor (rate base)
34	R-HDO2	C5	Product mixture was decreased temperature
35	C5	SEP2	Product mixture was sent to separate in three phase separation unit
FUEL-GAS	SEP2		Fuel gas mainly contained CO, CH_4, C_2H_6, C_3H_8, and H_2 residue
36	SEP2	SEP3	Water and Crude green diesel
S-WATER2	SEP3		Wastewater
CRUDE-GD	SEP3		Crude green diesel mainly consists of HEPD, HEXD, PEND, and OCTD

Table 4.6 Equipment description of hydrotreating of stearic acid demonstrated in Figure 4.15.

Model	**Name**	**Stream description**
COMPR	COM1	Adjust H_2 pressure before preheating
PUMP	P6	Pumps stearic acid to destination pressure
HEATER	HX4	Preheats H_2 to reaction temperature
	HX5	Preheats stearic acid to reaction temperature
	C5	Cools the product gas mixture from hydrotreating reactor before feeding to phase separation
RPLUG	R-HDO1	Simulates SA converting to various products in multiple bed reactor, which mainly comprises of HEPD, HEXD, PEND, and OCTD, by different pathways
REQUIL	R-HDO2	Simulates the methanation in multiple bed reactor
FLASH2	SEP2	Separates the vapor-liquid phase product including water, oil, and gas
DECANTER	SEP3	Separates the vapor-liquid phase product including water, and green diesel

CHAPTER V PROCESSS IMPROVEMENT

In this chapter proposed the combination process as a base case and improvement process.

5.1 Base case condition of combined process

5.1.1 Biodiesel production section

Base case process design including of homogeneous alkali-catalyzed biodiesel production process, hydrogen production via glycerol steam reforming, and hydrotreating of stearic acid, were simulated. Soybean oil, and steric acid, were used for fresh vegetable oil feedstock and free fatty acid for biodiesel and hydrotreating, respectively. 10,000 kg/hr of soybean oil were basis of feedstock for biodiesel production. In additional, the amounts of hydrogen is related directly to soybean oil via glycerol as a by-product. Process flow diagram of the base case with the detailed stream is presented in Figure 5.1

5.1.1.1 Biodiesel production using mechanically stirred tank reactor

For biodiesel production section, 10,000 kg/hr of soybean oil was preheated to 333 K before feeding to transesterification reactor (R-TRAN). Sodium methoxide-methanol solution was mixed with two stream of methanol (make-up methanol and recycle stream methanol) to obtain methanol to oil malar ratio of 6:1. This solution mixture was preheated to 333 K before feeding to transesterification reactor. All reactants was fed to adiabatic transesterification reactor at atmospheric pressure for 1 hr of residence time. Mechanically stirred tank reactor (CSTR) was assigned as a suitable reactor for transesterification of oil and methanol. The simulation result shows that the biodiesel yield was achieved 92.5 %wt. based on kinetic model as reported by Noureddini and Zhu [81].

5.1.1.2 Methanol recovery

Methanol residue was separated from transesterified product using first distillation column (DC-BD) where recycling methanol from overhead stream 07 (Figure 5.1). First distillation column (DC-BD) was operated 1 atm of pressure and fed above 4th stage with 7 theoretical stages, 2 mass reflux ratio, and 1130 kg/hr of distillate rate which 99.99 %wt. of methanol was achieved. The recovered methanol in stream 08 was recycled and mixed with the fresh methanol and catalyst in the first mixer (MIX1) as seen in Figure 5.1.

5.1.1.3 Water washing step

Extraction column (BD-WASH) was used to separate FAME from unreacted methanol, alkali catalyst and some intermediate such as diglyceride using water as solvent. Transesterified product in stream 09 was pumped and cooled to 333 K before sent to biodiesel washing column. Then, it was fed at 6th stage where is countercurrent with water from 1st stage under pressure of 0.987 atm in a FAME washing column with a total of 6 theoretical stages. The FAME rich product was withdrawn via stream 12. All glycerol, unreacted oil, methanol, water, and alkali catalyst were remained in the bottom stream 15.

จุฬาลงกรณ์มหาวิทยาลัย
Chulalongkorn University

5.1.1.4 FAME purification

According to ASTM specification, FAME must be purified to achieve >99.6 %wt. following this standard. The rich-FAME product in stream 12 from extraction column was sent to the third distillation column (DC-FAME) in order to obtain the high purity of FAME. A partial condenser was applied to separate methanol and water from FAME at the overhead of column where methanol and water were removed as vent gases. This column was operated under pressure of 0.0987 atm and fed above 4th stage with 7 theoretical stages, 2 mass reflux ratio, and 800 kg/hr of bottom rate. The purity of biodiesel was achieved to 99.89 %wt. in the liquid stream FAME (473 K). The bottom stream 14 mainly consisting of unrecovered oil was remove from process as a waste.

5.1.1.5 Catalyst neutralization

Isothermally neutralization reactor (R-NUET), an alkali catalyst containing in glycerol-rich stream (15) from extraction was neutralized by adding phosphoric acid (H_3PO_4) to precipitate sodium phosphate salt (Na_3PO_4), was operated at 1 atm and 323 K. Then, all sodium phosphate salt was separated via gravity separator (FILTER) to obtain glycerol purity of 85 %wt.

5.1.1.6 Glycerol purification

Typically, glycerol was widely used in the industrial such as cosmetics, food and pharmaceutical applications with 99% or higher purity. The crude glycerol stream (C-GLY) obtaining from previous separation was forwarded to the second distillation (DC-GLY) in order to achieve the high purity of glycerol. The second distillation column were operated under pressure of 0.395 atm and fed above 3rd stage with 6 theoretical stages, 2 mass reflux ratio, and 943 kg/hr of bottom rate. Methanol and water were left via distillate stream (RESIDUE). In this work, the purity of glycerol were achieved to 99.91 %wt.

5.1.2 Hydrogen production via glycerol steam reforming

Chulalongkorn University

5.1.2.1 Synthesis gas production

High purity of glycerol in GLY stream from biodiesel production section was mixed with water in STEAM stream to obtain 9 of WGSR. Then, glycerol-water mixture was pump to preheat to desire temperature before feeding to reformer. Glycerol-water mixture was converted to product under 1150 K and 14.31 atm at equilibrium reformer. The hydrogen yield was achieved via methanol reforming. In this work, coke deposition and methanation reactions can be neglected for any operating condition, because they do not take place in the reforming reactor (Figure 4.6). Glycerol conversion was always 100 % at equilibrium condition. Glycerol was converted to product gas consisting of H_2, CO, CO_2, and moisture.

5.1.2.2 CO conversion

Stream production gas leaving reforming reactor (stream 20) was cooled and forward to CO conversion unit. After cooling, CO was converted in this section via a two isothermal water-gas shift reactions in the series of equilibrium reactor. CO was firstly converted in the high water-gas shift reactor (HWGS) at 623 K and the low water-gas shift reaction in the second reactor was operated at 473 K. It was found that syngas (stream 24) contained very low CO content after CO conversion section.

5.1.2.3 Hydrogen purification

Pressure swing adsorption (PSA) is selected as hydrogen purification unit at the last process in the large-scale commercial hydrogen production. PSA is the most mature application for CO removal from the product gas mixture. “The advantages of PSA are described as: (1) The mean concentration of carbon dioxide can be less than 10 ppm; (2) PSA is able to remove other product gases (CH_4, CO, N_2, Ar_2, and moisture) to achieve a high purity of H_2 in the stream outlet from PSA; (3) small amounts of H_2 is lost during the bed regeneration step because it operated at the low temperature which provides a small adsorbent bed volume (low gas volume); (4) the high partial pressure promotes adsorption of sorbents against impurities [111]. In this simulation, the component separator in Aspen plus was represented PSA as an ideal separator. The efficient separation of PSA was supposed to offer a 99.999% of hydrogen purity with 80% of hydrogen recovery which are practical values for large-commercial scale [111]. Therefore, the off-gas consisting of H_2, CO_2, CO and water must be sent to the first phase separation unit (SEP1) in order to possibly remove moisture from product gas before entering PSA to minimize the adsorption capacity loss from water. Therefore, LWGS off-gas stream was cooled to 308 K and condense water was removed via the vapor-liquid separator (SEP1). High purity of hydrogen was prepared for the next hydrotreating of free fatty acid section (PURE-H2) and stored for the other applications (H2-STORE). Thus, green diesel production was in the consecutive process to utilize hydrogen via hydrotreating process.

5.1.3 Hydrotreating process

At the optimal condition, the molar flow rate of stearic is depended on H_2 feedstock which one mole of SA may be converted to other hydrocarbon products with two moles of H_2 and thus, SA flow rate is dependent parameter.

5.1.3.1 Green diesel production using multiple-bed reactor

Pressure and temperature of high purity of stearic acid in stream SA and hydrogen in stream PURE-H2 were firstly adjusted to 14.31 atm and 563 K, respectively before forwarding to hydrodeoxygenation reactor [116]. The hydrodeoxygenation reactor contains multiple-catalyst bed where the reactions mainly consisting of hydrodeoxygenation and decarbonylation, decarboxylation reaction can be simultaneously occurred over catalyst bed in this hydrotreating reactor. Based on the simulation, the reaction zones were altered in two zones where the SA was converted to products (R-HDO1) and CO was reacted with H_2 via methanation at equilibrium reaction (R-HDO2). Crude green diesel comprising of three phase products were liquid hydrocarbons as PEND, HEXD, HEPD, OCTD, and OCTDL, gas hydrocarbons as residue of hydrogen, carbon monoxide, methane, ethane and propane, and water which HEPD is the primary product.

จุฬาลงกรณ์มหาวิทยาลัย
Chulalongkorn University

5.1.3.2 Green diesel separation

Two-phase separator (SEP2) was applied to separate gas products from the liquid products from multiple-bed reactor after cooling. The gaseous portion of the stream (FUEL-GAS) was removed from the vessel and the mixture of water and crude green diesel in stream 36 was also separated in the liquid-liquid separator (SEP3). These liquid mixtures of green diesel in stream CRUDE-GD is readily for the further processes such as isomerization which it is not a main consideration in this work. Table 5.1 and 5.2 summarize the specification detailed such as equipment and operating condition and stream table using in the base case.

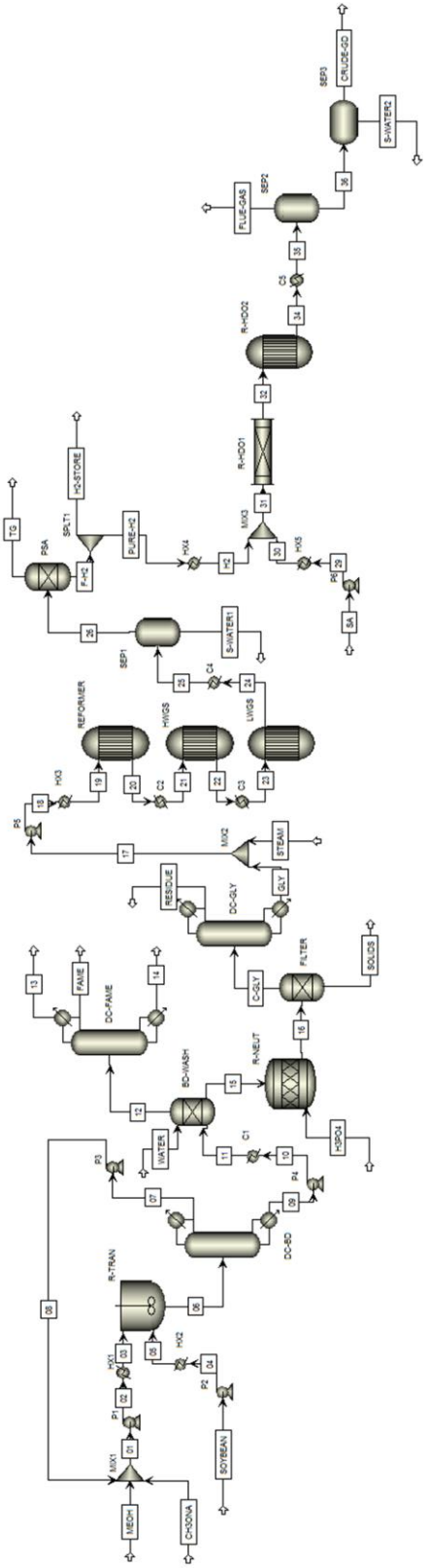

Figure 5. 1 Process flow diagram for base case condition of combined process.

Table 5.1 Unit specification for base case condition of combination process demonstrated in Figure 5.1.

CODE NAME	EQUIPMENT	DESIGN SPECIFICATION
MIX1-MIX3	Stream mixer	Pressure drop: 0.0 atm
SPLT1	Stream splitter	Pressure drop: 0.0 atm Split fraction H2GD: variable parameter (zero value for H_2 storage)
P1-P4	Pump	Discharge pressure: 1.1 atm Pump efficiencies: 0.75
P5	Pump	Discharge pressure: 20 atm Pump efficiencies: 0.75
P6	Pump	Discharge pressure: 14.31 atm Pump efficiencies: 0.75
HX1-HX2	Heater	Pressure drop: 0.0 atm Outlet temperature: 333 K
HX3	Heater	Pressure drop: 0.0 atm Outlet temperature: 1150 K
HX4-HX5	Heater	Pressure drop: 0.0 atm Outlet temperature: 563 K
C1	Coolers	Pressure drop: 0.0 atm Outlet temperature: 333 K
C2	Coolers	Pressure drop: 0.0 atm Outlet temperature: 623 K
C3	Coolers	Pressure drop: 0.0 atm Outlet temperature: 473 K
C4-C5	Coolers	Pressure drop: 0.0 atm Outlet temperature: 308 K
R-TRAN	Transesterification reactor	Adiabatic reactor (heat duty = 0) Pressure drop: 0 atm

Table 5.1 Unit specification for base case condition of combination process demonstrated in Figure 5.1 *(continue).*

CODE NAME	EQUIPMENT	DESIGN SPECIFICATION
DC-BD	Distillation column	Number of stages: 7 stages Above feed stage: 4 Column pressure: 0.98 atm Distillate rate: 1130 kg/hr Mass reflux ratio: 2
BD-WASH	Liquid-liquid extraction column	Number of stages: 6 stages Column pressure: 0.98 atm
DC-FAME	Distillation column	Number of stages: 7 stages Above feed stage: 4 Column pressure: 0.098 atm Bottom rate: 800 kg/hr Mass reflux ratio: 2
R-NUET	Neutralization reactor	Isothermal operation: 323 K Pressure: 1 atm
FILTER	Filter	Na_3PO_4 removal (split fraction = 1)
DC-DLY	Distillation column	Number of stages: 6 stages Above feed stage: 3 Column pressure: 0.098 atm Bottom rate: 943 kg/hr Mass reflux ratio: 2
REFORMER	Glycerol reforming reactor	$C_3H_8O_3 + 3H_2O \rightleftharpoons 3CO_2 + 7H_2$ $CH_3OH + H_2O \rightleftharpoons CO_2 + 3H_2$ Operating temperature = 1150 K Pressure drop: 0.0 atm

Table 5.1 Unit specification for base case condition of combination process demonstrated in Figure 5.1 *(continue).*

CODE NAME	EQUIPMENT	DESIGN SPECIFICATION
HWGS	High water gas shift reactor	$CO + H_2O \rightleftarrows CO_2 + H_2$ Operating temperature = 623 K Pressure drop: 0.0 atm
LWGS	Low water gas shift reactor	$CO + H_2O \rightleftarrows CO_2 + H_2$ Operating temperature = 473 K Pressure drop: 0.0 atm
SEP1	Separators (Two-outlet flash)	Heat duty: 0 Pressure drop: 0.0 atm
PSA	Pressure swing absorption unit	80% of H_2 from the other gases Pressure drop: 0.0 atm
R-HDO1	Hydrodeoxygenation reactor	Rate-controlled reaction: $SA + 2H_2 \overset{k_1}{\rightleftarrows} OCTDL + H_2O$ $OCTDL \overset{k_2}{\rightleftarrows} HEPD + H_2 + CO$ $OCTDL + H_2 \overset{k_3}{\rightleftarrows} OCTD + H_2O$ $OCTDL + 2H_2 \overset{k_4}{\rightleftarrows} PEND + C_3H_8 + H_2O$ $OCTDL + 2H_2 \overset{k_5}{\rightleftarrows} HEXD + C_2H_6 + H_2O$ Residence time: 6 hr Operating temperature: 563 K Pressure drop: 0.0 atm

Table 5.1 Unit specification for base case condition of combination process demonstrated in Figure 5.1 *(continue).*

CODE NAME	EQUIPMENT	DESIGN SPECIFICATION
R-HDO2	Hydrodeoxygenation reactor	Equilibrium reaction: $CO + 3H_2 \rightleftarrows CH_4 + H_2O$ Operating temperature: 563 K Pressure drop: 0.0 atm
SEP2	Separators (two-outlet flash)	Heat duty: 0 Pressure drop: 0.0 atm
SEP3	Separators (Decanter)	Heat duty: 0 Pressure drop: 0.0 atm

จุฬาลงกรณ์มหาวิทยาลัย
Chulalongkorn University

Table 5.2 Main stream of combination process demonstrated in Figure 5.1.

Stream name	SOYBEAN	MEOH	CH3ONA	01	06	07	09	12
Temperature (K)	298	298	298	319	332	337	432	332
Pressure (atm)	1	1	1	1	1.1	0.98	0.98	1.1
Vapor fraction	0	0	0	0	0	0	0	0
Mass flow rate (kg/hr)	10000	1010.58	90.04	2230.62	12230.62	1130.00	11100.62	10102.77
Volumetric flow rate (m^3/hr)	5.19	1.27	1.53	4.99	16.23	1.52	15.27	10.73
Component mass fraction								
TG-P	0.111	0	0	trace	trace	trace	trace	trace
TG-O	0.284	0	0	trace	0.004	trace	0.004	0.004
TG-L	0.605	0	0	trace	0.028	trace	0.030	0.033
METHANOL	0	1	0.7	0.988	0.097	1	0.005	0.004
GLY	0	0	0	trace	0.077	trace	0.085	trace
DG-P	0	0	0	trace	0.001	trace	0.001	0.001
DG-O	0	0	0	trace	0.005	trace	0.005	0.006
DG-L	0	0	0	trace	0.020	trace	0.022	0.024
MG-P	0	0	0	trace	0.001	trace	0.001	0.001
MG-O	0	0	0	trace	0.002	trace	0.003	0.003
MG-L	0	0	0	trace	0.005	trace	0.005	0.006
FAME-P	0	0	0	trace	0.089	trace	0.098	0.108
FAME-O	0	0	0	trace	0.223	trace	0.246	0.270
FAME-L	0	0	0	trace	0.446	trace	0.492	0.540
CH3ONA	0	0	0.3	0.012	0.002	trace	0.003	trace
H3PO4	0	0	0	0	0	0	0	trace
NA3PO4	0	0	0	0	0	0	0	trace
WATER	0	0	0	0	0	0	0	trace
H2	0	0	0	0	0	0	0	trace
CO	0	0	0	0	0	0	0	trace
CO2	0	0	0	0	0	0	0	trace
O2	0	0	0	0	0	0	0	trace
N2	0	0	0	0	0	0	0	trace
OCTD	0	0	0	0	0	0	0	trace
OCTDL	0	0	0	0	0	0	0	trace
PEND	0	0	0	0	0	0	0	trace
HEPD	0	0	0	0	0	0	0	trace
HEXD	0	0	0	0	0	0	0	trace
SA	0	0	0	0	0	0	0	trace
C3H8	0	0	0	0	0	0	0	trace
C2H6	0	0	0	0	0	0	0	trace
CH4	0	0	0	0	0	0	0	trace

Table 5.2 Main stream of combination process demonstrated in Figure 5.1 *(continue)*.

Stream name	FAME	C-GLY	GLY	STEAM	20	24	26	F-H2
Temperature (K)	467	323	528	298	1100	473	308	308
Pressure (atm)	0.098	1	0.395	1	20	20	20	20
Vapor fraction	0	0	0	0	1	1	1	1
Mass flow rate (kg/hr)	9253.61	1106.86	943.00	1658.76	2601.76	2601.76	1497.63	115.24
Volumetric flow rate (m^3/hr)	11.07	0.91	0.88	1.67	740.66	313.25	129.05	72.97
Component mass fraction								
TG-P	trace	0	0	0	0	0	0	0
TG-O	trace	0	0	0	0	0	0	0
TG-L	trace	0	0	0	0	0	0	0
METHANOL	trace	0.041	trace	0	trace	trace	trace	0
GLY	trace	0.851	0.999	0	trace	trace	0	0
DG-P	0.001	0	0	0	0	0	0	0
DG-O	trace	0	0	0	0	0	0	0
DG-L	trace	0	0	0	0	0	0	0
MG-P	trace	0	0	0	0	0	0	0
MG-O	trace	0	0	0	0	0	0	0
MG-L	trace	0	0	0	0	0	0	0
FAME-P	0.117	trace	trace	0	trace	trace	trace	0
FAME-O	0.293	trace	trace	0	trace	trace	trace	0
FAME-L	0.589	trace	trace	0	trace	trace	trace	0
CH3ONA	0	0	0	0	0	0	0	0
H3PO4	0	0	0	0	0	0	0	0
NA3PO4	0	0	0	0	0	0	0	0
WATER	0	0	0	0	0	0	0	0
H2	trace	0.108	0.001	1	0.519	0.426	0.003	0
CO	0	0	0	0	0.045	0.056	0.097	1
CO2	0	0	0	0	0.146	0.002	0.003	0
O2	0	0	0	0	0.290	0.516	0.897	0
N2	0	0	0	0	0	0	0	0
OCTD	0	0	0	0	0	0	0	0
OCTDL	0	0	0	0	0	0	0	0
PEND	0	0	0	0	0	0	0	0
HEPD	0	0	0	0	0	0	0	0
HEXD	0	0	0	0	0	0	0	0
SA	0	0	0	0	0	0	0	0
C3H8	0	0	0	0	0	0	0	0
C2H6	0	0	0	0	0	0	0	0
CH4	0	0	0	0	0	0	0	0

Table 5.2 Main stream of combination process demonstrated in Figure 5.1 *(continue)*.

Stream name	TG	SA	PURE-H2	32	FUEL-GAS	CRUDE-GD
Temperature (K)	308	298	30*	563	N/A	N/A
Pressure (atm)	20	1	20	14.31	1.1	1.1
Vapor fraction	1	0	1	N/A	N/A	N/A
Mass flow rate (kg/hr)	1382.39	N/A	N/A	N/A	N/A	N/A
Volumetric flow rate (m^3/hr)	54.64	N/A	N/A	N/A	N/A	N/A
Component mass fraction						
TG-P	0	0	0	N/A	N/A	N/A
TG-O	0	0	0	N/A	N/A	N/A
TG-L	0	0	0	N/A	N/A	N/A
METHANOL	trace	0	0	N/A	N/A	N/A
GLY	0	0	0	N/A	N/A	N/A
DG-P	0	0	0	N/A	N/A	N/A
DG-O	0	0	0	N/A	N/A	N/A
DG-L	0	0	0	N/A	N/A	N/A
MG-P	0	0	0	N/A	N/A	N/A
MG-O	0	0	0	N/A	N/A	N/A
MG-L	0	0	0	N/A	N/A	N/A
FAME-P	trace	0	0	N/A	N/A	N/A
FAME-O	trace	0	0	N/A	N/A	N/A
FAME-L	trace	0	0	N/A	N/A	N/A
CH3ONA	0	0	0	N/A	N/A	N/A
H3PO4	0	0	0	N/A	N/A	N/A
NA3PO4	0	0	0	N/A	N/A	N/A
WATER	0	0	0	N/A	N/A	N/A
H2	0.003	0	0	N/A	N/A	N/A
CO	0.021	0	1	N/A	N/A	N/A
CO2	0.003	0	0	N/A	N/A	N/A
O2	0.973	0	0	N/A	N/A	N/A
N2	0	0	0	N/A	N/A	N/A
OCTD	0	0	0	N/A	N/A	N/A
OCTDL	0	0	0	N/A	N/A	N/A
PEND	0	0	0	N/A	N/A	N/A
HEPD	0	0	0	N/A	N/A	N/A
HEXD	0	0	0	N/A	N/A	N/A
SA	0	0	0	N/A	N/A	N/A
C3H8	0	1	0	N/A	N/A	N/A
C2H6	0	0	0	N/A	N/A	N/A
CH4	0	0	0	N/A	N/A	N/A

5.1.4 Product price analysis

The resulting stream after F-H_2 cannot show in stream table because, they were depended on a portion of H_2 and SA as green diesel feedstocks which was used to produce green diesel. Thus, the function of H_2 spitting to green diesel (H2GD) can be written as:

$$\text{H2GD} = \frac{\text{Total amounts of hydrogen is fed to hydrotreating process (kg/hr)}}{\text{Total amounts of hydrogen is produced from GSM after PSA (kg/hr)}}$$

Thus, Table 5.1 demonstrates the products involve combination process in function of H2GD.

Table 5.3 Products involve combination process as H2GD function.

H2GD	Capacities (kg/hr)		
	Hydrogen	Green diesel	Biodiesel
0	115.24	0.00	9244.10
0.1	103.71	903.64	9244.10
0.2	92.19	1807.29	9244.10
0.3	80.66	2710.93	9244.10
0.4	69.14	3614.57	9244.10
0.5	57.62	4518.22	9244.10
0.6	46.09	5421.86	9244.10
0.7	34.57	6325.51	9244.10
0.8	23.05	7229.15	9244.10
0.9	11.52	8132.79	9244.10
1.0	0.00	9036.44	9244.10

For product price analysis, the price of three alternative fuel can be particularized which they are changed by market world. Hydrogen price deriving from International Energy Agency is depended on producing technologies as “reforming costs 2.23-4.12 USD/kg (16-29 USD/GJ), electrolysis costs 2.84-5.68 USD/kg (20-40

USD/GJ), and the large scale natural gas reforming cost 0.71-1.14 USD/kg (5-8 USD/GJ), which based on energy and investment costs. Moreover, the cost from transportation is added depending on distance as 2.13-2.84 USD/kg (15-20 USD/GJ) for 100 miles [117]. Thus, the hydrogen price for this work obtaining from average cost from reforming process is 3.20 USD/kg. For green diesel, the carbon range of the liquid products was achieved in C15 to C18 within C10-C28 of typical diesel range. Thus, this renewable diesel cost was estimated to petroleum based diesel. Both diesel and biodiesel (B100) prices were received from Alternative Fuels Data Center using national average price between 1 to 15 January 2015 that 0.94 USD/kg (3.06 USD/gallon) and 1.21 USD/kg (4.02 USD/gallon), respectively [117]. Thus, the linear function of product cost can be written by:

$$Y = 3.20 \times X_{Hydrogen} + 0.94 \times X_{Green\ diesel} + 1.21 \times X_{Biodiesel}$$

where: $X_{Hydrogen}$ = Total hydrogen capacities, kg/hr

$X_{Green\ diesel}$ = Total green diesel capacities, kg/hr

$X_{Biodiesel}$ = Total biodiesel capacities, kg/hr

Y = Total product incomes, USD/hr

In fact, three alternative fuel product distribution cannot be precised prediction due to depend on the world market demand. Thus, the total income was applied to obtain the suitable product distribution for maximum cost in this work. Table 5.3 and Figure 5.2 suggest that the total hydrogen production should be used for hydrotreating process to achieve the maximum total income. This result can be agreement because: (1) the process provides high of two renewable diesels capacity with low hydrogen consumption; (2) hydrogen fuel using for car becomes more expensive when it is replaced to existing infrastructure such as gasoline and diesel, because the additional cost from transportation to gas station; (3) hydrogen offers high energy density (142 MJ/kg) comparing with green diesel (44 MJ/kg) and biodiesel (38 MJ/kg), but it is highly inflammable; (4) liquid fuels can be transported through pipelines, coal can be carried on the trucks or belt, but hydrogen is hard to transport on the long distance which is suitable for industrial estate.

จุฬาลงกรณ์มหาวิทยาลัย
Chulalongkorn University

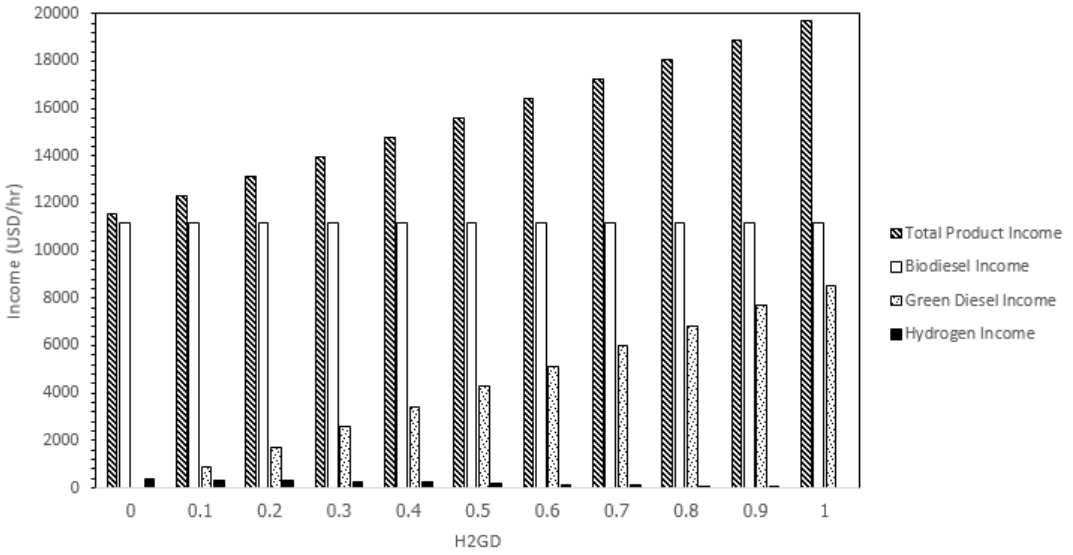

Figure 5.2 Total product income analysis of this combination process.

In additional, the overall energy consumption including heating and cooling for base case condition was also depended on H2GD as shown in Figure 5.3. The overall energy consumption was increased when increasing of hydrogen feed for green diesel production because the reactions occurring in multiple bed which reactor required high temperature. Heat requirement was related to preheat the reactants before feeding to process and cooling the product before phase separation. Table 5.4 shows the overall energy consumption for base case condition of combination process using H2GD = 1. Figure 5.4 surprisingly illustrates that the total energy consumption was existing into the biodiesel production section. However, based on energy consumption per capacities (Figure 5.5) clearly indicates that the hydrogen production section is the highest energy consumption.

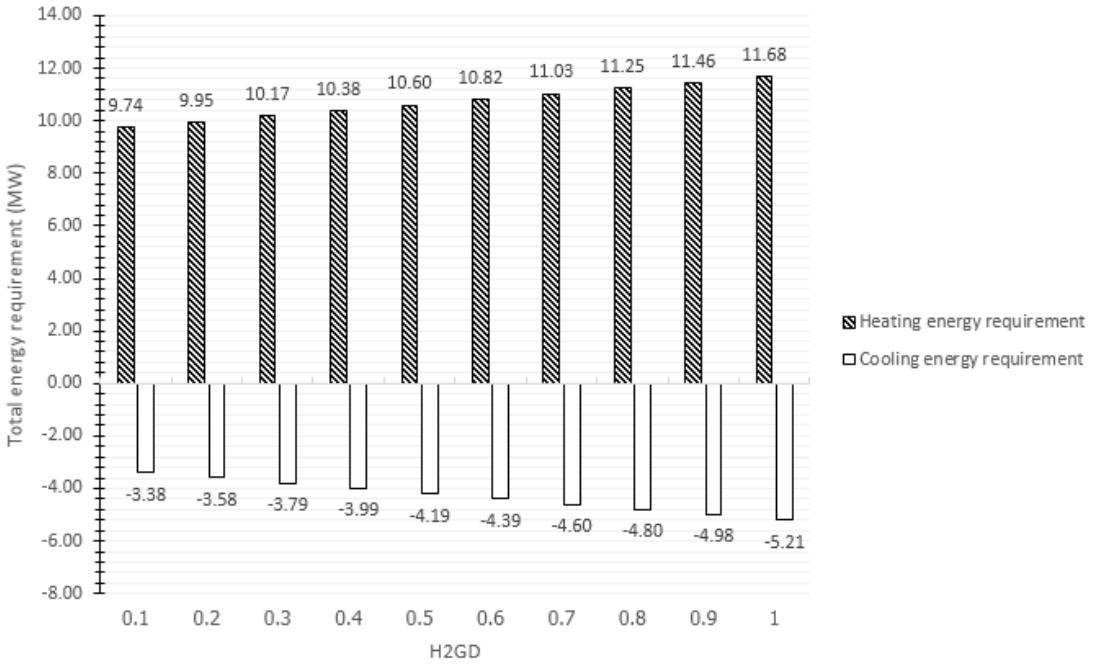

Figure 5.3 Energy analysis each of processes for base case condition of combined process against H2GD.

จุฬาลงกรณ์มหาวิทยาลัย
Chulalongkorn University

Table 5.4 Example of total energy requirement for the base case condition of combination process using H2GD = 1.

Equipment	Name	Energy requirement (MW)	
		Heat	Cooling
MIX	**MIX1**	0	0
	MIX2	0	0
Splitter	**SPLT1**	0	0
Pump	**P1**	0	0
	P2	0	0
	P3	0	0
	P4	0	0
	P5	0	0
	P6	0	0
Heater	**HX1**	0.030	0
	HX2	0.200	0
	HX3	2.601	0
	HX4	0.128	0
	HX5	1.941	0
Cooler	**C1**	0	-0.711
	C2	0	-0.981
	C3	0	-0.242
	C4	0	-1.015
	C5	0	-2.021
Valve	**V3**	0	0
Turbine	**TURB1**	0	0
Reactor	**R-TRAN**	0	0
	R-NUET	0	-0.067
	REFORMER	0.612	0
	HWGS	0	-0.127
	LWGS	0	-0.015
	R-HDO1	0.089	0
	R-HDO2	0	-0.007
Separator	**DC-BD**	1.749	0
	DC-FAME	3.908	0
	DC-GLY	0.421	0
	BD-WASH	0	0
	Filter	0	0
	SEP1	0	0
	SEP2	0	0
	PSA	0	0
Total		11.68	-5.21

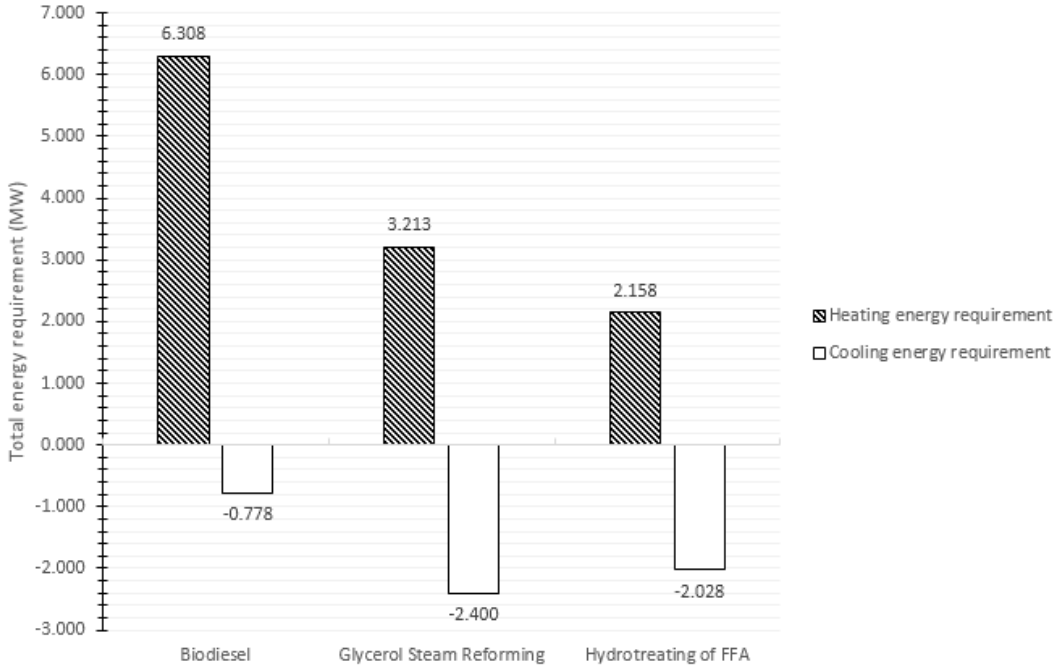

Figure 5.4 Energy analysis each of processes for base case condition of combined process using H2GD = 1.

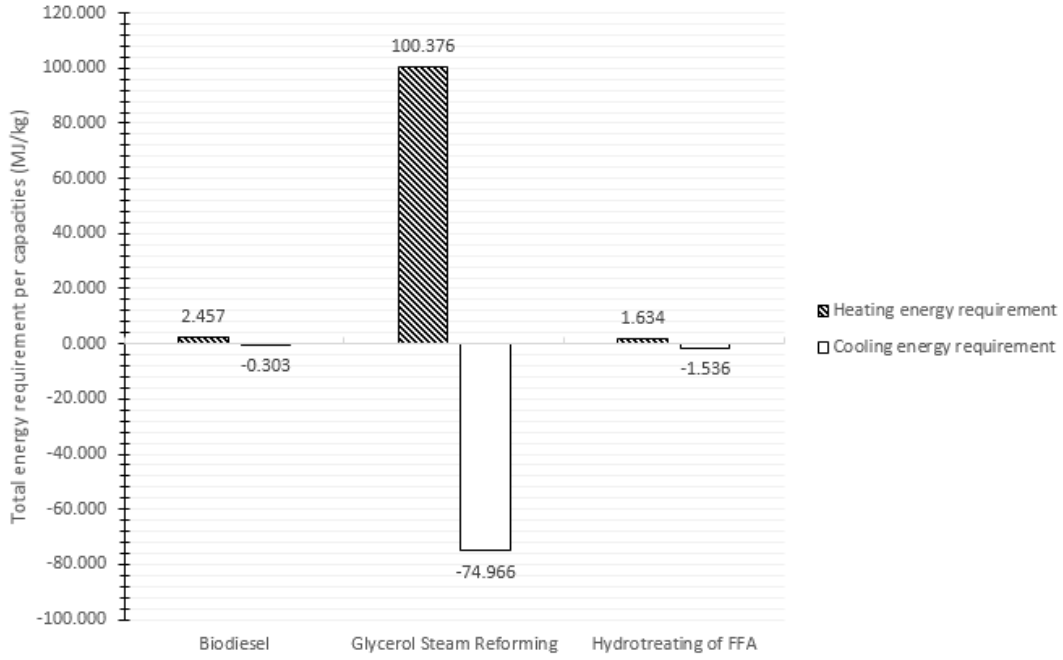

Figure 5.5 Energy consumption per capacities each of processes for base case condition of combined process using H2GD = 1.

5.2 Improvement strategies for combination process

5.2.1 Improvement strategy 1

To improve this combination process, the overall equipment in base case was analyzed based on the operating condition adjustment and the numbers of unit operation in order to achieve more efficiency process.

5.2.1.1 Biodiesel production improvement strategy 1

From base case condition (Figure 5.1), the mechanically stirred tank reactor is a suitable reactor to reduce mass transfer limitation between oil and alcohol as immiscible phase during reaction because no induction period was observed for all conditions (Figure 4.2). Although many researchers suggest that the decrease in mass transport limitation using several technologies such as ultrasonic irradiation and hydrodynamic cavitation, they suffer in industrial scale such as high energy consumption, equipment damage [118]. After transesterification reactor, recycle methanol from transesterified product is the main considered point due to it can reduce amount of methanol usage in this process. Distillation column (DC-BD) clearly uses to separate methanol from the other products, because of the low boiling point of methanol comparing to the other transesterified products (relative volatility >various product and glycerol might be decomposed at the high temperature during distillation process. Liquid-liquid extraction was used to separate polar as water methanol, and glycerol and non-polar as residue oil and FAMEs in the conventional biodiesel production. Water was used as a cheap solvent at low temperature extraction. FAMEs was separated from residue oil, water and methanol in the distillation column (DC-FAME) using partial condenser. Crude glycerol stream (C-GLY) comprising of glycerol, water, and methanol after solid filtration is also aimed to improve the biodiesel production efficiency. Typically, water and alcohol must be removed to obtain 50-80% of crude glycerol whereas 99% or higher purity is used for feeding in pharmaceutical and cosmetic industries and hence, distillation unit for glycerol purification is used in the conventional process. In this work, crude glycerol stream may be directly used as reactant for glycerol steam reforming process. Thus, the distillation of purification glycerol (DC-GLY) was discarded from the biodiesel production process.

5.2.1.2 Glycerol steam reforming improvement strategy 1

The mixture of glycerol, water and methanol from biodiesel production can be converted to hydrogen via glycerol and methanol stream reforming. In C-GLY stream, the molar ratio of glycerol-methanol is about 7.5, and then, the thermodynamic of two reforming reaction was recalculated as a function of steam to glycerol-methanol molar ratio (WGMR). The results of process improvement strategy 1 are shown in Figure 5.6-5.11 as comparable to Figure 4.4 - 4.8; (1) the molar feed ratio found in Figure 5.6 is corresponding to Hajjaji works [5] as 9 of WGMR; (2) The optimal temperature found in Figure 5.7 is obtained with the same value found in Figure 4.4; (3) No methanation occurs in reaction zone after 1150K (Figure 5.8 and 4.5); (4) Coke deposition can be neglected through the three reactors as see in Figure 5.9 and 4.6; (5) Mole of carbon monoxide reaction (Figure 5.10 and 4.7) and carbon dioxide produce (Figure 5.11 and 4.8) were in the similar trend during reaction via glycerol decomposition, water-gas shift, and methanol reforming reaction.

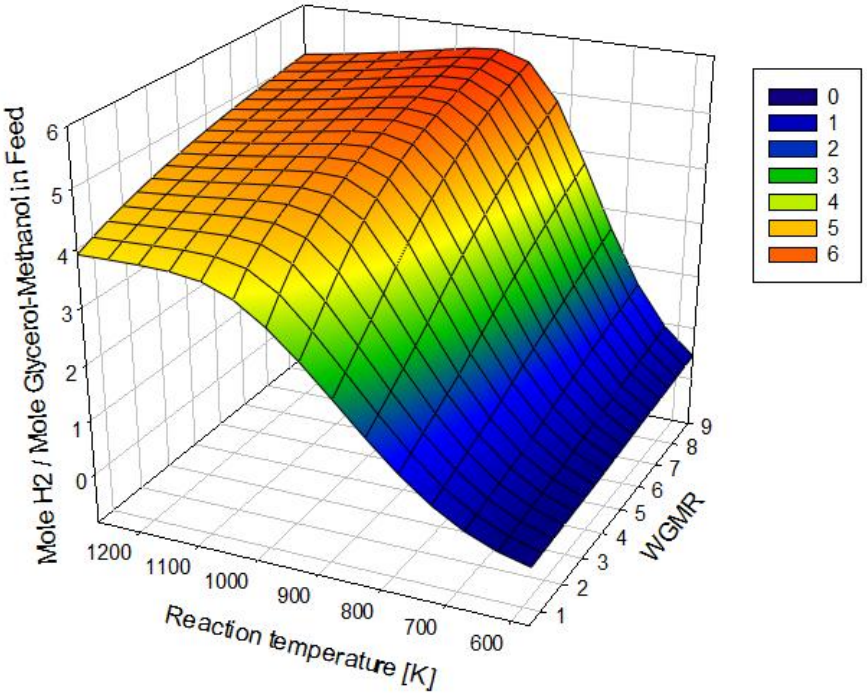

Figure 5.6 Mole of hydrogen produces per mole of glycerol-methanol as a function WGMR and temperature of reformer under 0.98 atm.

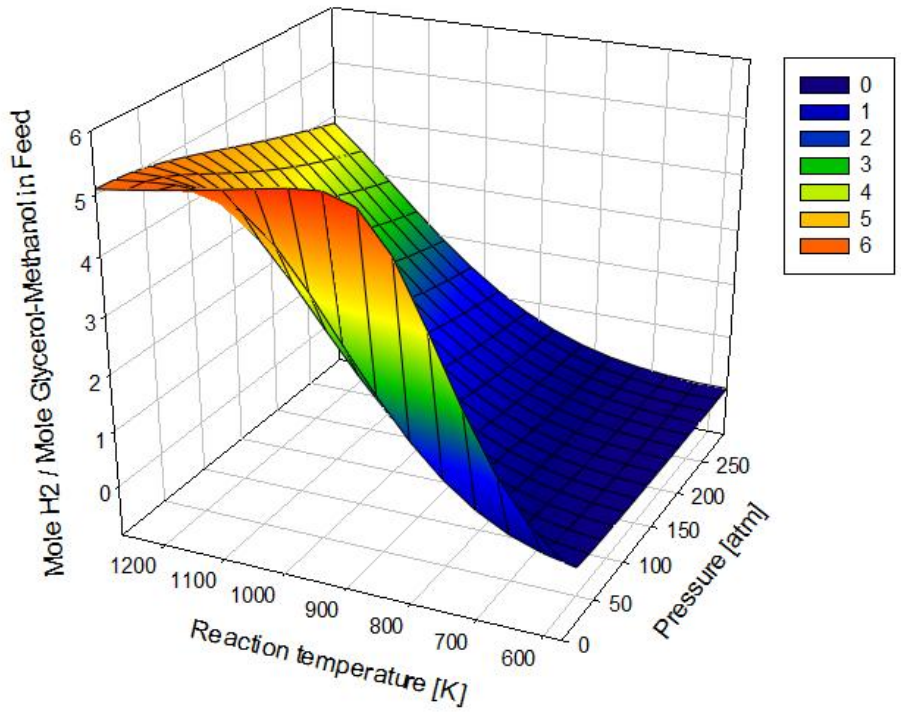

Figure 5.7 Mole of hydrogen produces per mole of glycerol-methanol as a function pressure and temperature of reformer for WGMR = 9.

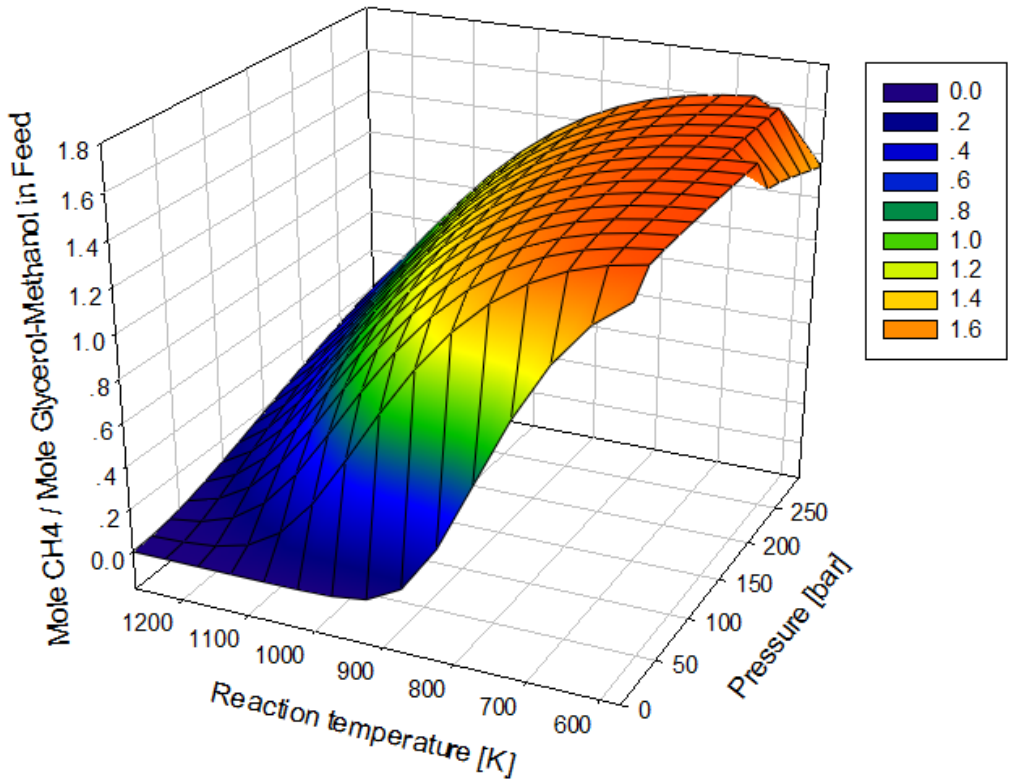

Figure 5.8 Mole of methane produces per mole of glycerol-methanol as a function temperature and pressure of reformer for WGMR = 9.

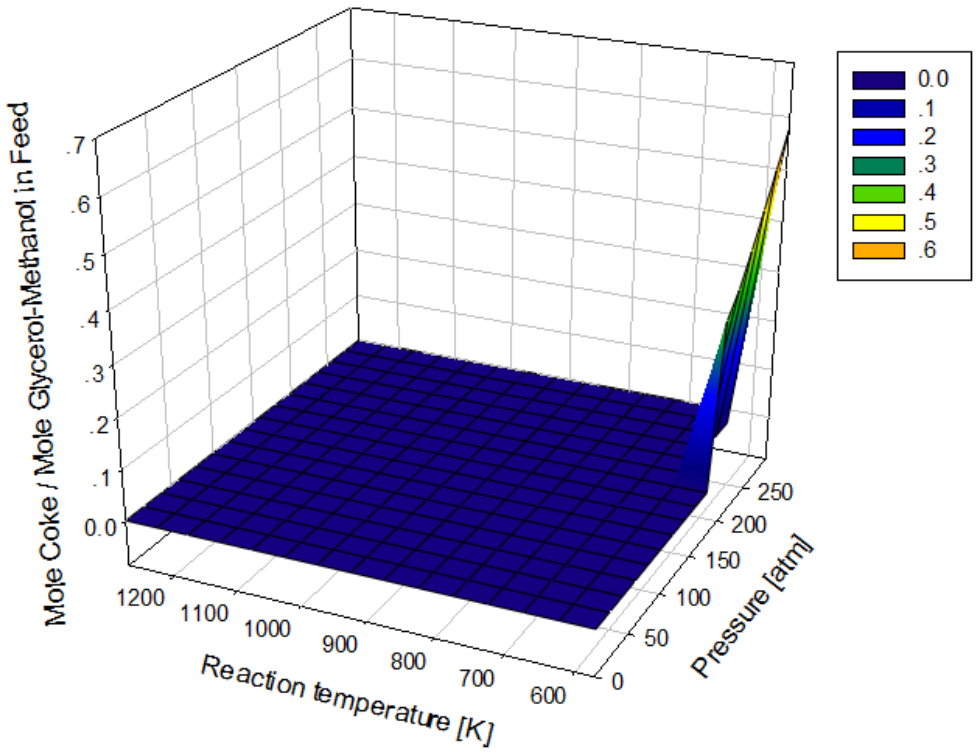

Figure 5.9 Mole of coke produces per mole of glycerol-methanol as a function temperature and pressure of reformer for WGMR = 9.

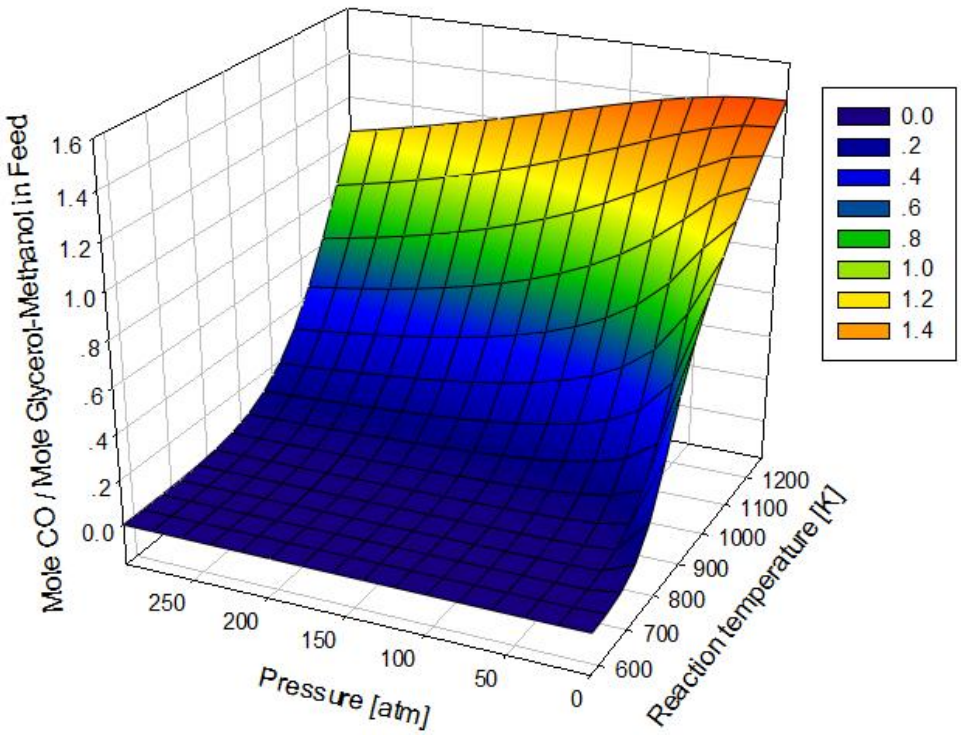

Figure 5.10 Mole of carbon monoxide produces per mole of glycerol-methanol as a function temperature and pressure of reformer for WGMR = 9.

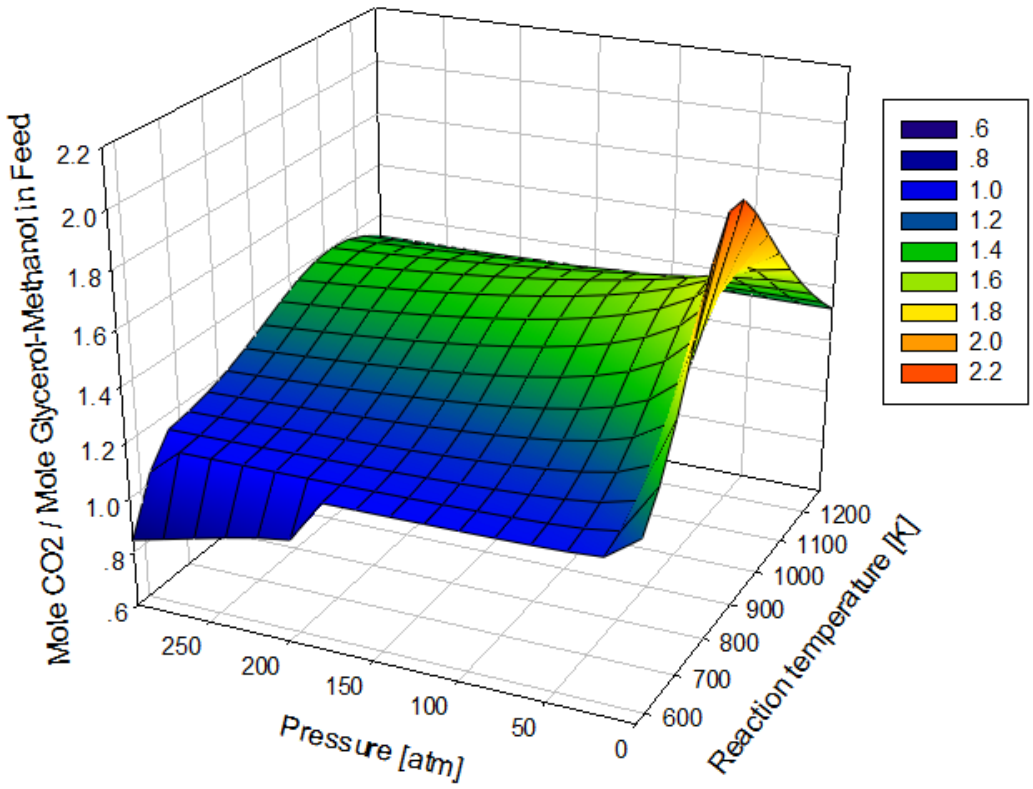

Figure 5.11 Mole of carbon dioxide produces per mole of glycerol-methanol as a function temperature and pressure of reformer for WGMR = 9.

Nevertheless, the optimal operating condition for the three reactors of glycerol steam reforming are related from the two process explaining biodiesel production at the glycerol-methanol stream (C-GLY) and the hydrotreating process for hydrogen feed stream (H2). From base case condition, the glycerol conversion reactor (REFORMER), high water-gas shift reactor (HWGS), and low water-gas shift reactor (LWGS) were operated under 14.31 atm. The hydrogen from LWGS off stream was purified from the other products via pressure swing adsorption unit (PSA). Mole of hydrogen at the optimal operating condition (P = 14.31 atm, T = 1150 K) was 5.43 as seen in Figure 4.4. Therefore, the new optimal operating condition might be adjusted by changing of temperature or WGMR to provide the same mole hydrogen production under the pressure of 14.31 atm. Figure 5.12 clearly illustrates that the glycerol-methanol mixture cannot provide hydrogen producing as same as the base case condition for any operating temperature. WGMR was adjusted to 13.5 to maintain the mole of hydrogen from base case as shown in Figure 5.13. Consequently, the operating condition for glycerol steam

reforming section was adjusted to 13.5 of WGMR using 14.31 atm of pressure, and 1150 K of reformer temperature. After adjust operating condition, hydrogen capacity increased because, methanol was converted to hydrogen via methanol steam reforming along with the energy consumption decreased due to the increase of steam ratio (Table 5.5).

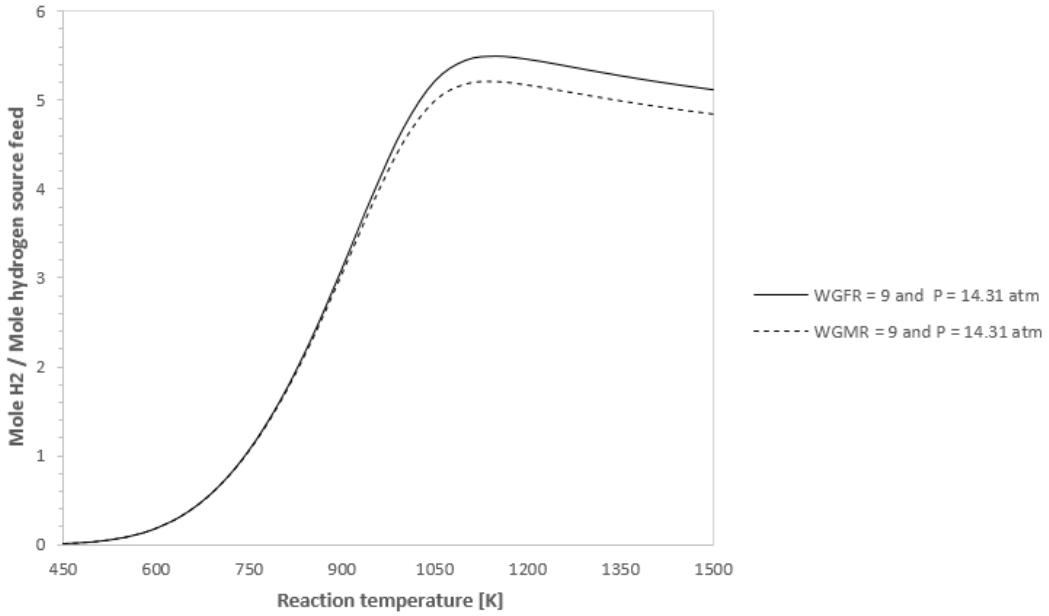

Figure 5.12 Comparison of operating pressure to mole of hydrogen produces per mole of hydrogen source as a function temperature of reformer at 9 of steam to hydrogen source feed molar ratio.

Chulalongkorn University

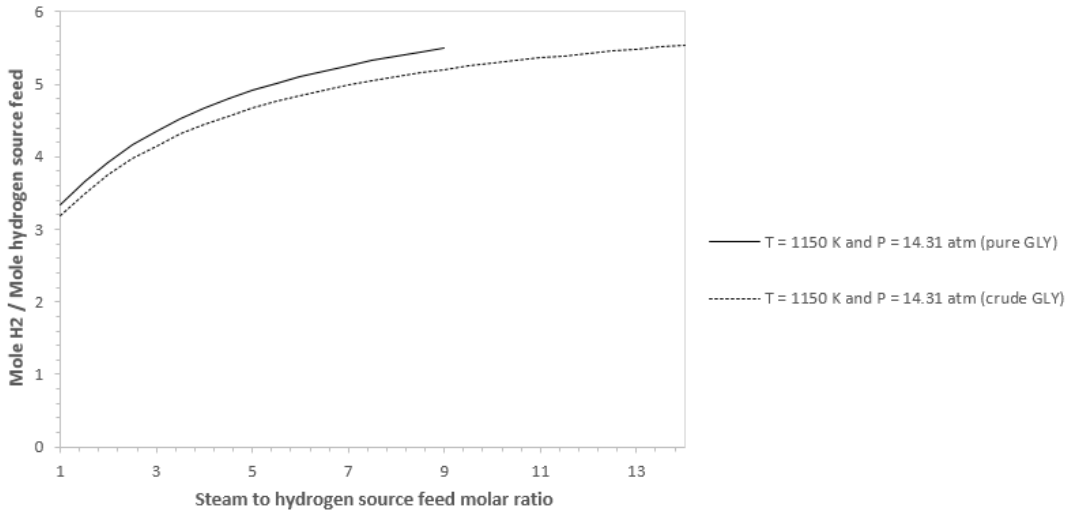

Figure 5.13 Evaluation of operating pressure to mole of hydrogen produces per mole of hydrogen source as a function steam to hydrogen source feed molar ratio at 1150 K of reformer temperature.

จุฬาลงกรณ์มหาวิทยาลัย
Chulalongkorn University

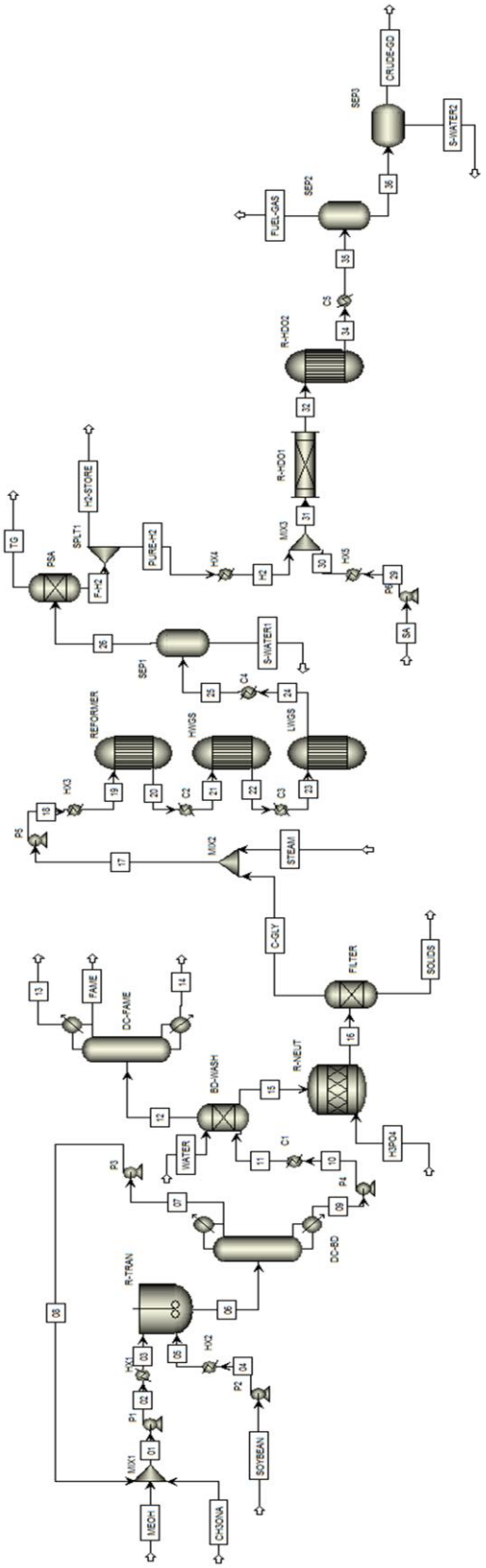

Figure 5.14 Process flow diagram for improvement strategy 1 of combined process.

Table 5.5 Comparison of base case and improvement strategy 1 processes.

Parameters	**Original**	**Improvement strategy 1**
Soybean feed rate (kg/hr)	10,000	10,000
Hydrogen source feed	99.9 wt.% glycerol	Glycerol-methanol
Steam to feed molar ratio	9	13.5
Hydrogen to SA feed molar ratio	1.5	1.5
Reformer T (K) and P (atm)	1150, 14.31	1150, 14.31
HWGS T (K) and P (atm)	623, 14.31	623, 14.31
LWGS T (K) and P (atm)	473, 14.31	473, 14.31
H2GD	1	1
Soybean oil conversion (%)	96.16	96.16
Feed conversion (%)	100	100
SA conversion (%)	99.79	99.79
Reactors	7	7
Columns	3	2
Pressure changers	6	6
Preheating units	6	6
Cooling units	6	6
Separators	3	3
FAMEs purity (wt.%)	99.80	99.80
Hydrogen purity (wt.%)	~100	~100
Green diesel purity (wt.%)	99.28	99.28
Biodiesel capacities (kg/hr)	9,244.10	9,244.10
Hydrogen capacities (kg/hr)	115.24	125.55
Green diesel capacities (kg/hr)	9034.56	9845.28
Heating energy requirement (MW)	12.66	14.02

จุฬาลงกรณ์มหาวิทยาลัย
Chulalongkorn University

5.2.2 Improvement strategy 2

The overall byproduct summarizing in Table 5.6 can be used in the each section as the aimed of this improvement strategy 2.

5.2.2.1 Biodiesel production improvement strategy 2

Table 5.6 shows the outlet stream of biodiesel production from the improvement strategy 1 flow sheet which the three streams are comprised of: (1) the solid of trisodium phosphate (Na_3PO_4) derived from alkali neutralization via stream SOLIDS; (2) methanol, FAMEs residue and water withdrawn from the top of distillation column (DC-FAME) by partial condenser via stream 13; (3) the components of vegetable oil residue from the bottom of the FAME purification column.

Table 5.6 Effluent stream table of biodiesel production from improvement strategy 1.

Stream name	**SOLIDS**	**13**	**14**
Temperature (K)	323	467	601
Pressure (atm)	1	0.0987	0.0987
Vapor fraction	0	1	0
Mass flow rate (kg/hr)	27.33	49.46	800.00
Volumetric flow rate (m^3/hr)	0.02	353.68	0.67
Component mass fraction			
TG-P	0.000	trace	0.006
TG-O	0.000	trace	0.051
TG-L	0.000	trace	0.422
METHANOL	0.000	0.530	trace
GLY	0.000	0.000	0.000
DG-P	0.000	trace	0.013
DG-O	0.000	trace	0.074
DG-L	0.000	trace	0.299
MG-P	0.000	trace	0.012
MG-O	0.000	trace	0.037
MG-L	0.000	trace	0.074
FAME-P	0.000	0.133	trace
FAME-O	0.000	0.138	0.012
FAME-L	0.000	0.195	trace
WATER	0.000	0.004	trace
NA3PO4	1	0	0

5.2.2.1.1 Stream SOLIDS

Trisodium phosphate is always used in the variously heavy cleaning application for household uses by dissolves with the solvent especially hot water. Trisodium phosphate offers a fast cleaning without scrubbing which can be used on wall, refrigerators, machines, and ceramic surface. Moreover, it can remove grease, grime and surface oil deposits motors, engines and other mechanical parts and then, also used as a pre-painting cleaner to surfaces. High concentration of trisodium phosphate can be also used to clean paint, varnish and shellac [119]. Thus, this stream may be sent to the further process in order to obtain trisodium phosphate used grade which this process is not main consideration.

5.2.2.1.2 Stream 13

Although the stream 13 was withdrawn from the FAME purification column contains methanol, water, and FAMEs. This stream cannot be recycled back to mix with fresh alcohol because the soap will be occurred by saponification reaction. Therefore, this stream must be sent to wastewater treatment.

5.2.2.1.3 Stream 14

Stream 14 should be considered since, this stream composes of the unconverted oil (~100 wt.% purity) with high mass flow rate (Table 5.8). Consequently, the stream 14 is recycled back to mix with fresh soybean oil and keep constant feed flow rate before feed to transesterification reactor. Thus, the FAMEs purification column must be adjust new optimal operating condition which offers biodiesel product greater than 99.6 wt.% as following ASTM specification [88]. Figure 5.15 clearly indicates that optimal operating condition for FAME distillation column can be carried out at 383 K of condenser temperature and 800 kg/hr of bottom rate which achieves biodiesel purity conformed ASTM standard.

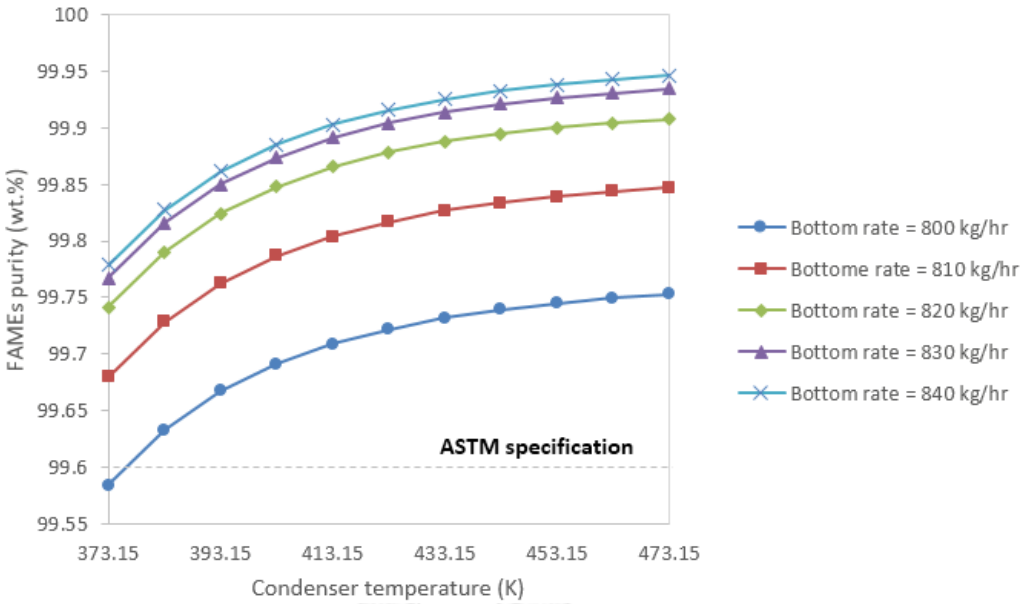

Figure 5.15 Influence of condenser temperature and bottom rate toward FAMEs purity.

The vessel (MIX4) and pump (P7) were installed for containing and transferring fresh soybean oil in stream SOYBEAN and unconverted oil via stream REC-OIL after adjusting the operating condition of FAME distillation column. The temperature of mixed vegetable oil (MIXEDOIL) rises from 298 to 328 K due to heat flow from recycled oil which the heat duty is extremely decreased from 0.20 MW to 0.03 MW.

5.2.2.2 Glycerol steam reforming improvement strategy 2

This section was also consideration to improve overall process as seen below:

Table 5.7 Effluent stream table of hydrogen production from improvement strategy 1.

Stream name	**S-WATER1**	**TG**
Temperature (K)	308	308
Pressure (atm)	14.31	14.31
Vapor fraction	0	0.999
Mass flow rate (kg/hr)	2312.82	1489.18
Volumetric flow rate (m^3/hr)	2.35	83.68
Component mass fraction		
WATER	1.000	0.005
H2	trace	0.021
CO	trace	0.002
CO2	trace	0.972

5.2.2.2.1 Stream S-WATER 1

Water, as a major reactant, was used in the excessive steam, especially, in the hydrogen producing reactors including of reformer, HWGS, and LWGS and operated at WGMR of 13.5. Hence, the reuse of water was absolutely required. The stream S-WATER1 (Table 5.7) is attractive for improvement purpose to recycle to hydrogen production process, because the water in this stream is almost separated from the other product gases to obtain high purity (~100 wt.%) with high mass flow rate. Thus, the large amounts of water from C-GLY, STEAM, and S-WATER1 stream were mixed in vessel (MIX2) as the operating feed ratio before sending to glycerol conversion.

5.2.2.2.2 Stream TG

The impurities such as CO and CO_2 were removed from H_2 by absorbents in the pressure swing adsorption unit (PSA). High pressure (after adjust operating condition from previous strategy) can enhance H_2 purity. The saturated solid containing impurities was fed to regeneration step. Components were desorbed in PSA bed and depressurized, where the species were removed via TG stream by total pressure reduction. Table 5.7 shows that the tail gas contains some hydrogen, because 20 % of total hydrogen is adsorbed by adsorbent and the, this hydrogen is desorbed after sorbent regeneration step. TG stream with high concentration of CO_2 can be used as s fuel stream [120].

จุฬาลงกรณ์มหาวิทยาลัย
Chulalongkorn University

5.2.2.3 Hydrotreating process improvement strategy 2

Table 5.8 Effluent stream table of green diesel production after biodiesel production improvement strategy 2.

Stream name	**S-WATER2**	**FUEL-GAS**
Temperature (K)	308	308
Pressure (atm)	14.31	14.31
Vapor fraction	0	1
Mass flow rate (kg/hr)	857.24	1056.46
Volumetric flow rate (m^3/hr)	0.87	64.81
Component mass fraction		
WATER	1.000	0.002
H2	trace	trace
CO	trace	0.876
OCTD	trace	trace
OCTDL	trace	trace
PEND	trace	trace
HEPD	trace	trace
HEXD	trace	trace
SA	trace	trace
C3H8	trace	0.036
C2H6	trace	0.084
CH4	trace	0.002

จุฬาลงกรณ์มหาวิทยาลัย
Chulalongkorn University

5.2.2.3.1 Stream S-WATER2

The simulation result reveals that this stream (S-WATER2) has high purity of water after separation from phase separator (SEP2). In detailed, stream S-WATER2 should not be reused to glycerol stream reforming process as same as stream S-WATER1. The large amounts of residue water obtaining from stream S-WATER1 were separated from vapor-liquid mixture which a portion of water (liquid phase) in flash drum with some trace of CO, CO_2, and H_2. The less amount of CO, CO_2, and H_2 do not effect on the reaction zone in hydrogen producing reactors which this water can be directly recycled to the process. On the other hand, the water in stream S-WATER2 derived from phase separation was contaminated with some liquid such as oil compounds (OCTD, PEND, HEPD, HEXD). This water must be treated in the water treatment before utilization.

5.2.2.3.2 Stream FUEL-GAS

Byproduct gases consisting of CH_4, C_2H_6, C_3H_8, CO, moisture, and hydrogen residue are attractive purpose to mix (MIX5) with stream TG from PSA off-gas (Table 5.8). The furnace-combustor was installed to produce the energy from the fuel gas in the proposed process which the stoichiometric reactor is selected as suitable model for simulation with the air. This required an oxidizing agent, compressed by fan (FAN1) and preheated combustion air (HX6). In additional, the operating condition and specification of furnace and preheated combustion air are presented in the next improvement strategy.

จุฬาลงกรณ์มหาวิทยาลัย
Chulalongkorn University

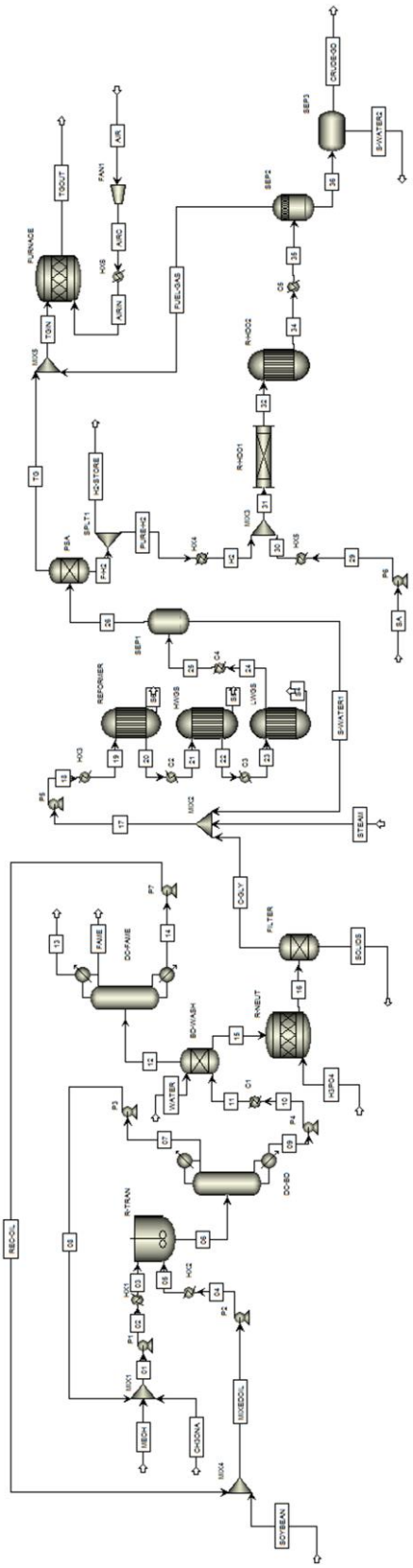

Figure 5.16 Process flow diagram for improvement strategy 2 of combined process.

5.2.3 Improvement strategy 3

5.2.3.1 Heat improvement of combined process.

Heat requirement in the process was aimed to recover crossing with the heat exchangers to preheat heat stream before sending to destination equipment such as reactor. From the improvement strategy 2, tail gas from the PSA outlet stream after adsorbent regeneration (TG) and light gas stream (FUEL) after phase separation were attractive in this strategy. The components (Table 5.9) were fed to furnace-combustor (FURNACE) to oxidize with O_2 in air which is compressed by FAN1 (21 mol% O_2 in air).

Table 5.9 The component mass fraction of gas mixture before sending to combustor.

Stream name	**TGIN**
Temperature (K)	306
Pressure (atm)	1.1
Vapor fraction	0
Mass flow rate (kg/hr)	2547.95
Volumetric flow rate (m^3/hr)	1981.28
Component mass fraction	
METHANOL	trace
FAME-P	trace
FAME-O	trace
FAME-L	trace
WATER	0.025
H2	0.012
CO	0.356
CO2	0.568
OCTD	trace
OCTDL	trace
PEND	trace
HEPD	trace
HEXD	trace
SA	trace
C3H8	0.010
C2H6	0.028
CH4	0.001

Generally, the heater model as a HX6 is represented to preheated combustion air. This unit is the one of the popular technology to improve the heat efficiency and

preheat inlet air before forward to fuel-burners. Industrial Technologies Program Energy Efficiency and Renewable Energy U.S suggests the value of fuel (natural gas) can reduce the energy consumption for different furnace off-gas temperature and preheated combustion air temperature which can be estimated the energy cost reduction following the Table 5.10 [121].

Table 5.10 Percentage of fuel cost saving derived from using preheated combustion air [121].

Furnace exhaust temperature, K	**Preheated air temperature, K**					
	589	**700**	**811**	**922**	**1033**	**1144**
811	13	18	-	-	-	-
922	14	19	23	-	-	-
1033	15	20	24	28	-	-
1144	17	22	26	30	34	-
1255	18	24	28	33	37	40
1367	20	26	31	35	39	43
1478	23	29	34	39	43	47
1589	26	32	38	43	47	51

Note: 10% excess air required for natural gas

จุฬาลงกรณ์มหาวิทยาลัย
Chulalongkorn University

Although, the fuel sources of furnace combustor uses only residue gas stream from the process, and likewise, the energy from furnace are only obtained from the inlet enthalpy from air (stream AIRIN) and tail gas mixture (stream TGIN), and oxidation of combustible component. Table 5.10 may be used as guideline for preheated air temperature in order to achieve the possible heat recovery from the heat exchanger network, because the energy consumption for the whole process is related with the preheated air temperature. Process flow diagram from the improvement strategy 2 was developed to obtain the new process before the heat recovery analysis as given in Figure 5.17.

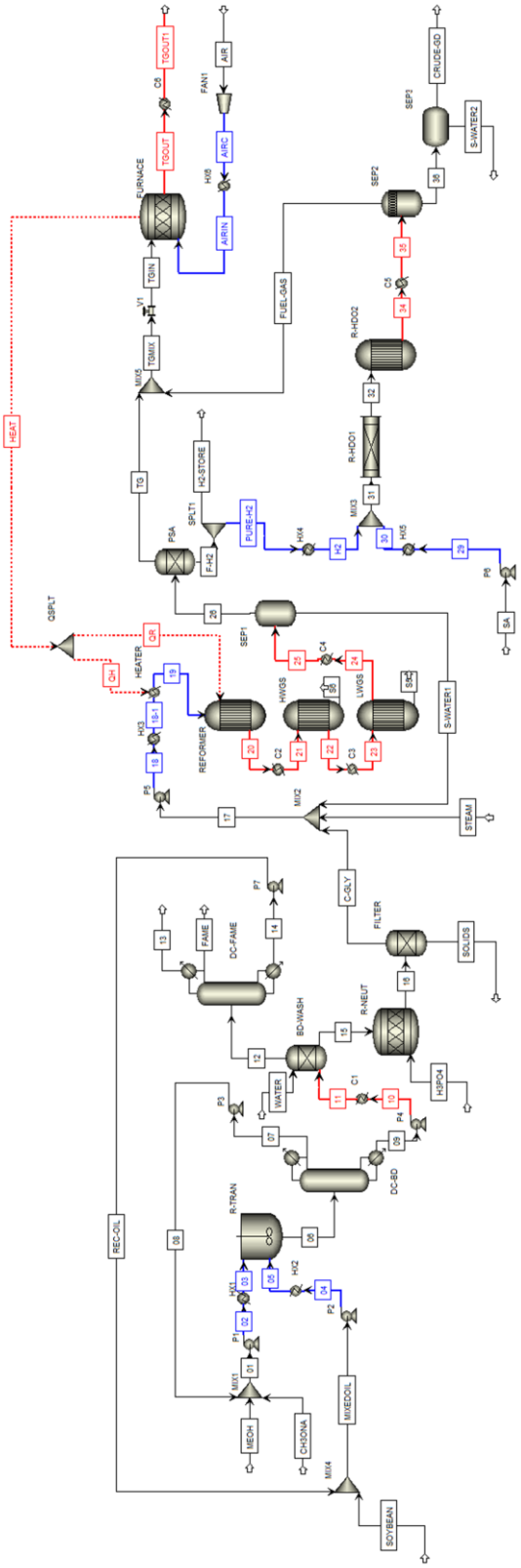

Figure 5.17 Process flow diagram for improvement strategy 3 of combined process before heat recovery analysis; (1) hot stream = red; (2) cold stream = blue.

The heater (HEATER) is represented the tube bundles in the furnace which received the all heat duty in order to provide the desirable temperature before feeding to reforming reactor. Thus, the exhaust temperature of the preheated combustion air is an independent variable. The cooler (C6) was installed to decrease the exhaust gas stream temperature before releasing from the process. In fact, the main reason of C6 was installed in the process, because, it was used to recover the large amounts of enthalpy in exhaust gas stream back to the process via heat integration. Table 5.11 shows a list of hot and cold streams which were taken from the overall process in the Figure 5.17.

Table 5.11 Energy loads in each of heat exchangers presented in Figure 5.18.

Type	**Name**	**Inlet temperature (K)**	**Outlet temperature (K)**	**mCp (W/K)**	**Enthalpy (W)**
Cold	**HX1**	319	333	2102.69	30000.61
Cold	**HX2**	328	333	5846.27	30077.60
Cold	**HX3**	301	NA	NA	NA
Cold	**HX4**	309	563.	506.57	128937.69
Cold	**HX5**	308	563	8045.80	2049103.45
Cold	**HX6**	310	NA	NA	NA
Hot	**C1**	429	333	7159.04	-682628.45
Hot	**C2**	1150	623	2537.65	-1336963.25
Hot	**C3**	623	473	2382.71	-357405.86
Hot	**C4**	473	308	11946.67	-1971200.52
Hot	**C5**	563	308	9568.81	-2438611.98
Hot	**C6**	1250	313	2750.27	-2576592.83

N/A Presented by authors as “not available” in bibliography.

Pinch technology is a practical methodology to minimize the energy consumption in the chemical process using the First and Second law of Thermodynamics to achieve the feasible energy result. The First Law of Thermodynamics offers the energy balance to calculate the change of enthalpy and The

Second Law of Thermodynamic provides the heat flow direction which the heat must flow from the higher temperature to lower temperature and temperature crossover is prohibited. The pinch analysis is applied to identify the number of heat exchanger network which it is the first design from minimum the external heat utility requirement via pinch point [125].

Energy integration was used to manage the amounts of heat (Figure 5.17) by the minimum approach temperature (ΔT_{min}) as estimated at first of calculation. ΔT_{min} = 15 K was chosen to use in this simulation and then, the pinch temperature and minimum energy requirement were derived by the software The Heat Exchanger Network version 1.0.

According to the result of pinch analysis in Table 5.12 shows that the combined process in the improvement strategy 3 do not need the minimum heat requirement for any preheated combustion air temperature (K) which the heater is not additional installed in the process. When the inlet temperature of air stream increases, the total heat recovery increases and the number of total heat exchanger in process decreases. The optimal operating temperature of preheated combustion air temperature (Figure 5.17) may be obtained at 850-1150 K with 16 heat exchangers, but at low temperature range (850-950 K) provides the low energy from furnace which relates to HX3 duty requirement. The comparison of coolers required in of 1050 and 1150 K showed that the exhaust gas stream in Table 5.13 was used in pinch analysis. This result may not be agreed, because: (1) the heat flow in reformer and LWGS outlet stream (C2 and C4) were not used in the heat exchanger network which they should be firstly used to connect with other heat exchangers in the process; (2) Enthalpy in LWGS outlet stream (C3) was used in the small amounts; (3) The exhaust gas stream was not directly used to supply energy to unit operation because, it can be corrosive equipment ,which the energy of this gas is apply to produce steam to supply heat for any equipment required high temperature. Unlike preheated combustion air temperature of 1050 K (Table 5.14), the energy in the process is firstly used in energy integration. Furthermore, the cooler (C6) can be discarded from the process which decrease the minimum cooling requirement from 4,639,498.5 W to 2,062,905.5 W as 55.54 % cooling energy saving and then, the simple and detailed heat exchangers networks are illustrated in Figure 5.18 and 5.19.

Table 5.12 Influence of preheated combustion air temperature (K) toward the pinch analysis result.

Preheated combustion air temperature (K)	Heat duty from furnace (W)	Minimum heat requirement (W)	Minimum cooling requirement (W)	No. heat exchanger	No. heater requirement	No. cooler requirement	Heat recovery from heat exchangers (W)	Total heat recovery (W)
550	~2,797,030	0	~4,639,498	17	0	4	~4,648,756	~7,444,677
650	~2,954,466	0	~4,639,498	12	0	5	~4,648,756	~7,602,112
750	~3,115,472	0	~4,639,498	11	0	5	~4,648,756	~7,763,119
850	~3,280,045	0	~4,639,498	10	0	6	~4,648,756	~7,927,692
950	~3,447,968	0	~4,639,498	10	0	6	~4,648,756	~8,095,615
1050	~3,618,929	0	~4,639,498	10	0	6	~4,648,756	~8,266,575
1150	~3,792,589	0	~4,639,498	10	0	6	~4,648,756	~8,440,236

Table 5.13 Energy loads in coolers and heaters after pinch analysis presented in Figure 5.17 using preheated combustion air temperature = 1150 K.

No.	**Heat stream**	**Temperature inlet (K)**	**Temperature outlet (K)**	**Heat (W)**
Cooler 1	C1	429	333	682,628.4
Cooler 2	C2	1150	623	1,336,963.5
Cooler 3	C3	559	473	204,097.3
Cooler 4	C4	391	308	986,459.8
Cooler 5	C5	344	308	344,246.4
Cooler 6	C6	708	313	1,085,103.1
The minimum cold utility requirement				**4,639,498.5**

Table 5.14 Energy loads in coolers and heaters after pinch analysis presented in Figure 5.17 using preheated combustion air temperature = 1050 K.

No.	**Heat stream**	**Temperature inlet (K)**	**Temperature outlet (K)**	**Heat (W)**
Cooler 1	C1	429	333	682,628.4
Cooler 2	C2	631	623	19,133.4
Cooler 3	C3	559	473	204,097.3
Cooler 4	C4	377	308	817,876.9
Cooler 5	C5	344	308	339,169.5
Cooler 6	C6	1250	313	2,576,593
The minimum cold utility requirement				**4,639,498.5**

จุฬาลงกรณ์มหาวิทยาลัย
Chulalongkorn University

Table 5.15 Summarization of pinch temperature and heat recovery each of heat exchangers after pinch analysis at 1050 K of preheated air temperature.

No. heat exchangers	Cold stream	Heat stream	Temperature hot inlet (K)	Temperature hot outlet (K)	Temperature cold inlet (K)	Temperature cold outlet (K)	Heat recovery (W)
1	**HX6**	**C2**	1150	682	310	1050	1,182,763.60
2	**HX5-4**	**C3**	623	563	545	563	135,770.13
3	**HX4**	**C2**	682	631	309	563	121,731.27
4	**HX5-3**	**C3**	563	559	544	545.	2,787.84
5	**HX5-2**	**C5**	563	488	454	544	713,712.30
6	**HX3-2**	**C5**	488	473	453	473	130,815.03
7	**HX5-1**	**C5**	473	344	298	453	1,232,965.25
8	**HX3-1**	**C4**	473	382	301	453	1,082,568.64
9	**HX2**	**C4**	382	379	328	333	22,875.71
10	**HX1**	**C4**	379	377	319	333	22,756.60
Total heat recovery							**4,648,756.52**

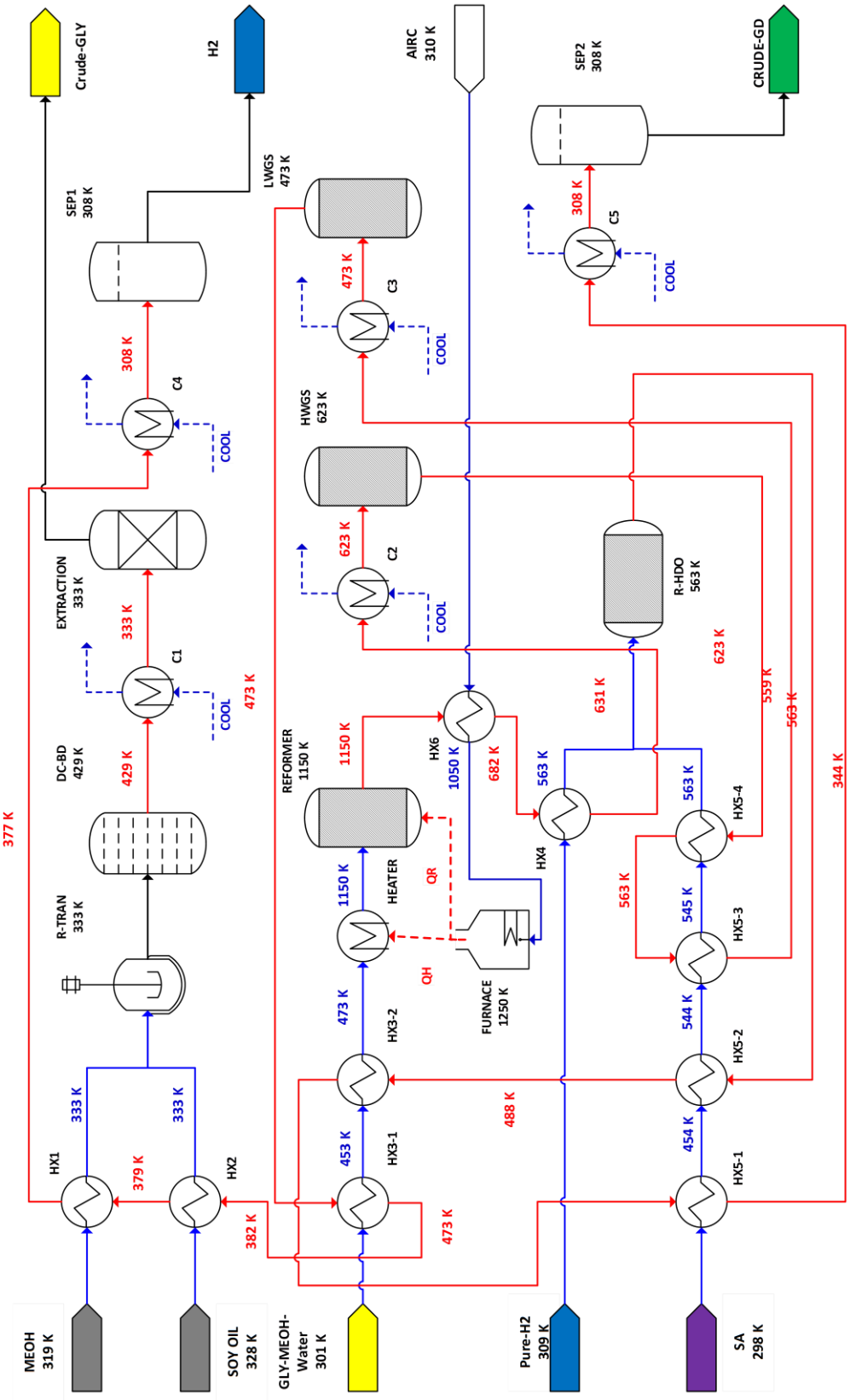

Figure 5.18 The simple heat exchangers networks and heat flow after pinch analysis; (1) hot stream = red; (2) cold stream = blue.

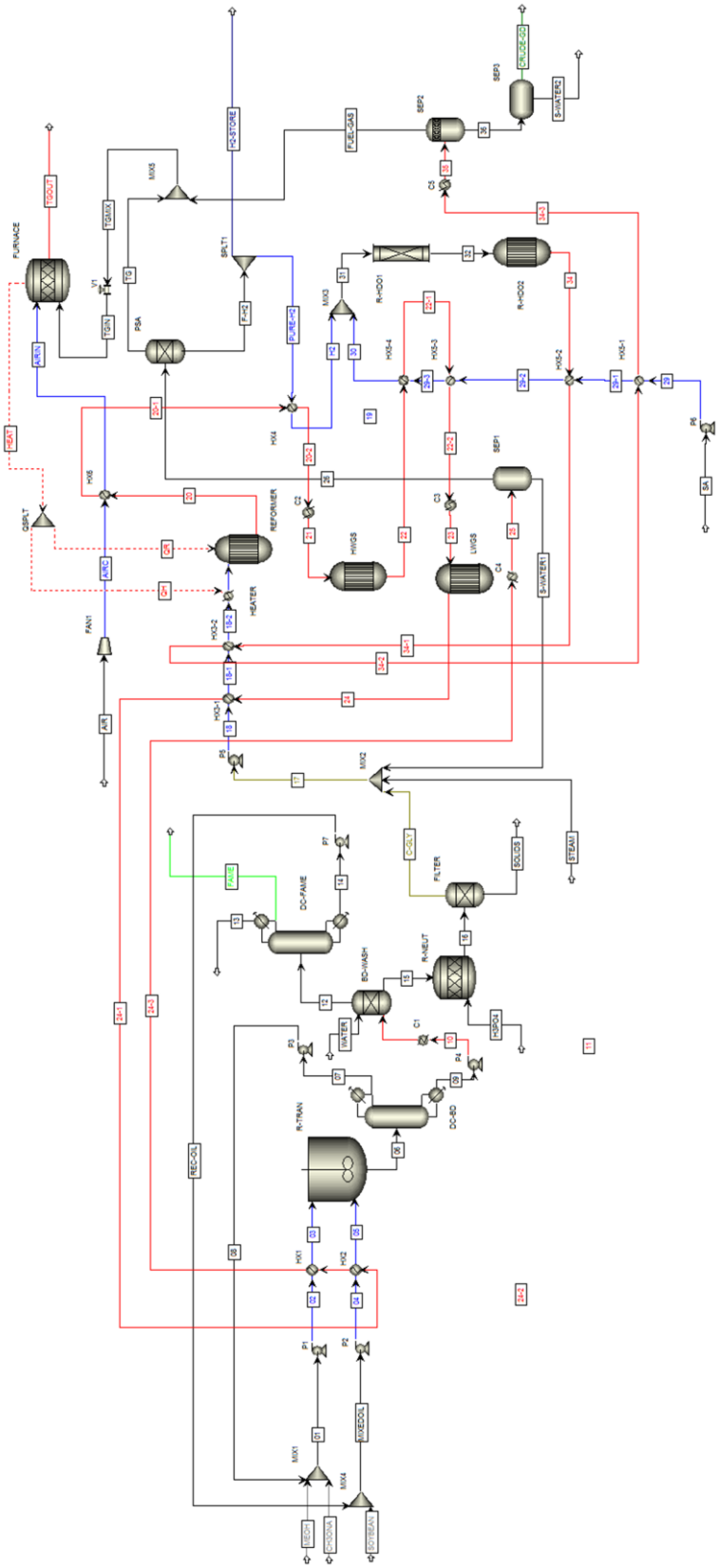

Figure 5.19 Heat exchangers networks and heat flow after pinch analysis details; (1) hot stream = red; (2) cold stream = blue.

5.2.3.2 Heat improvement of the three conventional processes.

Energy integration of three processes consisting of the conventional biodiesel production, hydrogen production via stream reforming, and hydrotreating of stearic acid were investigated in this section using ΔT_{min} = 15 K for all processes.

5.2.3.2.1 Heat improvement of the conventional biodiesel production

Process flow diagram of the conventional biodiesel production in Figure 4.3 was used pinch analysis to determine the heat recovery. Table 5.17 and 5.18 summarize the total number of heat exchangers, total heat recovery, and the energy utility requirement which this result suggested that the heat of products withdrawn from methanol recovery column (DC-BD) can offer the sufficient energy for total feed comprising of oil and methanol. The cooling utility is required for remove the excess enthalpy before forwarding to liquid-liquid extraction hot and cold stream details are illustrated as following Figure 5.20, and 5.21. Table 5.16 also concludes the main results after heat improvement.

Table 5.16 Process performance comparison of the conventional process and its heat integration

Parameters	**Conventional**	**Heat improvement**
Soybean feed rate (kg/hr)	10,000	10,000
Soybean oil conversion (%)	96.16	96.16
Reactors	2	2
Columns	3	3
Separators	5	5
FAMEs yield (wt.%)	92.5	92.5
Biodiesel capacities (kg/hr)	9,244.10	9,244.10
Preheating units	2	0
Cooling units	1	1
Heat exchanger units	0	2
Energy consumption (MW)	6.32	6.09
Energy consumption per kg (MJ/kg)	2.27	2.19

Table 5.17 Summarization of pinch temperature and heat recovery each of heat exchangers after pinch analysis of the conventional biodiesel production.

No. heat exchangers	Cold stream	Heat stream	Temperature hot inlet (K)	Temperature hot outlet (K)	Temperature cold inlet (K)	Temperature cold outlet (K)	Heat recovery (W)
1	**HX2**	**C1**	432	405	298	333	200,297.94
2	**HX1**	**C1**	405	401	319	333	30,000.61
Total heat recovery							**230,298.55**

Table 5.18 Energy loads in coolers and heaters after pinch analysis of the conventional biodiesel production.

No.	Heat stream	Temperature inlet (K)	Temperature outlet (K)	Heat (W)
Cooler 1	C1	401	333	485,921.9
The minimum cold utility requirement				**485,921.9**

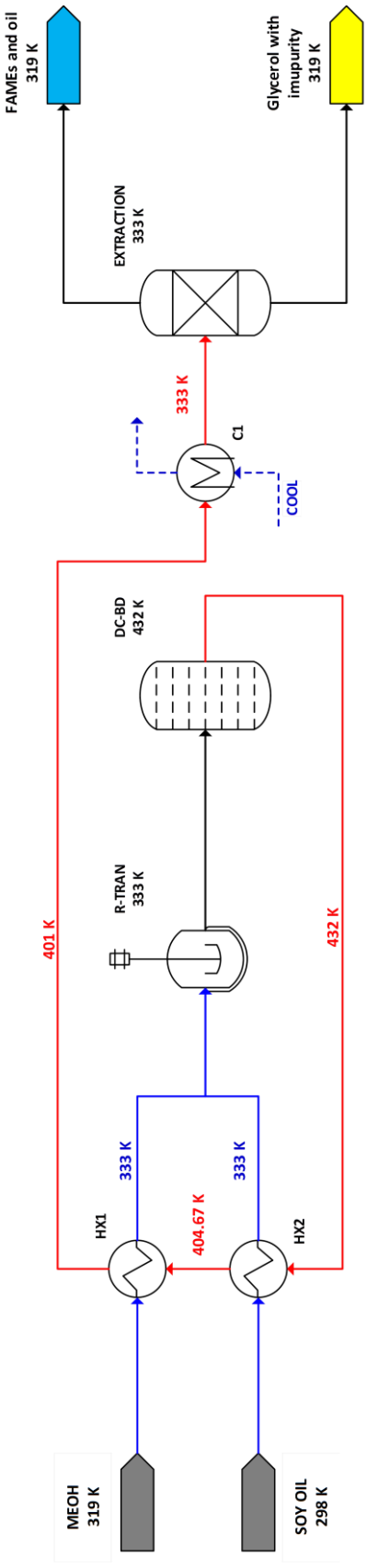

Figure 5.20 Simple heat exchangers networks and heat flow of the conventional biodiesel production after pinch analysis; (1) hot stream = red; (2) cold stream = blue.

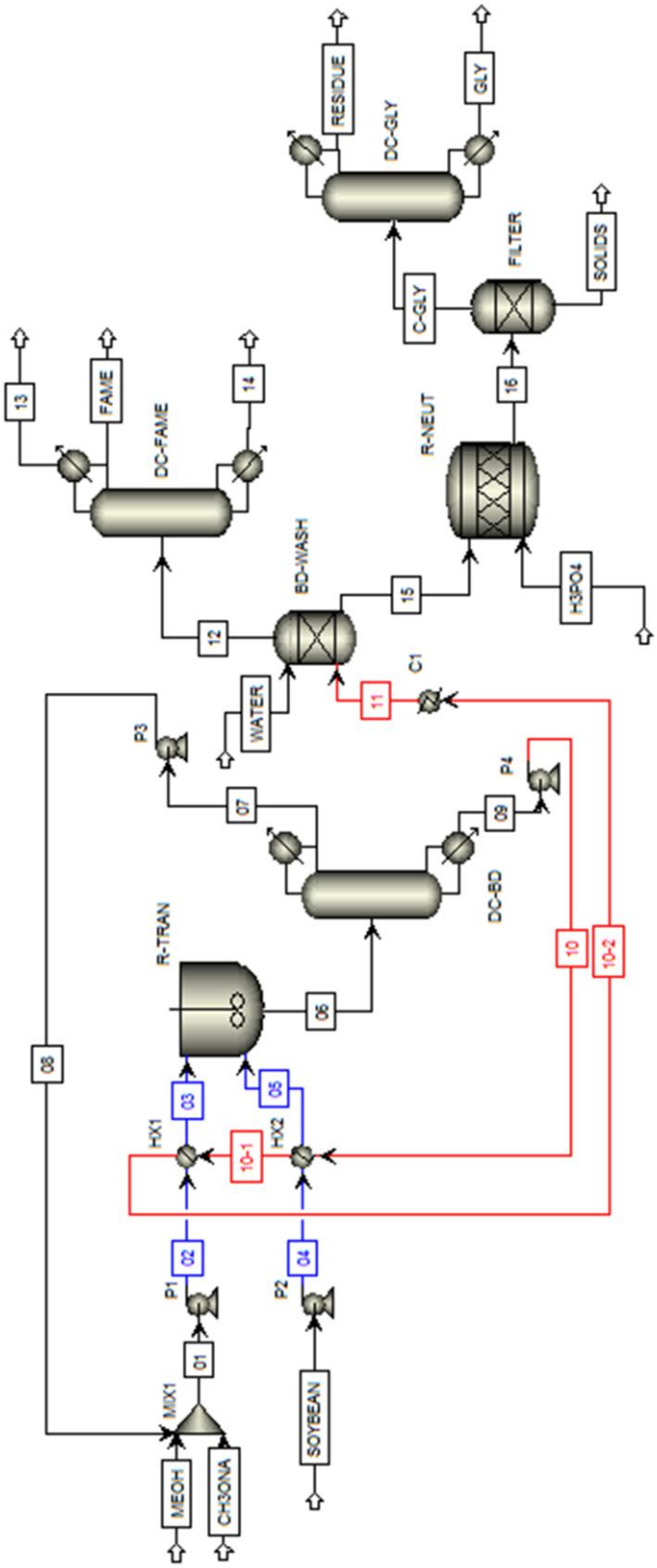

Figure 5.21 Heat exchangers networks and heat flow after pinch analysis of the conventional biodiesel production details ; (1) hot stream = red; (2) cold stream = blue.

5.2.3.2.2 Heat improvement of hydrogen production via glycerol steam reforming

The heat integration was applied to hydrogen production via glycerol steam reforming in Figure 4.10. Although this process must be made up the external energy for heater as found in Table 5.20 and 5.21. Table 5.19 concludes that heat exchangers can almost recover 51 % of energy back to the process. The hot and cold stream details are illustrated as following Figure 5.22, and 5.23.

Table 5.19 Process performance comparison of the conventional process and its heat integration.

Parameters	**Conventional**	**Heat improvement**
Hydrogen source feed	99.9 wt.% glycerol	99.9 wt.% glycerol
Hydrogen source feed rate (kg/hr)	943	943
Steam to feed molar ratio	9	9
Reformer T (K) and P (atm)	1200, 14.31	1200, 14.31
HWGS T (K) and P (atm)	623, 14.31	623, 14.31
LWGS T (K) and P (atm)	473, 14.31	473, 14.31
Reactors	3	3
Columns	0	0
Separators	2	2
Feed conversion (%)	100	100
Hydrogen purity (wt.%)	~100	~100
Hydrogen capacities (kg/hr)	115.24	115.24
Preheating units	1	1
Cooling units	3	1
Heat exchanger units	0	3
Energy consumption (MW)	3.27	1.61
Energy consumption per kg (MJ/kg)	102.05	50.16

จุฬาลงกรณ์มหาวิทยาลัย
Chulalongkorn University

Table 5.20 Summarization of pinch temperature and heat recovery each of heat exchangers after pinch analysis of the hydrogen production via glycerol steam reforming.

No. heat exchangers	Cold stream	Heat stream	Temperature hot inlet (K)	Temperature hot outlet (K)	Temperature cold inlet (K)	Temperature cold outlet (K)	Heat recovery (W)
1	**HX3-1**	**C4**	473	409	301	458	761,073.3
2	**HX3-2**	**C4**	623	473	458.	608	363,486.1
3	**HX3-3**	**C4**	1150	623	608	984	1,238,561.3
Total heat recovery							**2,461,120.7**

Table 5.21 Energy loads in coolers and heaters after pinch analysis of the hydrogen production via glycerol steam reforming.

No.	Heat stream	Temperature inlet (K)	Temperature outlet (K)	Heat (W)
Heater 1	HEATER1	984	1150	1,726,776
The minimum hot utility requirement				**1,727,463.16**
Cooler 4	C4	409	308	-1,205,356.09
The minimum cold utility requirement				**-1,205,356.09**

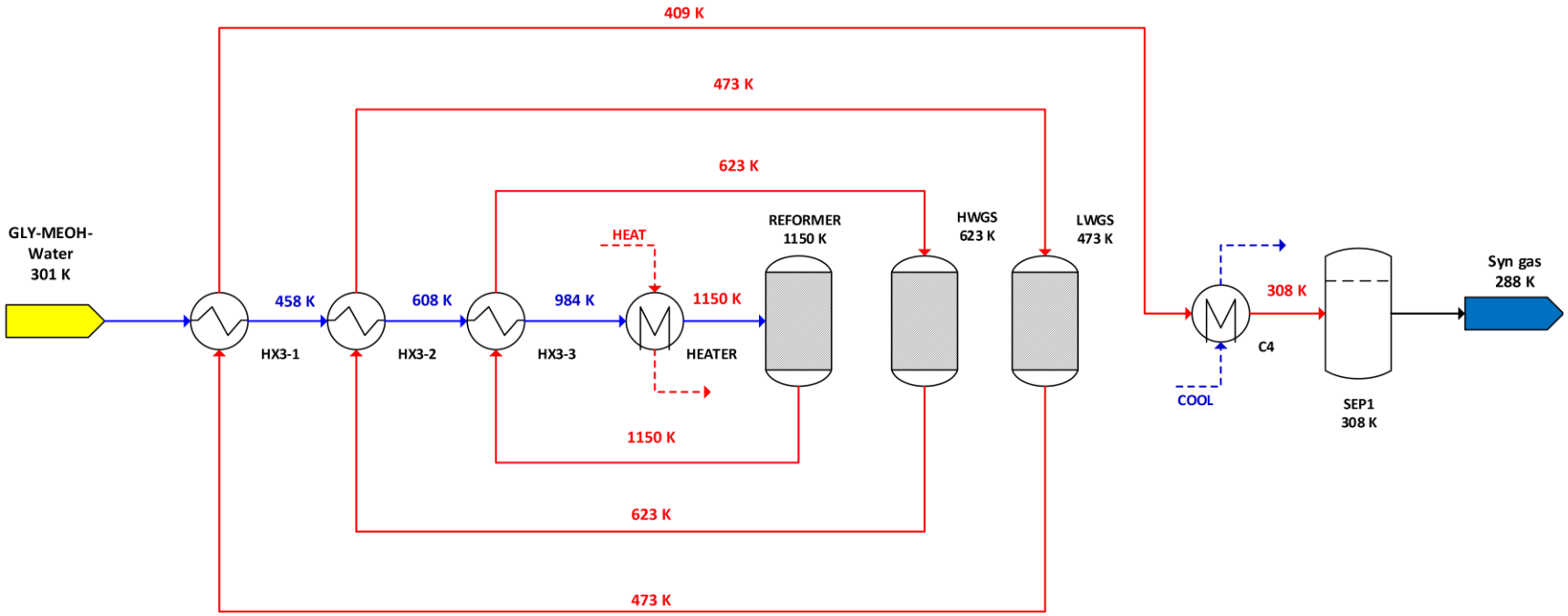

Figure 5.22 Simple heat exchangers networks and heat flow of the hydrogen production via glycerol steam reforming after pinch analysis; (1) hot stream = red; (2) cold stream = blue.

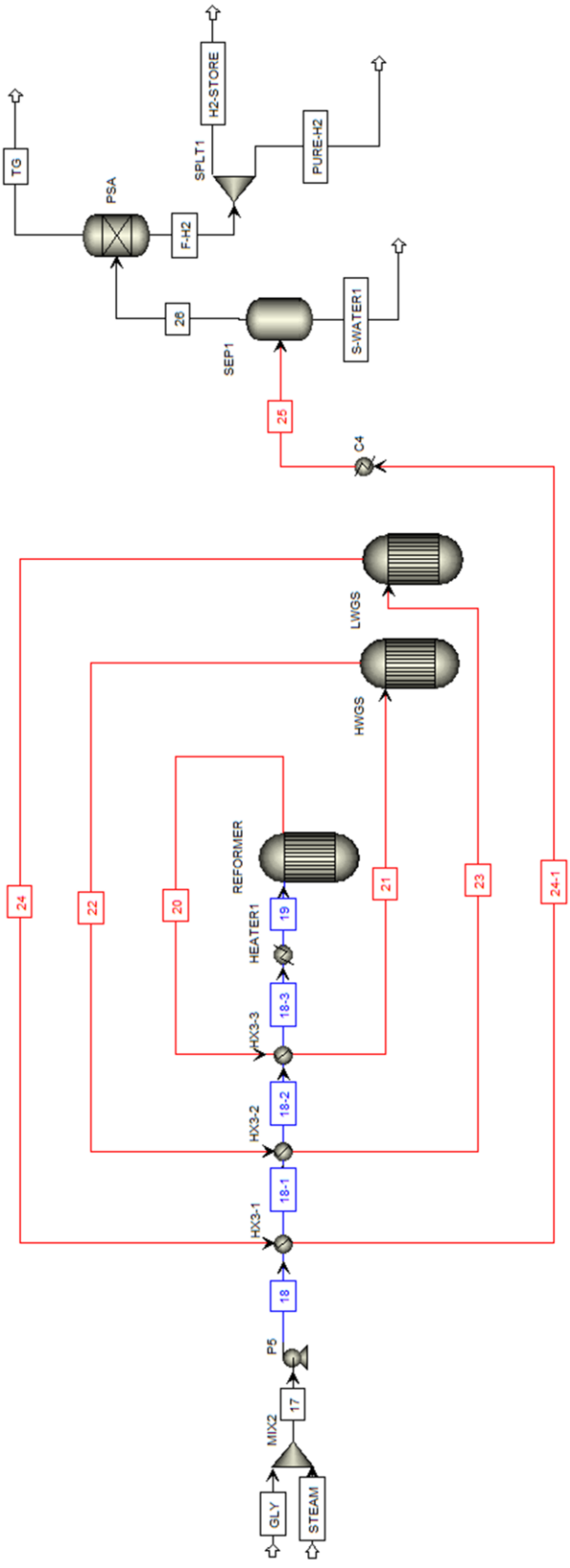

Figure 5.23 Heat exchangers networks and heat flow after pinch analysis of hydrogen production via glycerol stream reforming details; (1) hot stream = red; (2) cold stream = blue.

5.2.3.2.3 Heat improvement of the hydrotreating of stearic acid

The total heat consumption of the hydrotreating of stearic acid, was recalculated (see in Figure 5.24 and 5.25). This process produced the low energy itself which required more energy adding in the heater. Although the heat was recovery (Table 5.23 and 5.24). After pinch analysis, it was found that this process showed the lowest the energy consumption comparing with biodiesel and glycerol steam reforming (Table 5.22).

Table 5.22 Process performance comparison of the conventional process and its heat integration.

Parameters	**Conventional**	**Heat improvement**
Stearic acid (SA) feed rate (kg/hr)	10841.84	10841.84
Hydrogen to SA feed ratio	1.5	1.5
SA conversion (%)	99.79	99.79
Reactors	2	2
Columns	0	0
Separators	2	2
Green diesel purity (wt.%)	97.46	97.46
Green diesel capacities (kg/hr)	9036.81	9036.81
Preheating units	2	2
Cooling units	1	1
Heat exchanger units	0	1
Energy consumption (MW)	2.28	0.47
Energy consumption per kg (MJ/kg)	0.91	0.19

จุฬาลงกรณ์มหาวิทยาลัย
CHULALONGKORN UNIVERSITY

Table 5.23 Summarization of pinch temperature and heat recovery each of heat exchangers after pinch analysis of green diesel production.

No. heat exchangers	Cold stream	Heat stream	Temperature hot inlet (K)	Temperature hot outlet (K)	Temperature cold inlet (K)	Temperature cold outlet (K)	Heat recovery (W)
1	**HX5**	**C5**	298	548	563	394	1,811,958.41
Total heat recovery							**1,811,958.41**

Table 5.24 Energy loads in coolers and heaters after pinch analysis of green diesel production.

No.	Heat stream	Temperature inlet (K)	Temperature outlet (K)	Heat (W)
Heater 2	HEATER2	308	563	128,937.70
Heater 3	HEATER3	548	563	128,765.61
The minimum hot utility requirement				**257,703.31**
Cooler 5	C5	361	308	426,400.16
The minimum cold utility requirement				**426,400.16**

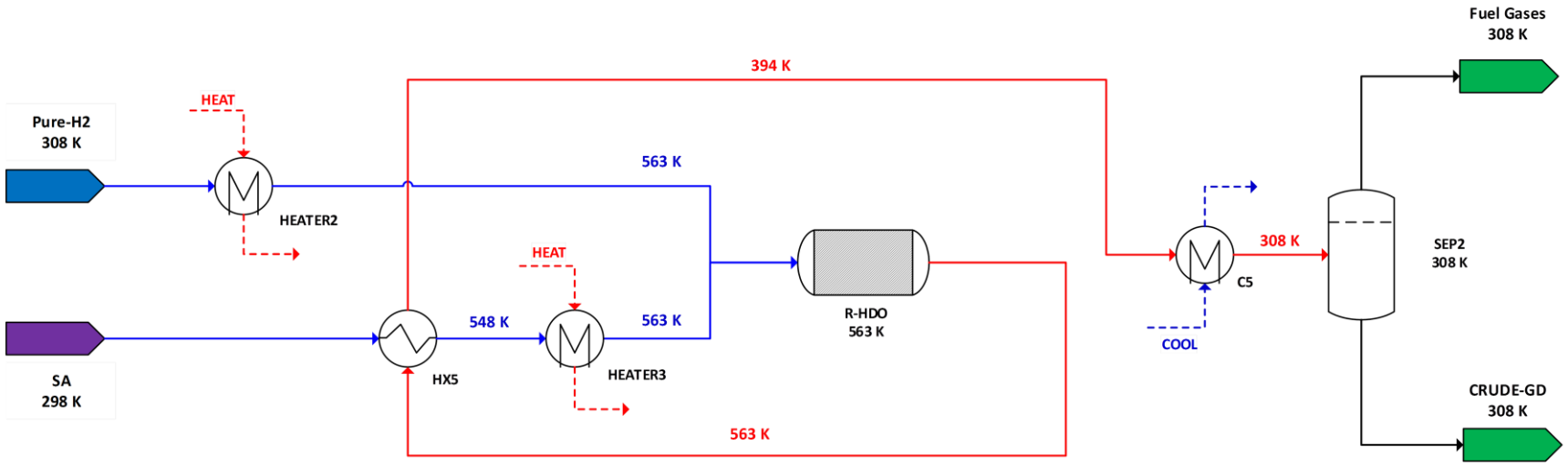

Figure 5.24 Simple heat exchangers networks and heat flow of the hydrotreating process of stearic acid after pinch analysis; (1) hot stream = red; (2) cold stream = blue.

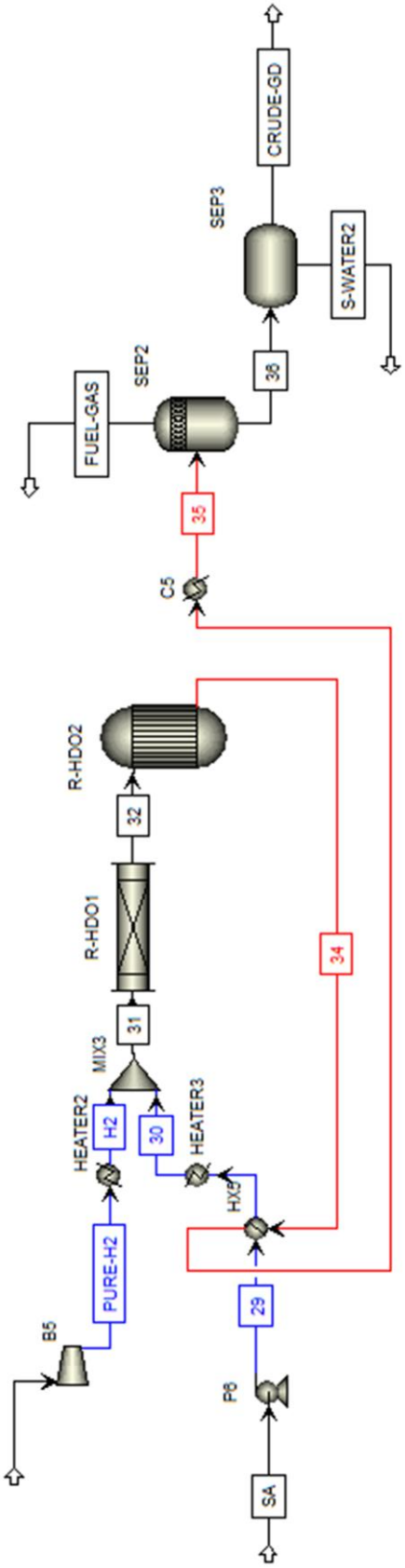

Figure 5.25 Heat exchangers networks and heat flow after pinch analysis of hydrotreating of stearic acid details; (1) hot stream = red; (2) cold stream = blue.

5.2.3.2.4 Process performance comparison of the three original processes and the combined process.

According to the result from Table 5.25, the original base case was lower the energy requirement than that of the improvement strategy 1 and 2. This result can be described that the large amounts of feed stock of improvement strategy 1 and 2 were directly obtained from crude glycerol consisting of glycerol, water, and methanol (stream C-GLY) after solid filtration and high water to feed ratio. Crude glycerol-methanol mixture are benefit toward the hydrogen capacity and no waste as water and methanol residue when glycerol distillation column was installed. Hot residue oil provides the enthalpy to fresh oil after recycle in the vessel (MIX4) in outlet stream utilization (improvement strategy 2) which this result can decrease the oil heating requirement from 0.2 MW to 0.03 MW and energy saving rate can be obtained in the improvement strategy 3 as 47.24%.

Process performance comparison of the three conventional process and the combination process analyzed by heat integration are presented in Table 5.26. The combination process can reduce the energy used in the process. 6.68 MW of energy consumption is mainly obtained from the two distillation column in biodiesel section as methanol recovery (DC-BD) and FAMEs purification (DC-FAME). Total number of equipment in the proposed process is higher than the three conventional processes, but the preheating unit used in the process is lower than the three conventional processes and the large amount of energy requirement of glycerol purification can be neglected and then, the energy consumption extremely decreases even though comparing with individual processes modified energy integration which offered 31.41 % of energy saving rate.

จุฬาลงกรณ์มหาวิทยาลัย
CHULALONGKORN UNIVERSITY

Table 5.25 Comparison of base case and other improvement strategy processes.

Parameters	Original	Strategy 1	Strategy 2	Strategy 3
Soybean feed rate (kg/hr)	10,000	10,000	10,000	10,000
Feed	99.9 wt.% glycerol	Glycerol-methanol	Glycerol-methanol	Glycerol-methanol
Steam to feed molar ratio	9	13.5	13.5	13.5
Hydrogen to SA feed molar ratio	1.5	1.5	1.5	1.5
Soybean oil conversion (%)	96.16	96.16	96.16	96.16
Hydrogen source feed conversion (%)	100	100	100	100
SA conversion (%)	99.79	99.79	99.79	99.79
FAMEs purity (wt.%)	99.80	99.80	99.6	99.6
Hydrogen purity (wt.%)	~100	~100	~100	~100
Green diesel purity (wt.%)	99.28	99.28	99.28	99.28
Biodiesel kg (kg/hr)	9,244.10	9,244.10	9221.75	9221.75
Hydrogen kg (kg/hr)	115.24	125.55	125.55	125.55
Green diesel kg (kg/hr)	9034.56	9845.28	9845.28	9845.28
Heating energy requirement (MW)	12.66	14.02	13.85	6.68

Table 5.26 Process performance comparison of the three conventional process and the combination process are analyzed by heat integration.

Individual units	Individual conventional local process			Propose process Combination process (This work)
	Biodiesel	Glycerol Steam reforming	Hydrotreating	
Reactor	2	3	2	7
Distillation	2	0	0	1
Heater	0	1	2	1
Coolers	1	3	1	5
Heat exchanger	2	3	1	10
Flash	0	1	2	3
Pump	3	1	2	7
Compressor	0	0	1	1
Valve	0	0	0	1
Furnace	0	0	0	1
Total equipment	33			37
Total heat energy requirement (MW)	7.10	2.35	0.29	6.68
	9.74			

CHAPTER VI CONCLUSION AND RECOMMENDATION

6.1 Conclusion

In this work, the novel combined processes comprising of the conventional biodiesel production, hydrogen production via glycerol reforming, and green diesel production using stearic acid as free fatty acid model was simulated and, the following conclusion can be written below;

6.1.1 Base case condition

1) An alkali catalytic biodiesel production process was selected to simulate in biodiesel production section ,because this provides high yield in a short residence time, low operating condition, effective catalyst cost, no mass transfer limitation between catalyst and reactant, using simple equipment and process.

2) The optimal condition from the proposed biodiesel production process was 6 of methanol to oil molar ratio, 1 hr. of residence time of mechanical stirred tank reactor, 333 K of reaction temperature which this process offers 99.60 wt.% of biodiesel purity with 92.7 wt.% yield of FAMEs yield.

3) Glycerol was converted by steam reforming process which offers high hydrogen yield, no coke formation, and methanation occurring during reaction zone.

4) The operating condition for GSM was selected at 9 of steam to glycerol feed ratio, 1150 K and 14.31 atm which operated in the range of conventional steam reforming process as 3-25 atm and 973 – 1373 K.

5) The total product income suggests that the total hydrogen produced should be used for green diesel production to obtain the higher income (H2GD = 1).

6) For green diesel production, SA can be converted to HEPD via dehydrogenation and followed by decarboxylation over nickel supported catalyst which allows the low hydrogen used in process. The optimal condition can be operated at 1.5 of hydrogen to SA molar ratio at 563 K and 14.31 atm.

7) 10,000 kg/hr of soybean oil was converted to 9,244 kg/hr of biodiesel. 115.24 kg/hr of hydrogen obtaining from PSA was produced from 942 kg/hr of 99.9 wt.% of

glycerol withdrawn from glycerol distillation column and then, 9,034.56 kg/hr of C16-C18 of diesel range was derived along with H2GD = 1.

6.1.2 Improvement strategy 1

1) Crude glycerol consisting of glycerol, methanol, and water can be directly used for GSM process and then, the glycerol purification column was discarded from the process with the energy consumption of this column is 0.42 MW per 9,244.10 kg/hr of biodiesel.

2) Due to the glycerol purification column neglected from the process, thermodynamic was recalculated in function of 7.5 glycerol to methanol mole ratio in hydrogen feed source, water, and reaction temperature and pressure. The glycerol-methanol mixture cannot offers a hydrogen yield as same as 99.9 wt.% of glycerol any reaction temperature, but the increase of steam ratio provided the same hydrogen yield. Thus, the optimal of steam ratio from 9 to 13.5.

3) Total heat requirement increases from 12.66 to 14.02 MW because of steam ratio increase from 9 to 13.5 when crude glycerol is substituted the glycerol after discarded glycerol purification column.

4) Green diesel capacity increased from 9034.56 to 9845.28 kg because, the additional of hydrogen was produced via the methanol reforming reaction.

จุฬาลงกรณ์มหาวิทยาลัย
Chulalongkorn University

6.1.3 Improvement strategy 2

1) The hot unconverted oil (606 K) withdrawn from the bottom of FAMEs purification column was recycled to mix with fresh soybean oil to remain 10,000 kg/hr can decrease the total energy from 14.02 MW to 13.85 MW .

2) Although the large amounts of steam from the steam ratio was adjust from 9 to 13.5, the high purity of used condensed water after separated from phase separation (SEP1) can be directly recycle to use as reactant without any treatment.

3) Tailed gas from adsorbent regeneration of PSA in stream TG and the fuel gas in stream FUEL-GAS were mixed as the fuel for furnace combustor which is installed in the process in order to produce heat for the process.

6.1.4 Improvement strategy 3

1) Preheat combustion air is widely in industrial process which installed along with furnace combustor by reducing the cost of fuel gas for make up or provide high heat duty from air enthalpy.

2) When the temperature of preheat combustion air increases the total number of exchanger units was decrease which at 1050 K of temperature of preheat combustion air was given the suitable operation because, lower heat exchangers used and exhausted gas stream is not used in heat integration which the minimum cooling utility requirement was decreased from 4,639,498.5 W to 2,062,905.5 W as 55.54 % cooling energy saving.

3) The minimum heat utility is not required in 550 to 1150 K of the temperature of preheat combustion air operated for the process. This result clearly indicated that the heat produced from the furnace is excessive when the three processes is combined whereas, the more heat is required when three processes is not combined even though the energy integration is applied to recover heat back to processes.

4) Comparison of three processes and the combined process obliviously demonstrated that the proposed process offers 31.41 % of energy saving which 6.68 MW of this process is mainly obtained from the two distillation column in biodiesel section as methanol recovery (DC-BD) and FAMEs purification (DC-FAME).

จุฬาลงกรณ์มหาวิทยาลัย
Chulalongkorn University

6.2 Recommendations

1) Combined process uses SA as the model of free fatty acid which is not the main component of free fatty acid in soybean likewise, the soybean oil and their fatty acid as waste cooking oil have attractive to be further investigated

2) Modified combined process with energy integration provides the higher heat exchangers than other processes and then should be further analyzed.

3) This work does not consider the detailed of total cost such as capital investment, operating cost to decide the plant operation. Therefore, the comparison of cost or amounts of total utility is strongly comment in the future.

4) Large amounts of enthalpy in exhausted gas stream was not used in the pinch analysis and suitable using to directly exchange the heat in the process. This gas is more

attractive to produce steam to supply the energy to equipment such as distillation column to reduce the heat consumption in the proposed process.

5) Although this proposed process can handle the large amount of glycerol converted to hydrogen, the high concentration of CO_2 in the exhausted gas stream is more interesting to combine with other processes which used CO_2 as raw material such as methanol production.

จุฬาลงกรณ์มหาวิทยาลัย
Chulalongkorn University

REFERENCES

1. Canıaz, R.O. and C. Erkey, *Process intensification for heavy oil upgrading using supercritical water.* Chemical Engineering Research and Design, 2014. **92**(10): p. 1845-1863.

2. H. Bridjanian, A.K.S., *BOTTOM OF THE BARREL, AN IMPORTANT CHALLENGE OF THE PETROLEUM REFINING INDUSTRY.* Petroleum & Coal, 2011 **53**(1): p. 13-21.

3. Hajjaji, N., I. Baccar, and M.-N. Pons, *Energy and exergy analysis as tools for optimization of hydrogen production by glycerol autothermal reforming.* Renewable Energy, 2014. **71**(0): p. 368-380.

4. Yoon, J.J., *What's the Difference between Biodiesel and Renewable (Green) Diesel* Advanced Biofuels USA.

5. Hajjaji, N., et al., *A comprehensive energy–exergy-based assessment and parametric study of a hydrogen production process using steam glycerol reforming.* Energy, 2014. **64**(0): p. 473-483.

6. Adhikari, S., S.D. Fernando, and A. Haryanto, *Kinetics and Reactor Modeling of Hydrogen Production from Glycerol via Steam Reforming Process over Ni/CeO2 Catalysts.* Chemical Engineering & Technology, 2009. **32**(4): p. 541-547.

7. Pairojpiriyakul, T., et al., *Catalytic reforming of glycerol in supercritical water with nickel-based catalysts.* International Journal of Hydrogen Energy, 2014. **39**(27): p. 14739-14750.

8. *VEGETABLE OILS IN FOOD TECHNOLOGY: Composition, Properties and Uses*. 1 ed, ed. R.J. Hamilton. 2002: Blackwell Publishing. 337.

CHULALONGKORN UNIVERSITY

9. Ulf Schuchardt, R.S., and Rogério Matheus Vargas and I. Baccar, *Transesterification of Vegetable Oils: a Review.* J. Braz. Chem. Soc., 1997. **9**: p. 199-210.

10. Borges, M.E. and L. Díaz, *Recent developments on heterogeneous catalysts for biodiesel production by oil esterification and transesterification reactions: A review.* Renewable and Sustainable Energy Reviews, 2012. **16**(5): p. 2839-2849.

11. Liu, W., et al., *Biodiesel production from the esterification of fatty acid over organophosphonic acid.* Journal of Industrial and Engineering Chemistry, 2015. **21**(0): p. 893-899.

12. Eze, V.C., A.P. Harvey, and A.N. Phan, *Determination of the kinetics of biodiesel saponification in alcoholic hydroxide solutions.* Fuel, 2015. **140**(0): p. 724-730.

13. Cheng, C.K., S.Y. Foo, and A.A. Adesina, *H2-rich synthesis gas production over Co/Al2O3 catalyst via glycerol steam reforming.* Catalysis Communications, 2010. **12**(4): p. 292-298.

14. Silva, J.M., M.A. Soria, and L.M. Madeira, *Challenges and strategies for optimization of glycerol steam reforming process.* Renewable and Sustainable Energy Reviews, 2015. **42**(0): p. 1187-1213.

15. Liejin Guo, C.C.a.Y.L., *Supercritical Water Gasification of Biomass and Organic Wastes*. 2010, Sciyo.

16. Markočič, E., et al., *Glycerol reforming in supercritical water; a short review.* Renewable and Sustainable Energy Reviews, 2013. **23**(0): p. 40-48.

จุฬาลงกรณ์มหาวิทยาลัย
Chulalongkorn University

17. Wang, W., *Thermodynamic analysis of glycerol partial oxidation for hydrogen production.* Fuel Processing Technology, 2010. **91**(11): p. 1401-1408.

18. Iliuta, I., et al., *Integrated aqueous-phase glycerol reforming to dimethyl ether synthesis—A novel allothermal dual bed membrane reactor concept.* Chemical Engineering Journal, 2012. **187**(0): p. 311-327.

19. Siew, K.W., et al., *Characterization of La-promoted Ni/Al2O3 catalysts for hydrogen production from glycerol dry reforming.* Journal of Energy Chemistry, 2014. **23**(1): p. 15-21.

20. Lee, H.C., et al., *Synthesis and characterisation of cement clinker-supported nickel catalyst for glycerol dry reforming.* Chemical Engineering Journal, 2014. **255**(0): p. 245-256.

21. Choudhary, T.V. and C.B. Phillips, *Renewable fuels via catalytic hydrodeoxygenation.* Applied Catalysis A: General, 2011. **397**(1–2): p. 1-12.

22. Srifa, A., et al., *Production of bio-hydrogenated diesel by catalytic hydrotreating of palm oil over NiMoS2/γ-Al2O3 catalyst.* Bioresource Technology, 2014. **158**(0): p. 81-90.

23. Kim, M., et al., *Competitive transesterification of soybean oil with mixed methanol/ethanol over heterogeneous catalysts.* Bioresour Technol, 2010. **101**(12): p. 4409-14.

24. Bhatti, H.N., et al., *Biodiesel production from waste tallow.* Fuel, 2008. **87**(13–14): p. 2961-2966.

25. Chongkhong, S., C. Tongurai, and P. Chetpattananondh, *Continuous esterification for biodiesel production from palm fatty acid distillate using economical process.* Renewable Energy, 2009. **34**(4): p. 1059-1063.

จุฬาลงกรณ์มหาวิทยาลัย
Chulalongkorn University

26. Antolín, G., et al., *Optimisation of biodiesel production by sunflower oil transesterification.* Bioresource Technology, 2002. **83**(2): p. 111-114.

27. Canoira, L., et al., *Biodiesel from Jojoba oil-wax: Transesterification with methanol and properties as a fuel.* Biomass and Bioenergy, 2006. **30**(1): p. 76-81.

28. Cardone, M., et al., *Brassica carinata as an alternative oil crop for the production of biodiesel in Italy: agronomic evaluation, fuel production by transesterification and characterization.* Biomass and Bioenergy, 2003. **25**(6): p. 623-636.

29. Dmytryshyn, S.L., et al., *Synthesis and characterization of vegetable oil derived esters: evaluation for their diesel additive properties.* Bioresource Technology, 2004. **92**(1): p. 55-64.

30. Foidl, N., et al., *Jatropha curcas L. as a source for the production of biofuel in Nicaragua.* Bioresource Technology, 1996. **58**(1): p. 77-82.

31. Nabi, M.N., M.M. Rahman, and M.S. Akhter, *Biodiesel from cotton seed oil and its effect on engine performance and exhaust emissions.* Applied Thermal Engineering, 2009. **29**(11–12): p. 2265-2270.

32. Nakpong, P. and S. Wootthikanokkhan, *Roselle (Hibiscus sabdariffa L.) oil as an alternative feedstock for biodiesel production in Thailand.* Fuel, 2010. **89**(8): p. 1806-1811.

33. Hotti, S.R. and O.D. Hebbal, *Biodiesel Production Process Optimization from Sugar Apple Seed Oil (Annona squamosa) and Its Characterization.* Journal of Renewable Energy, 2015. **2015**: p. 6.

จุฬาลงกรณ์มหาวิทยาลัย
Chulalongkorn University

34. Puhan, S., et al., *Performance and emission study of Mahua oil (madhuca indica oil) ethyl ester in a 4-stroke natural aspirated direct injection diesel engine.* Renewable Energy, 2005. **30**(8): p. 1269-1278.

35. Ghadge, S.V. and H. Raheman, *Biodiesel production from mahua (Madhuca indica) oil having high free fatty acids.* Biomass and Bioenergy, 2005. **28**(6): p. 601-605.

36. Tomasevic, A.V. and S.S. Siler-Marinkovic, *Methanolysis of used frying oil.* Fuel Processing Technology, 2003. **81**(1): p. 1-6.

37. Usta, N., *Use of tobacco seed oil methyl ester in a turbocharged indirect injection diesel engine.* Biomass and Bioenergy, 2005. **28**(1): p. 77-86.

38. Zullaikah, S., et al., *A two-step acid-catalyzed process for the production of biodiesel from rice bran oil.* Bioresource Technology, 2005. **96**(17): p. 1889-1896.

39. Encinar, J.M., J.F. González, and A. Rodríguez-Reinares, *Ethanolysis of used frying oil. Biodiesel preparation and characterization.* Fuel Processing Technology, 2007. **88**(5): p. 513-522.

40. Patil, P.D. and S. Deng, *Optimization of biodiesel production from edible and non-edible vegetable oils.* Fuel, 2009. **88**(7): p. 1302-1306.

41. Yang, Z. and W. Xie, *Soybean oil transesterification over zinc oxide modified with alkali earth metals.* Fuel Processing Technology, 2007. **88**(6): p. 631-638.

42. Guo, F., et al., *Calcined sodium silicate as solid base catalyst for biodiesel production.* Fuel Processing Technology, 2010. **91**(3): p. 322-328.

จุฬาลงกรณ์มหาวิทยาลัย
Chulalongkorn University

43. Ren, Q., et al., *Nano KF/ g-Al 2 O 3 catalyzed transesterification of soybean oil for biodiesel production by using ultrasonic irradiation.* J Cent South Univ (Sci Technol), 2010. **41**: p. 883.

44. Wen, Z., et al., *Synthesis of biodiesel from vegetable oil with methanol catalyzed by Li-doped magnesium oxide catalysts.* Applied Energy, 2010. **87**(3): p. 743-748.

45. Tantirungrotechai, J., P. Chotmongkolsap, and M. Pohmakotr, *Synthesis, characterization, and activity in transesterification of mesoporous Mg–Al mixed-metal oxides.* Microporous and Mesoporous Materials, 2010. **128**(1–3): p. 41-47.

46. Silva, C.C.C.M., et al., *Biodiesel production from soybean oil and methanol using hydrotalcites as catalyst.* Fuel Processing Technology, 2010. **91**(2): p. 205-210.

47. Samart, C., C. Chaiya, and P. Reubroycharoen, *Biodiesel production by methanolysis of soybean oil using calcium supported on mesoporous silica catalyst.* Energy Conversion and Management, 2010. **51**(7): p. 1428-1431.

48. Kim, M.J., et al., *Transesterification of vegetable oils over a phosphazenium hydroxide catalyst incorporated onto silica.* Fuel Processing Technology, 2011. **92**(1): p. 126-131.

49. Di Serio, M., et al., *Vanadyl phosphate catalysts in biodiesel production.* Applied Catalysis A: General, 2007. **320**(0): p. 1-7.

50. Furuta, S., H. Matsuhashi, and K. Arata, *Biodiesel fuel production with solid superacid catalysis in fixed bed reactor under atmospheric pressure.* Catalysis Communications, 2004. **5**(12): p. 721-723.

จุฬาลงกรณ์มหาวิทยาลัย
Chulalongkorn University

51. Chung, K.-H. and B.-G. Park, *Esterification of oleic acid in soybean oil on zeolite catalysts with different acidity.* Journal of Industrial and Engineering Chemistry, 2009. **15**(3): p. 388-392.

52. Mo, X., et al., *A Novel Sulfonated Carbon Composite Solid Acid Catalyst for Biodiesel Synthesis.* Catalysis Letters, 2008. **123**(1-2): p. 1-6.

53. Semwal, S., et al., *Biodiesel production using heterogeneous catalysts.* Bioresource Technology, 2011. **102**(3): p. 2151-2161.

54. Suppes, G.J., et al., *Transesterification of soybean oil with zeolite and metal catalysts.* Applied Catalysis A: General, 2004. **257**(2): p. 213-223.

55. Kim, H.-J., et al., *Transesterification of vegetable oil to biodiesel using heterogeneous base catalyst.* Catalysis Today, 2004. **93–95**(0): p. 315-320.

56. Ilham, Z. and S. Saka, *Dimethyl carbonate as potential reactant in non-catalytic biodiesel production by supercritical method.* Bioresource Technology, 2009. **100**(5): p. 1793-1796.

57. Ilham, Z. and S. Saka, *Optimization of supercritical dimethyl carbonate method for biodiesel production.* Fuel, 2012. **97**(0): p. 670-677.

58. Tan, K.T., K.T. Lee, and A.R. Mohamed, *Optimization of supercritical dimethyl carbonate (SCDMC) technology for the production of biodiesel and value-added glycerol carbonate.* Fuel, 2010. **89**(12): p. 3833-3839.

59. Saka, S. and Y. Isayama, *A new process for catalyst-free production of biodiesel using supercritical methyl acetate.* Fuel, 2009. **88**(7): p. 1307-1313.

จุฬาลงกรณ์มหาวิทยาลัย
Chulalongkorn University

60. Campanelli, P., M. Banchero, and L. Manna, *Synthesis of biodiesel from edible, non-edible and waste cooking oils via supercritical methyl acetate transesterification.* Fuel, 2010. **89**(12): p. 3675-3682.

61. Tan, K.T., K.T. Lee, and A.R. Mohamed, *A glycerol-free process to produce biodiesel by supercritical methyl acetate technology: an optimization study via Response Surface Methodology.* Bioresour Technol, 2010. **101**(3): p. 965-9.

62. Niza, N., et al., *Comparison and optimisation of biodiesel production from Jatropha curcas oil using supercritical methyl acetate and methanol.* Chemical Papers, 2011. **65**(5): p. 721-729.

63. Doná, G., et al., *Biodiesel production using supercritical methyl acetate in a tubular packed bed reactor.* Fuel Processing Technology, 2013. **106**(0): p. 605-610.

64. Saka, S. and D. Kusdiana, *Biodiesel fuel from rapeseed oil as prepared in supercritical methanol.* Fuel, 2001. **80**(2): p. 225-231.

65. Madras, G., C. Kolluru, and R. Kumar, *Synthesis of biodiesel in supercritical fluids.* Fuel, 2004. **83**(14–15): p. 2029-2033.

66. Cao, W., H. Han, and J. Zhang, *Preparation of biodiesel from soybean oil using supercritical methanol and co-solvent.* Fuel, 2005. **84**(4): p. 347-351.

67. Yin, J.-Z., M. Xiao, and J.-B. Song, *Biodiesel from soybean oil in supercritical methanol with co-solvent.* Energy Conversion and Management, 2008. **49**(5): p. 908-912.

68. Du, W., et al., *Comparative study on lipase-catalyzed transformation of soybean oil for biodiesel production with different acyl acceptors.* Journal of Molecular Catalysis B: Enzymatic, 2004. **30**(3–4): p. 125-129.

จุฬาลงกรณ์มหาวิทยาลัย
Chulalongkorn University

69. Noureddini, H., X. Gao, and R.S. Philkana, *Immobilized Pseudomonas cepacia lipase for biodiesel fuel production from soybean oil.* Bioresour Technol, 2005. **96**(7): p. 769-77.

70. Samukawa, T., et al., *Pretreatment of immobilized Candida antarctica lipase for biodiesel fuel production from plant oil.* Journal of Bioscience and Bioengineering, 2000. **90**(2): p. 180-183.

71. Hama, S., et al., *Effect of fatty acid membrane composition on whole-cell biocatalysts for biodiesel-fuel production.* Biochemical Engineering Journal, 2004. **21**(2): p. 155-160.

72. Xu, W.D., Jing Zeng and Y. Dehua Liu, *Conversion of Soybean Oil to Biodiesel Fuel Using Lipozyme TL IM in a Solvent-free Medium.* Biocatalysis and Biotransformation, 2004. **22**(1): p. 45-48.

73. Luo, Y., et al., *A novel psychrophilic lipase from Pseudomonas fluorescens with unique property in chiral resolution and biodiesel production via transesterification.* Appl Microbiol Biotechnol, 2006. **73**(2): p. 349-55.

74. Shieh, C.J., H.F. Liao, and C.C. Lee, *Optimization of lipase-catalyzed biodiesel by response surface methodology.* Bioresource Technology, 2003. **88**(2): p. 103-106.

75. Kaieda, M., et al., *Effect of Methanol and water contents on production of biodiesel fuel from plant oil catalyzed by various lipases in a solvent-free system.* Journal of Bioscience and Bioengineering, 2001. **91**(1): p. 12-15.

76. de Oliveira, D., et al., *Kinetics of Enzyme-Catalyzed Alcoholysis of Soybean Oil in n-Hexane,* in *Twenty-Sixth Symposium on Biotechnology for Fuels and Chemicals*, B. Davison, et al., Editors. 2005, Humana Press. p. 231-241.

จุฬาลงกรณ์มหาวิทยาลัย
Chulalongkorn University

77. Souza, M.S., et al., *Biodiesel synthesis via esterification of feedstock with high content of free fatty acids.* Appl Biochem Biotechnol, 2009. **154**(1-3): p. 74-88.

78. Chouhan, A.P.S. and A.K. Sarma, *Modern heterogeneous catalysts for biodiesel production: A comprehensive review.* Renewable and Sustainable Energy Reviews, 2011. **15**(9): p. 4378-4399.

79. Lam, M.K., K.T. Lee, and A.R. Mohamed, *Homogeneous, heterogeneous and enzymatic catalysis for transesterification of high free fatty acid oil (waste cooking oil) to biodiesel: A review.* Biotechnology Advances, 2010. **28**(4): p. 500-518.

80. Rashid, U., et al., *Production of sunflower oil methyl esters by optimized alkali-catalyzed methanolysis.* Biomass and Bioenergy, 2008. **32**(12): p. 1202-1205.

81. Noureddini, H. and D. Zhu, *Kinetics of transesterification of soybean oil.* Journal of the American Oil Chemists' Society, 1997. **74**(11): p. 1457-1463.

82. Vicente, G., M. Martínez, and J. Aracil, *Integrated biodiesel production: a comparison of different homogeneous catalysts systems.* Bioresource Technology, 2004. **92**(3): p. 297-305.

83. Wang, B., et al., *A new solid base catalyst for the transesterification of rapeseed oil to biodiesel with methanol.* Fuel, 2013. **104**(0): p. 698-703.

84. Bharathiraja, B., et al., *Biodiesel production using chemical and biological methods – A review of process, catalyst, acyl acceptor, source and process variables.* Renewable and Sustainable Energy Reviews, 2014. **38**(0): p. 368-382.

85. Chen, C.-L., et al., *Biodiesel synthesis via heterogeneous catalysis using modified strontium oxides as the catalysts.* Bioresource Technology, 2012. **113**(0): p. 8-13.

86. Tariq, M., S. Ali, and N. Khalid, *Activity of homogeneous and heterogeneous catalysts, spectroscopic and chromatographic characterization of biodiesel: A review.* Renewable and Sustainable Energy Reviews, 2012. **16**(8): p. 6303-6316.

87. Zheng, S., et al., *Acid-catalyzed production of biodiesel from waste frying oil.* Biomass and Bioenergy, 2006. **30**(3): p. 267-272.

88. Zhang, Y., et al., *Biodiesel production from waste cooking oil: 1. Process design and technological assessment.* Bioresource Technology, 2003. **89**(1): p. 1-16.

89. West, A.H., D. Posarac, and N. Ellis, *Assessment of four biodiesel production processes using HYSYS.Plant.* Bioresource Technology, 2008. **99**(14): p. 6587-6601.

90. Lee, S., D. Posarac, and N. Ellis, *Process simulation and economic analysis of biodiesel production processes using fresh and waste vegetable oil and supercritical methanol.* Chemical Engineering Research and Design, 2011. **89**(12): p. 2626-2642.

91. Sawangkeaw, R., K. Bunyakiat, and S. Ngamprasertsith, *A review of laboratory-scale research on lipid conversion to biodiesel with supercritical methanol (2001–2009).* The Journal of Supercritical Fluids, 2010. **55**(1): p. 1-13.

92. Serrera, A., F.J. Gutiérrez Ortiz, and P. Ollero, *Syngas methanation from the supercritical water reforming of glycerol.* Energy, 2014. **76**(0): p. 584-592.

จุฬาลงกรณ์มหาวิทยาลัย
Chulalongkorn University

93. Kamonsuangkasem, K., S. Therdthianwong, and A. Therdthianwong, *Hydrogen production from yellow glycerol via catalytic oxidative steam reforming.* Fuel Processing Technology, 2013. **106**(0): p. 695-703.

94. Byrd, A.J., K.K. Pant, and R.B. Gupta, *Hydrogen production from glycerol by reforming in supercritical water over Ru/Al2O3 catalyst.* Fuel, 2008. **87**(13–14): p. 2956-2960.

95. Wen, G., et al., *Production of hydrogen by aqueous-phase reforming of glycerol.* International Journal of Hydrogen Energy, 2008. **33**(22): p. 6657-6666.

96. Ciftci, A., et al., *Support effects in the aqueous phase reforming of glycerol over supported platinum catalysts.* Applied Catalysis A: General, 2012. **431–432**(0): p. 113-119.

97. Menezes, A.O., et al., *Production of renewable hydrogen from aqueous-phase reforming of glycerol over Pt catalysts supported on different oxides.* Renewable Energy, 2011. **36**(2): p. 595-599.

98. Ciftci, A., et al., *Pt-Re synergy in aqueous-phase reforming of glycerol and the water–gas shift reaction.* Journal of Catalysis, 2014. **311**(0): p. 88-101.

99. Lehnert, K. and P. Claus, *Influence of Pt particle size and support type on the aqueous-phase reforming of glycerol.* Catalysis Communications, 2008. **9**(15): p. 2543-2546.

100. Tuza, P.V., et al., *Production of renewable hydrogen by aqueous-phase reforming of glycerol over Ni–Cu catalysts derived from hydrotalcite precursors.* Renewable Energy, 2013. **50**(0): p. 408-414.

จุฬาลงกรณ์มหาวิทยาลัย
Chulalongkorn University

101. Guo, Y., et al., *Hydrogen production by aqueous-phase reforming of glycerol over Ni-B catalysts.* International Journal of Hydrogen Energy, 2012. **37**(1): p. 227-234.

102. Manfro, R.L., et al., *Hydrogen production by aqueous-phase reforming of glycerol over nickel catalysts supported on CeO2.* Fuel Processing Technology, 2011. **92**(3): p. 330-335.

103. He, C., et al., *Sorption enhanced aqueous phase reforming of glycerol for hydrogen production over Pt-Ni supported on multi-walled carbon nanotubes.* Applied Catalysis B: Environmental, 2015. **162**(0): p. 401-411.

104. Wang, C., et al., *Hydrogen production from steam reforming of glycerol by Ni–Mg–Al based catalysts in a fixed-bed reactor.* Chemical Engineering Journal, 2013. **220**(0): p. 133-142.

105. Kale, G.R. and B.D. Kulkarni, *Thermodynamic analysis of dry autothermal reforming of glycerol.* Fuel Processing Technology, 2010. **91**(5): p. 520-530.

106. Pairojpiriyakul, T., et al., *Hydrogen production from supercritical water reforming of glycerol in an empty Inconel 625 reactor.* International Journal of Hydrogen Energy, 2014. **39**(1): p. 159-170.

107. Gutiérrez Ortiz, F.J., et al., *Optimization of power and hydrogen production from glycerol by supercritical water reforming.* Chemical Engineering Journal, 2013. **218**(0): p. 309-318.

108. Gutiérrez Ortiz, F.J., et al., *Autothermal Reforming of Glycerol with Supercritical Water for Maximum Power through a Turbine Plus a Fuel Cell.* Energy & Fuels, 2013. **27**(1): p. 576-587.

จุฬาลงกรณ์มหาวิทยาลัย
Chulalongkorn University

109. Fermoso, J., L. He, and D. Chen, *Production of high purity hydrogen by sorption enhanced steam reforming of crude glycerol.* International Journal of Hydrogen Energy, 2012. **37**(19): p. 14047-14054.

110. Huber, G.W., P. O'Connor, and A. Corma, *Processing biomass in conventional oil refineries: Production of high quality diesel by hydrotreating vegetable oils in heavy vacuum oil mixtures.* Applied Catalysis A: General, 2007. **329**(0): p. 120-129.

111. Kubička, D. and L. Kaluža, *Deoxygenation of vegetable oils over sulfided Ni, Mo and NiMo catalysts.* Applied Catalysis A: General, 2010. **372**(2): p. 199-208.

112. Šimáček, P., et al., *Hydroprocessed rapeseed oil as a source of hydrocarbon-based biodiesel.* Fuel, 2009. **88**(3): p. 456-460.

113. Zhang, H., et al., *Hydroprocessing of waste cooking oil over a dispersed nano catalyst: Kinetics study and temperature effect.* Applied Catalysis B: Environmental, 2014. **150–151**(0): p. 238-248.

114. Yakovlev, V.A., et al., *Development of new catalytic systems for upgraded bio-fuels production from bio-crude-oil and biodiesel.* Catalysis Today, 2009. **144**(3–4): p. 362-366.

115. Boda, L., et al., *Catalytic hydroconversion of tricaprylin and caprylic acid as model reaction for biofuel production from triglycerides.* Applied Catalysis A: General, 2010. **374**(1–2): p. 158-169.

116. Kumar, P., et al., *Kinetics of hydrodeoxygenation of stearic acid using supported nickel catalysts: Effects of supports.* Applied Catalysis A: General, 2014. **471**(0): p. 28-38.

จุฬาลงกรณ์มหาวิทยาลัย
Chulalongkorn University

117. *HYDROGEN PRODUCTION AND STORAGE*. 2006, INTERNATIONAL ENERGY AGENCY. p. 1-38.

118. Ramachandran, K., et al., *Recent developments for biodiesel production by ultrasonic assist transesterification using different heterogeneous catalyst: A review*. Renewable and Sustainable Energy Reviews, 2013. **22**(0): p. 410-418.

119. *TRI SODIUM SPECIALTY PHOSPHATE CLEANER All Purpose Cleaner*. 2008, Empire Blended Products, Inc: 250 Hickory Lane C Bayville, NJ 08721. p. 1-2.

120. William Bachop Dolan, M.J.M., *Heavy hydrocarbon recovery from pressure swing adsorption unit tail gas*. 26 August 2003, Engelhard Coporation. p. 1-14.

121. *Preheated Combustion Air*. 2007 Industrial Technologies Program Energy Efficiency and Renewable Energy U.S. Department of Energy Washington, DC 20585-0121 p. 1-2.

จุฬาลงกรณ์มหาวิทยาลัย
Chulalongkorn University

จุฬาลงกรณ์มหาวิทยาลัย
Chulalongkorn University

VITA

Mr. Bamrung Sungnoen was born on February 8th, 1990 in Bangkok,Thailand. He received his Bachelor degree in Chemical Engineering (2nd class honors) from Faculty of Engineering, Naresuan University in 2013. After obtaining first degree, he continued his study in the Master's Degree program of Chemical Engineering, Chulalongkorn University since the academic year 2013.